


Grenoble INP – ENSIMAG
École Nationale Supérieure d'Informatique et de Mathématiques Appliquées

UGA – UFR IM²AG
Université Grenoble Alpes – Unité de Formation et de Recherche en Informatique, Mathématiques et Mathématiques Appliquées de Grenoble

Master's Thesis

Asymptotic expansion and numerical simulation in viscoelastic fluids with application to biological tissues

Nathan Shourick

Third Year Engineering Option MMIS – M.Sc. MSIAM Option MSCI

March 2020, 1st – June 2020, 15th

Laboratoire Jean Kuntzmann
Bâtiment IMAG
Université Grenoble Alpes
700 Avenue Centrale
Campus de Saint Martin d'Hères
38401 Domaine Universitaire de Saint-Martin-d'Hères

Supervisors
Pierre Saramito
Research Director at the CNRS, LJK
Ibrahim Cheddadi
Associate Professor, TIMC-IMAG

Acknowledgements

My thanks go first of all to my two internship supervisors, Mr Pierre Saramito, research director at the CNRS, and Mr Ibrahim Cheddadi, associate professor, thanks to whom the internship took place in the best possible conditions. I would like to express my gratitude for their welcome, their kindness and their many pieces of advice. I was really able to progress and learn (a lot) of new things with them.

I am very grateful to François Graner, research director at the CNRS, Hélène Delanoë-Ayari, associate professor, Sham Tlili, postdoctoral student, and Mélina Durande, doctoral student, for taking the time to discuss with my supervisors and myself about the first results I obtained. A special thank you to François Graner for reviewing this master's thesis.

I would also like to thank the staff of the LJK who contributed to ensure that my internship went well within the structure.

Finally, I would like to thank the teaching and administrative teams of MSIAM and Ensimag, who made this internship possible.

Remerciements

Mes remerciements vont tout d'abord à mes deux responsables de stage, MM. Pierre Saramito, directeur de recherche au CNRS, et Ibrahim Cheddadi, maître de conférence, grâce à qui le stage a pu se dérouler dans les meilleures conditions possibles. Je leur exprime toute ma gratitude pour leur accueil, leur bienveillance et leurs nombreux conseils. J'ai vraiment pu progresser et apprendre (beaucoup) de nouvelles choses à leurs côtés.

Je remercie vivement François Graner, directeur de recherche au CNRS, Hélène Delanoë-Ayari, maître de conférence, Sham Tlili, post-doctorante, et Mélina Durande, doctorante, pour avoir pris le temps de discuter avec mes responsables et moi-même sur les premiers résultats que j'ai obtenus. J'adresse un merci tout particulier à François Graner pour avoir bien voulu relire le présent mémoire.

Je tiens également à remercier le personnel du LJK qui a contribué au bon déroulement de mon stage au sein de la structure.

Je remercie enfin les équipes pédagogique et administrative du MSIAM et de l'Ensimag, sans qui ce stage n'aurait pas été possible.

Abstract

This master's thesis addresses the mathematical and numerical modelling of collective movement in thin biological tissues, epithelia. It is part of a long-standing project, initiated by a team of biophysicists, whose aim is to improve knowledge of the biophysical mechanisms involved in developmental biology. From our point of view, the behavior of epithelia is described by a viscoelastic fluid model. The laws associated with it then lead to the formulation of the problem as a coupled system of time-dependent partial differential equations. The transition to a variational formulation is based on the discontinuous Galerkin method and allows to obtain first results in the inelastic case. These results are compared with the experimental data available to the above-mentioned team of biophysicists, which gives us the opportunity to identify the limits of our model and the perspectives to be considered.

Keywords: Collective cell migration in epithelial tissues; shallow viscoelastic fluids; asymptotic expansion; thin-layer approximation; variational formulation; discontinuous Galerkin method; comparison with experimental data.

Résumé

Ce mémoire aborde la modélisation mathématique et numérique du mouvement collectif dans des tissus biologiques minces, les épithéliums. Elle s'inscrit dans un projet de longue date, initié par une équipe de biophysiciens, dont le but est d'améliorer les connaissances sur les mécanismes biophysiques qui intervienent en biologie du développement. De notre point de vue, le comportement des épithéliums est décrit par un modèle de type fluide viscoélastique. Les lois qui lui sont associées amènent alors à formuler le problème sous la forme d'un système couplé d'équations aux dérivées partielles dépendantes du temps. Le passage à une formulation variationnelle s'appuie sur la méthode de Galerkin discontinue et permet d'obtenir de premiers résultats dans le cas non élastique. Ces résultats sont comparés avec les données expérimentales dont dispose l'équipe de biophysiciens déjà mentionnée, ce qui nous offre la possibilité de dégager les limites de notre modèle et les perspectives à envisager.

Mots-clés: Migration cellulaire collective dans les épithéliums; fluides viscoélastiques minces; analyse asymptotique; approximation en couche mince; formulation variationnelle; méthode de Galerkin discontinue; comparaison avec des données expérimentales.

Contents

Notations

Domain description

Notation	Description
$\Lambda(t)$	flow domain at time t
$\Gamma_f(t)$	upper free surface at time t
Γ_0	lower horizontal plane substrate in 3D
$\Gamma = \Gamma_{\text{obstacle}} \cup \Gamma_{\text{wall}}$	vertical obstacles and domain limits
Ω	lower horizontal plane substrate in 2D
$\Omega_c(t) = h(t,\cdot)^{-1}([h_c, +\infty[)$	tissue domain for the thin layer approximation
$\boldsymbol{n}$	outer unit normal vector in 3D
$\boldsymbol{\nu}$	outer unit normal vector in 2D

Material parameters

Notation	Description	Unit	Num. exp.
$\boldsymbol{u}$	cell velocity field	$\text{m} \cdot \text{s}^{-1}$	
ρ	fluid density	$\text{kg} \cdot \text{m}^{-3}$	
h	cell height	$\text{kg} \cdot \text{m}^{-3}$	
$\boldsymbol{\sigma}$	Cauchy stress tensor	$\text{N} \cdot \text{m}^{-2}$	
$\boldsymbol{\tau}$	elastic stress tensor	$\text{N} \cdot \text{m}^{-2}$	
p	pressure	Pa	
η_m	viscosity of the material	$\text{Pa} \cdot \text{s}$	
η_s	viscosity of the solvent	$\text{Pa} \cdot \text{s}$	
$\eta = \eta_m + \eta_s$	total viscosity	$\text{Pa} \cdot \text{s}$	
μ	elasticity modulus of the material	Pa	
$\lambda = \eta_m/\mu$	relaxation time	s	
ζ	friction coefficient	$\text{Pa} \cdot \text{s} \cdot \text{m}^{-1}$	
$\boldsymbol{f}_a$	active force	$\text{N} \cdot \text{m}^{-2}$	
L	characteristic length of the domain	m	75 μm
H	characteristic height of the domain	m	
U	characteristic planar velocity	$\text{m} \cdot \text{s}^{-1}$	10/9 $\mu\text{m} \cdot \text{min}^{-1}$
$\varepsilon = H/L$	low aspect ratio of the geometry	-	
$Re = \rho UL/\eta$	Reynolds number	-	
$We = \lambda U/L$	Weissenberg number	-	
$\alpha = \varepsilon^{-1} L\zeta/\eta$	dimensionless friction parameter	-	
$\beta = \eta_m/\eta$	dimensionless viscosity parameter	-	
$x_f(t)$	position of the tissue front at time t	m	
d_{mean}	mean cell surface density	$\text{kg} \cdot \text{m}^{-2}$	
r_{mean}	mean cell radius	m	

Mathematical notations

Notation	Description
$\boldsymbol{D}(\boldsymbol{u}) = \frac{1}{2}\left(\nabla \boldsymbol{u} + \nabla \boldsymbol{u}^\top\right)$	rate of deformation
$D_t = \partial_t + (\boldsymbol{u} \cdot \nabla)$	Lagrange derivative
$\overset{\nabla}{\boldsymbol{\tau}} = \partial_t \boldsymbol{\tau} + (\boldsymbol{u} \cdot \nabla)\boldsymbol{\tau} - (\nabla \boldsymbol{u})\boldsymbol{\tau} - \boldsymbol{\tau}(\nabla \boldsymbol{u})^\top$	upper convected derivative
$v_{\boldsymbol{n}} = \boldsymbol{v} \cdot \boldsymbol{n}$	normal component of $\boldsymbol{v}$
$\boldsymbol{v_t} = \boldsymbol{v} - v_{\boldsymbol{n}}\boldsymbol{n}$	tangential component of $\boldsymbol{v}$
$\tau_{\boldsymbol{nn}} = (\boldsymbol{\tau n}) \cdot \boldsymbol{n}$	normal component of $\boldsymbol{\tau n}$
$\boldsymbol{\tau_{nt}} = \boldsymbol{\tau n} - \tau_{\boldsymbol{nn}}\boldsymbol{n}$	tangential component of $\boldsymbol{\tau n}$
$\boldsymbol{I}$	identity tensor
$\lfloor x \rceil = \lfloor x + 1/2 \rfloor$	nearest integer to x
$[\![a, b]\!] = [a, b] \cap \mathbb{N}$	integer interval where $a \leqslant b$ are two integers
$\mathcal{P}_k$	set of polynomial functions of degree at most k
∇_h	broken gradient
q_{ext}	external trace of q
$[\![q]\!] = q - q_{\text{ext}}$	jump of q across the associated face
$\{\!\{q\}\!\} = \frac{1}{2}(q + q_{\text{ext}})$	average of q on the associated face

Numerical parameters

Notation	Description	Num. exp.
t_f	final time	20/3
$\xi = \ln h$	log-height	-
$n_{\max}$	number of time iterations	5000
$\Delta t^{(n)}$	$(n+1)^{\text{th}}$ time step	-
$\Delta t_{\text{init}} = t_f / n_{\max}$	canonical time step	-
Δt_{ref}	reference time step	-
Δt_0	a possible initial time step	10^{-7}
$n^\star$	number of adaptations of the time step	-
κ	parameter used for the purpose of the aforementioned adaptation	1.1
$\mathcal{T}_h$	finite element mesh	-
N	number of elements in the mesh $\mathcal{T}_h$	1000
$\mathscr{S}_h^{(i)}$	set of internal faces of the mesh $\mathcal{T}_h$	-
ε_h	lower bound for h when computing the initial velocity	10^{-2}
ε_r	regularization parameter of the boundary condition on the obstacle	10^{-7}
δ	error tolerance used as stopping criterion for the fixed-point loop	10^{-5}
$k_{\max}$	number of iterations in the aforementioned loop	100

Introduction

Epithelia are tissues, i.e. clusters of similar cells, made up of cells juxtaposed by so-called cell junctions. For example, they cover the walls of the digestive tract or the pulmonary alveoli. Generally speaking, epithelial tissues are involved in many biological processes, whether it is embryonic development, tumor proliferation or wound healing. This intervention will result in a flow of tissue, a phenomenon more commonly known as collective cell migration and illustrated in Figure 0.1.

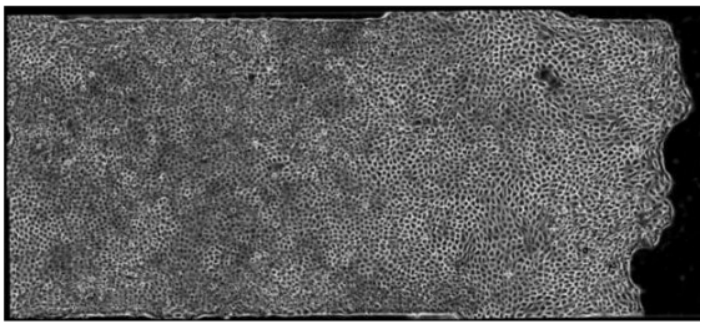

Figure 0.1: Epithelium is seen from above and cells are migrating from left to right. Extracted from Tlili et al. [2018b, Supporting Movie S1].

Here we are faced with an active material that is at the origin of complex dynamics. The tissue can undergo large deformations and the cells do not necessarily remain attached to their neighbors. In particular, the following effects will be observed:

- friction: the cells slide against the substrate on which they evolve;
- elasticity: the cells are not rigid and can stretch;
- and viscosity: the cells slide against each other, slowing down any movement.

All these characteristics, present on a microscopic scale, make the epithelium a material that can be described on a macroscopic scale as a viscoelastic fluid. A more complete description would also take into account the ability of the cells to exert a force on the substrate on their own in order to migrate, known as the active force. Finally, the cells are capable of adopting a privileged direction, or polarity, which will condition their movements, the forces they exert, the stresses they undergo, etc. The observed movement is then collective: the cells interact with each other, they exchange various mechanical constraints and their polarities tend to align with those of their neighbors. A summary is shown in Figure 0.2.

This coupling between viscoelastic fluid mechanics and polarity is very rich, especially from the point of view that interests us here: continuous mathematical and numerical modelling. Together with the work of biophysicists, the project in which this internship is part could lead to a better understanding of the phenomenon presented here. Tlili et al. [2018b] and Tlili et al. [2018a] have carried out experiments highlighting these phenomena of migration and polarity and have designed them with a view to what this report intends to begin to lead to: the mathematical modelling of collective epithelial migration and the numerical resolution of the resulting problem.

We will start in section 1 by setting up a first model, formulated by a system of partial differential equations, decoupled from any polarity, whose mathematical writing is still an

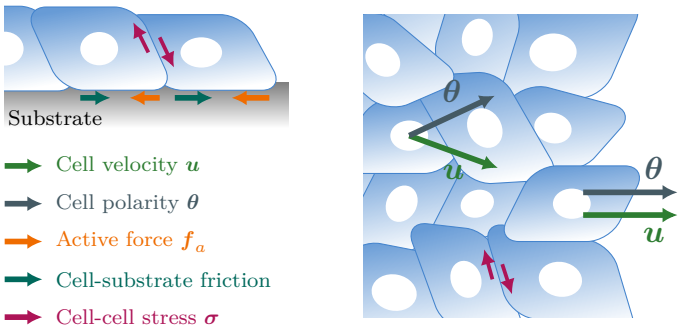

Figure 0.2: Forces and interactions of migrating cells. This figure was inspired by Alert and Trepat [2020, Figure 2].

open question. The thin-layer structure of the considered medium will allow an asymptotic expansion, a process that will transform the initial system into a simpler approximated system. Bouchut and Boyaval [2013] were the first to apply this method for viscoelastic fluids. They did it for turbulent flows where inertial forces are preponderant while we will do it for laminar flows where viscous forces are more important. In section 2, we will propose a numerical resolution algorithm for the very special case where elasticity is neglected and leave the other case for perspective. In particular, we will use a discontinuous Galerkin method to handle transport terms involving constant functions in pieces. The method developed in this report has been implemented in `C++` using the Rheolef (Saramito [2020]) `C++` finite element library. Finally, in section 3, we will present the results obtained and will then be able to compare them with the database developed in the two papers cited in the previous paragraph. In particular, we will try to highlight the limits of the model and the perspectives that are available to us.

1 Mathematical modelling of collective epithelial migration and asymptotic expansion

1.1 Introduction

As announced in the introduction, we choose to continuously model the collective behavior of epithelia on a macroscopic scale. The aggregate of cells is then represented by a viscoelastic fluid. This type of fluid is already well studied and we will therefore be able to use the tools of continuum mechanics to describe its behavior mathematically.

Like any fluid, ours is governed by well-known principles such as the laws of conservation. We are particularly interested in the conservation laws of mass and linear momentum[1]. That should bring us to our first two equations. However, a viscoelastic fluid has its own characteristics that must be exhibited by means of laws of mechanical behavior, called constitutive equations, of which there will be two. Finally, the boundary and initial conditions will completely close the system.

Before we begin, let us first introduce some notations that we will use throughout this document. The tissue geometry, or flow domain, $\Lambda(t) \subset \mathbb{R}^3$ is an open bounded subset of the three-dimensional physical space, depending on time $t \in \mathbb{R}_+$; the initial set $\Lambda(0)$ is assumed to be known. The domain has an evolving free surface $\Gamma_f(t)$ over time on its upper part and an horizontal plane substrate Γ_0 on its lower part on which cells are moving. Eventually, vertical obstacles and domain limits, represented by Γ, lead to very general and thus possibly complex geometries. Figure 1.1 shows an example of such a domain.

To characterize the cell flow, we will use the Eulerian description. The framework that the latter offers automatically places the velocity as unknown in the equations. The velocity field[2], namely a real vector with three components is denoted by $\boldsymbol{u} = (u_x, u_y, u_z)$. The fluid density $\rho > 0$ is supposed to be constant on $\Lambda(t)$, at any time $t \geqslant 0$. The last variable we will use to fully set our model up is the height of the tissue, a real scalar field denoted by h. Both of them are assumed to be sufficiently smooth so that each invoked calculus result can be applied.

1.2 Conservation laws

Let $t \geqslant 0$ and $\omega \subset \Lambda(t)$ be an open connected elementary volume, strictly interior to the flow domain. Let us introduce the characteristic curve $\boldsymbol{X}(t, \boldsymbol{x}; \cdot)$ passing through position $\boldsymbol{x} \in \Lambda(t)$[3]. Then, let $\omega(t) = \boldsymbol{X}(0, \omega; t)$ be the set of positions at time t of particles which were initially in ω[4]. In other words, we follow in its movement an elementary volume transported by the velocity field $\boldsymbol{u}$.

[1] See Germain and Muller [1995, First part, III], Saramito [2016, Chapter 1] and Maitre [2010, Section 3] for more details.

[2] Here, a field is a function of $(t, \boldsymbol{x}) \in \mathbb{R}_+ \times \Lambda(t)$, which are the Eulerian variables.

[3] See appendix A.0.1 for a definition.

[4] I borrowed this notation in Maitre [2010, Section 2].

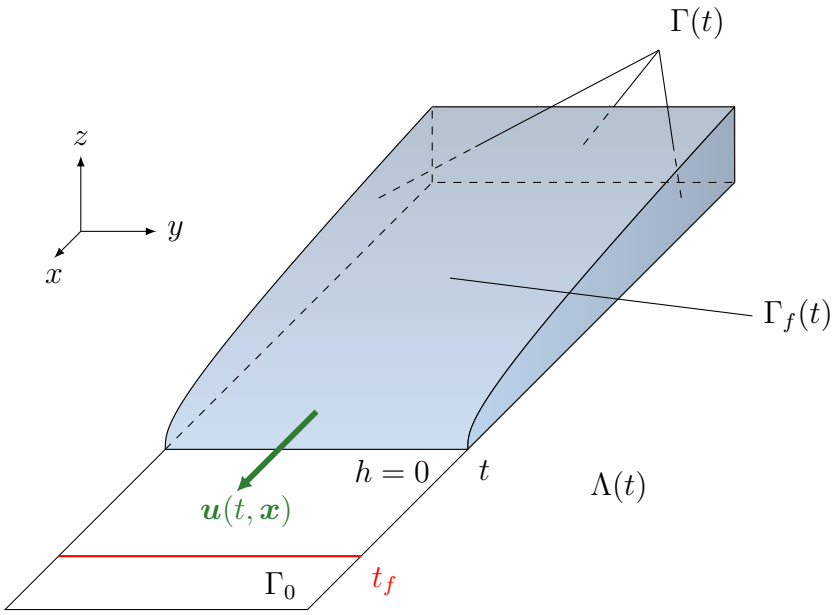

Figure 1.1: Simplest possible geometry of the tissue domain.

1.2.1 Conservation of mass

The postulate is as follows: the mass $\int_{\omega(t)} \rho \, \mathrm{d}\boldsymbol{x}$ of the fluid is conserved in time inside $\omega(t)$. Mathematically, since ρ is constant, we have

$$\forall t \geqslant 0, \quad \frac{\mathrm{d}}{\mathrm{d}t} \int_{\omega(t)} \rho \, \mathrm{d}\boldsymbol{x} = \rho \frac{\mathrm{d}\,|\omega|}{\mathrm{d}t}(t) = 0 \tag{1.2.1}$$

where $|\omega(t)|$ is the Lebesgue measure of $\omega(t)$. Thanks to Reynolds formula (B.0.2) and by arguments of density, or by what is referred to as the fundamental lemma of continuum mechanics, we can rewrite this law of conservation in local form:

$$\operatorname{div} \boldsymbol{u} = 0 \quad \text{in } \mathbb{R}_+ \times \Lambda(t) \tag{1.2.2}$$

Remark. Whenever ρ is constant, we say the flow is incompressible. Thus, the latter equation only describes this property.

1.2.2 Conservation of linear momentum

The postulate is as follows: in any inertial frame of reference, the time derivative of the linear momentum $\int_{\omega(t)} \rho \boldsymbol{u}(t, \boldsymbol{x}) \, \mathrm{d}\boldsymbol{x}$ of $\omega(t)$ is equal to the sum of the forces applied to it. Actually, it is nothing but the Newton's second law of motion applied to an elementary volume of a fluid. On one side are the volume forces, on the other side are the surface forces. In our case, we assume that only the latter apply to our elementary volume. The density of surface forces, of the form $\boldsymbol{\sigma n}$, where $\boldsymbol{\sigma}$ is the (symmetric) Cauchy stress tensor and $\boldsymbol{n}$ is the outer unit normal vector to the boundary $\partial\omega(t)$ at position $\boldsymbol{x}$, reflects local contact actions at the interface of $\omega(t)$. Mathematically, since ρ is constant, we have

$$\forall t \geqslant 0, \quad \frac{\mathrm{d}}{\mathrm{d}t} \int_{\omega(t)} \rho \boldsymbol{u}(t, \boldsymbol{x}) \, \mathrm{d}\boldsymbol{x} = \int_{\partial\omega(t)} \boldsymbol{\sigma}(t, \boldsymbol{x}) \boldsymbol{n}(t, \boldsymbol{x}) \, \mathrm{d}s \tag{1.2.3}$$

Again, thanks to Reynolds transport formula (B.0.3) and by the fundamental lemma of continuum mechanics, we can rewrite this law of conservation in local form:

$$\rho(\partial_t \boldsymbol{u} + (\boldsymbol{u}\cdot\nabla)\boldsymbol{u}) - \mathbf{div}\,\boldsymbol{\sigma} = \mathbf{0} \quad \text{in } \mathbb{R}_+ \times \Lambda(t) \tag{1.2.4}$$

Remark. This principle applies more generally to a screw, a pair formed by the linear and angular momentum.

1.3 Constitutive equations

On a microscopic scale, a tissue is an aggregate of cells assumed to be an elastic material. On a macroscopic scale, the cell-cell friction is described by a viscous mechanism and the tissue could be represented as a continuum by a viscoelastic fluid model. The latter is characterized by an elastic stress tensor $\boldsymbol{\tau}$ satisfying the following partial differential equation:

$$\lambda D_t \boldsymbol{\tau} + \boldsymbol{\tau} = 2\eta_m \boldsymbol{D}(\boldsymbol{u}) \quad \text{in } \mathbb{R}_+ \times \Lambda(t) \tag{1.3.1}$$

where $D_t = \partial_t + (\boldsymbol{u}\cdot\nabla)$ is the so-called Lagrangian or particle derivative – it represents the time derivative in the Eulerian description – and

$$\boldsymbol{D}(\boldsymbol{u}) = \frac{1}{2}\left(\nabla\boldsymbol{u} + \nabla\boldsymbol{u}^\top\right) \tag{1.3.2}$$

is the rate of deformation. It is a symmetric tensor. $\lambda = \eta_m/\mu$ is the relaxation time. It is the time it takes for the material to return to its equilibrium configuration when it is no longer under stress. η_m is the viscosity of the material. It quantifies the frictional forces between polymers and solvent molecules. Finally, μ is the elastic modulus of the material. It is a quantity that reflects the elastic deformation of the material subjected to certain stresses.

Unfortunately, the Lagrangian derivative is not an *objective tensor derivative*[5]: it depends on the frame of reference. Even though the latter is in translation or rotation, the intrinsic properties of the material must not change. A widely used solution is to replace the particle derivation D_t with the *upper convected* or *covariant* derivative, denoted by $\overset{\nabla}{\cdot}$ and defined for any sufficiently regular symmetric tensor τ by

$$\overset{\nabla}{\boldsymbol{\tau}} = \partial_t \boldsymbol{\tau} + (\boldsymbol{u}\cdot\nabla)\boldsymbol{\tau} - (\nabla\boldsymbol{u})\boldsymbol{\tau} - \boldsymbol{\tau}(\nabla\boldsymbol{u})^\top \tag{1.3.3}$$

As a consequence, the constitutive (1.3.1) becomes

$$\lambda \overset{\nabla}{\boldsymbol{\tau}} + \boldsymbol{\tau} = 2\eta_m \boldsymbol{D}(\boldsymbol{u}) \quad \text{in } \mathbb{R}_+ \times \Lambda(t) \tag{1.3.4}$$

The Cauchy stress tensor $\boldsymbol{\sigma}$ must depend on the rate of deformation; this is what mathematically differentiates a fluid from any other continuum medium. In the case of viscoelastic fluids, a possible relation is

$$\boldsymbol{\sigma} = \boldsymbol{\tau} + 2\eta_s \boldsymbol{D}(\boldsymbol{u}) - p\boldsymbol{I} \quad \text{in } \mathbb{R}_+ \times \Lambda(t) \tag{1.3.5}$$

where p is the pressure, η_s is the viscosity of the solvent and $\boldsymbol{I}$ is the identity tensor.

[5] See [Saramito, 2016, Chapter 4] for more details.

1.4 Boundary conditions

Let Ω be the plane on which the substrate rests, in such a way that, for every $t \in \mathbb{R}_+$, we have

$$\begin{aligned}\Lambda(t) &= \Omega \times \{z \in [0, h(t,x,y)],\ (x,y) \in \Omega\} \\ \Gamma_f(t) &= \Omega \times \{h(t,x,y),\ (x,y) \in \Omega\} \\ \Gamma &= \partial\Omega \times I_z \\ \Gamma_0 &= \Omega \times \{0\}\end{aligned}$$

where $I_z \subset \mathbb{R}_+$ is a closed interval such that $h(t,x,y) \in I_z$, for any $(t,(x,y)) \in \mathbb{R}_+ \times \Omega$.

1.4.1 On the free surface

The free surface is the interface between the tissue and the air. At any time $t \geqslant 0$, a point $\boldsymbol{x} = (x,y,z) \in \mathbb{R}^3$ is on the free surface $\Gamma_f(t)$ if

$$h(t,x,y) - z = 0 \tag{1.4.1}$$

The free surface condition states that a point on $\Gamma_f(t)$ at a given time t always remains on it at any other time. By taking the Lagrangian derivative, we end up with the desired boundary condition:

$$\partial_t h + u_x\big|_{z=h}\partial_x h + u_y\big|_{z=h}\partial_y h - u_z\big|_{z=h} = 0 \quad \text{on } \mathbb{R}_+ \times \Omega \tag{1.4.2}$$

In addition, there is no stress, or density of surface forces, at the air-cell interface:

$$\boldsymbol{\sigma n} = 0 \quad \text{on } \mathbb{R}_+ \times \Gamma_f(t) \tag{1.4.3}$$

where, in this particular case,

$$\boldsymbol{n} = \frac{(-\partial_x h, -\partial_y h, 1)}{\sqrt{(\partial_x h)^2 + (\partial_y h)^2 + 1}} \tag{1.4.4}$$

1.4.2 On the substrate

Since the substrate Γ_0 is a stationary wall through which the fluid cannot flow, we must impose a *no-penetration* condition. Mathematically, this consists of writing that the normal component of velocity is zero:

$$u_{\boldsymbol{n}} = \boldsymbol{u} \cdot \boldsymbol{n} = 0 \quad \text{on } \mathbb{R}_+ \times \Gamma_0 \tag{1.4.5}$$

where, in this particular case, $\boldsymbol{n} = (0,0,-1)$.

On the substrate, cells are subjected to three external forces, all tangential to Γ_0:

- the viscous frictional force, which in our case of laminar flow, i.e. low velocity flow, is written $-\zeta \boldsymbol{u_t}$, where $\zeta > 0$ is the friction coefficient;
- the tangential part of the density of surface forces, which is written $\boldsymbol{\sigma_{nt}}$;
- the active force $\boldsymbol{f}_a$, mentioned in the introduction, for which a mathematical expression has yet to be found.

where $\boldsymbol{u_t}$ and $\boldsymbol{\sigma_{nt}}$ are the tangential components of $\boldsymbol{u}$ and $\boldsymbol{\sigma n}$ respectively, namely

$$\boldsymbol{u_t} = \boldsymbol{u} - u_{\boldsymbol{n}}\boldsymbol{n} \tag{1.4.6}$$

$$\boldsymbol{\sigma_{nt}} = \boldsymbol{\sigma n} - \sigma_{\boldsymbol{nn}}\boldsymbol{n} \tag{1.4.7}$$

$\sigma_{\boldsymbol{nn}} = (\boldsymbol{\sigma n}) \cdot \boldsymbol{n}$ being the normal component of $\boldsymbol{\sigma n}$. The state of equilibrium of the solid on the substrate is then translated, by invoking Newton's first law of motion, by the following relation:

$$\boldsymbol{\sigma_{nt}} - \zeta \boldsymbol{u_t} + \boldsymbol{f}_a = \boldsymbol{0} \quad \text{on } \mathbb{R}_+ \times \Gamma_0 \tag{1.4.8}$$

In order to set up numerical experiments, we propose below a possible form of the active force:

$$\boldsymbol{f}_a = -\gamma\, h^{-1} \cdot \nabla h\, \mathbb{1}_{\Omega_c(t)} \tag{1.4.9}$$

The term h^{-1} reflects the (assumed) inverse proportionality relation between the height and the active force. This corresponds to the intuitive idea of active force: if a cell has a constant volume, the smaller its height, the larger the contact surface of the cell with the substrate and, therefore, the greater the force it can exert on the substrate. $\gamma > 0$ is a supposed physical coefficient. Then, $\Omega_c(t) = h(t,\cdot)^{-1}([h_c, +\infty[) = \{(x,y) \in \Omega \mid h(t,x,y) \geqslant h_c\} \subset \Omega$ represents the tissue domain. Actually, we assume that the cells cannot spread out indefinitely (the height cannot tend towards 0), so there is a height, called critical height and noted h_c, below which the tissue cannot sink. Finally, the term $-\nabla h$ gives the overall direction of the active force, it is the outer (non-unitary) normal to the front in the plane. The reason we have not taken a normalized version is that the current form allows the active force to be rewritten in a different way, opening up the possibility of other proposals involving, in this case, tensors:

$$\boldsymbol{f}_a = -\gamma\, \mathbf{div}(\ln(h)\boldsymbol{I})\, \mathbb{1}_{\Omega_c(t)} \tag{1.4.10}$$

We discuss this choice in subsubsection 3.3.4.

1.4.3 On obstacles and domain limits

For the same reasons as in subsubsection 1.4.2, the condition

$$u_{\boldsymbol{n}} = \boldsymbol{u} \cdot \boldsymbol{n} = 0 \quad \text{on } \mathbb{R}_+ \times \Gamma \tag{1.4.11}$$

has to be satisfied. When the domain exhibits a curved boundary, which is true in our case with an obstacle, it is necessary to separate the boundary into two disjoint parts Γ_{wall} and Γ_{obstacle}, so that their union is exactly Γ. According to Saramito [2020, section 2.3], we regularize the previous Dirichlet no-penetration condition on the curved boundary domain as follows:

$$\sigma_{\boldsymbol{nn}} + \varepsilon_r^{-1} \boldsymbol{u} \cdot \boldsymbol{n} = 0 \quad \text{on } \mathbb{R}_+ \times \Gamma_{\text{obstacle}} \tag{1.4.12}$$

where $\varepsilon_r > 0$ is the regularization parameter.

In all cases, a no-grip condition complements the previous one:

$$\boldsymbol{\sigma_{nt}} = \boldsymbol{0} \quad \text{on } \mathbb{R}_+ \times \Gamma \tag{1.4.13}$$

Note that we did not introduce any friction coefficient here, unlike what we had for the substrate. In practice, there is no vertical material barrier, only a chemical process prevents the cells from venturing outside the predefined area.

1.5 Asymptotic expansion

By combining equations (1.2.2), (1.2.4), (1.3.4), (1.3.5), (1.4.2), (1.4.3), (1.4.5), (1.4.8), (1.4.11) and (1.4.13), we end up with the following coupled system of evolutionary equations:

(P): Find $\boldsymbol{\tau}$ and $\boldsymbol{u}$ defined in $]0,t_f[\times\Lambda(t)$ and h defined in $]0,t_f[\times\Gamma_0$ such that

$$\begin{cases} \rho\left(\partial_t \boldsymbol{u} + (\boldsymbol{u}\cdot\nabla)\boldsymbol{u}\right) - \mathbf{div}\,\boldsymbol{\sigma} = \mathbf{0} & \text{in }]0,t_f[\times\Lambda(t) \quad (1.5.1a)\\ -\mathrm{div}\,\boldsymbol{u} = 0 & \text{in }]0,t_f[\times\Lambda(t) \quad (1.5.1b)\\ \boldsymbol{\sigma} = \boldsymbol{\tau} + 2\eta_s\,\boldsymbol{D}(\boldsymbol{u}) - p\mathbf{I} & \text{in }]0,t_f[\times\Lambda(t) \quad (1.5.1c)\\ \lambda\overset{\nabla}{\boldsymbol{\tau}} + \boldsymbol{\tau} - 2\eta_m\,\boldsymbol{D}(\boldsymbol{u}) = \mathbf{0} & \text{in }]0,t_f[\times\Lambda(t) \quad (1.5.1d)\\ \partial_t h + u_x\partial_x h + u_y\partial_y h - u_z = 0 \text{ and } \boldsymbol{\sigma}\boldsymbol{n} = \mathbf{0} & \text{on }]0,t_f[\times\Gamma_f(t) \quad (1.5.1e)\\ \boldsymbol{u}\cdot\boldsymbol{n} = 0 \text{ and } \boldsymbol{\sigma}_{\boldsymbol{nt}} - \zeta\boldsymbol{u}_{\boldsymbol{t}} + \boldsymbol{f}_a = \mathbf{0} & \text{on }]0,t_f[\times\Gamma_0 \quad (1.5.1f)\\ \boldsymbol{u}\cdot\boldsymbol{n} = 0 \text{ and } \boldsymbol{\sigma}_{\boldsymbol{nt}} = \mathbf{0} & \text{on }]0,t_f[\times\Gamma \quad (1.5.1g)\\ h(0,\cdot) = h_0 & \text{on } \Gamma_0 \quad (1.5.1h)\\ \boldsymbol{u}(0,\cdot) = \boldsymbol{u}_0 \text{ and } \boldsymbol{\tau}(0,\cdot) = \boldsymbol{\tau}_0 & \text{in } \Lambda(0) \quad (1.5.1i) \end{cases}$$

where $\boldsymbol{u}_0$, $\boldsymbol{\tau}_0$ and h_0 are the initial conditions and t_f is the final time.

1.5.1 Thin-layer approximation

As it stands, the model cannot be expected to be solved numerically in a reasonable time. The idea would therefore be to perform a thin-layer approximation (the height is very small compared to the length of the substrate) to get back to a two-dimensional system in the horizontal plane of the substrate, process known as *asymptotic expansion*. To this end, let us introduce the following notations, before we state the thin-layer approximation as a theorem:

Definitions 1.1. Let $\boldsymbol{x} = (x,y,z) \in \mathbb{R}^3$ be a point, ϕ be a smooth scalar field, $\boldsymbol{v}$ be a smooth vector field and $\boldsymbol{\tau}$ be a smooth symmetric tensor field. We define

- $\boldsymbol{s} = \begin{pmatrix} x \\ y \end{pmatrix}$ the planar components of $\boldsymbol{x}$;
- $\boldsymbol{v_s} = \begin{pmatrix} v_x \\ v_y \end{pmatrix}$ the planar components of $\boldsymbol{v}$;
- $\boldsymbol{\tau_s} = \begin{pmatrix} \tau_{xx} & \tau_{xy} \\ \tau_{xy} & \tau_{yy} \end{pmatrix}$ the planar components of $\boldsymbol{\tau}$, and $\boldsymbol{\tau_{sz}} = \begin{pmatrix} \tau_{xz} \\ \tau_{yz} \end{pmatrix}$;
- $\nabla_{\boldsymbol{s}}\phi = \begin{pmatrix} \partial_x\phi \\ \partial_y\phi \end{pmatrix}$ the planar gradient of ϕ;
- $\nabla_{\boldsymbol{s}}\boldsymbol{v_s} = \begin{pmatrix} \partial_x\boldsymbol{v}_x & \partial_y\boldsymbol{v}_x \\ \partial_x\boldsymbol{v}_y & \partial_y\boldsymbol{v}_y \end{pmatrix}$ the planar gradient of $\boldsymbol{v}$;
- $\mathrm{div}_{\boldsymbol{s}}\boldsymbol{v_s} = \partial_x v_x + \partial_y v_y$ the planar divergence of $\boldsymbol{v}$;
- $\mathbf{div}_{\boldsymbol{s}}\boldsymbol{\tau_s} = \begin{pmatrix} \partial_x\tau_{xx} + \partial_y\tau_{xy} \\ \partial_x\tau_{xy} + \partial_y\tau_{yy} \end{pmatrix}$ the planar divergence of $\boldsymbol{\tau}$;
- $\boldsymbol{D_s}(\boldsymbol{v_s}) = \frac{1}{2}\left(\nabla_{\boldsymbol{s}}\boldsymbol{v_s} + (\nabla_{\boldsymbol{s}}\boldsymbol{v_s})^\top\right)$ the planar rate of deformation of $\boldsymbol{v}$;
- $D_{t,\boldsymbol{s}} = \partial_t + (\boldsymbol{u_s}\cdot\nabla_{\boldsymbol{s}})$ the planar particle derivative;
- $\overset{\nabla_{\boldsymbol{s}}}{\boldsymbol{\tau}_{\boldsymbol{s}}} = D_{t,\boldsymbol{s}}\boldsymbol{\tau_s} - (\nabla_{\boldsymbol{s}}\boldsymbol{u_s})\boldsymbol{\tau_s} - \boldsymbol{\tau_s}(\nabla_{\boldsymbol{s}}\boldsymbol{u_s})^\top$ the planar upper convected derivative of $\boldsymbol{\tau}$.

Theorem 1.1 (Thin-layer approximation)**.** *Let L be the characteristic length, H the characteristic height, U the characteristic planar velocity U, V the characteristic vertical velocity V, $T = L/U = H/V$ the characteristic time and $\Sigma = \eta U/L$ the characteristic stress. Let also $\eta = \eta_m + \eta_s$ be the total viscosity, $Re = \rho UL/\eta$ the Reynolds number, $We = \lambda U/L$ the Weissenberg number, $\alpha = \varepsilon^{-1}\zeta U/\Sigma$, $\beta = \eta_m/\eta$ and $\varepsilon = H/L \ll 1$ the low aspect ratio of the geometry.*

Let us make the following changes of variable, called nondimensionalization*:*

$$\widetilde{\boldsymbol{s}} = \frac{\boldsymbol{s}}{L} \qquad \widetilde{z} = \frac{z}{H} \qquad \widetilde{t} = \frac{t}{T} \qquad \widetilde{\boldsymbol{u}}_{\boldsymbol{s}} = \frac{\boldsymbol{u}_{\boldsymbol{s}}}{U} \qquad \widetilde{u}_z = \frac{u_z}{V}$$
$$\widetilde{h} = \frac{h}{H} \qquad \widetilde{\boldsymbol{\tau}}_{\boldsymbol{s}} = \frac{\boldsymbol{\tau}_{\boldsymbol{s}}}{\Sigma} \qquad \widetilde{\boldsymbol{\tau}}_{\boldsymbol{sz}} = \frac{\boldsymbol{\tau}_{\boldsymbol{sz}}}{\Sigma} \qquad \widetilde{\tau}_{zz} = \frac{\tau_{zz}}{\Sigma} \qquad \widetilde{p} = \frac{p}{\Sigma}$$
$$\widetilde{\boldsymbol{\sigma}}_{\boldsymbol{s}} = \frac{\boldsymbol{\sigma}_{\boldsymbol{s}}}{\Sigma} \qquad \widetilde{\boldsymbol{\sigma}}_{\boldsymbol{sz}} = \frac{\boldsymbol{\sigma}_{\boldsymbol{sz}}}{\Sigma} \qquad \widetilde{\sigma}_{zz} = \frac{\widetilde{\sigma}_{zz}}{\Sigma} \qquad \widetilde{\boldsymbol{f}}_a = \frac{\boldsymbol{f}_a}{\Sigma}$$

As a result, we shall note $\widetilde{\mathcal{X}}$ the associated dimensionless set to $\mathcal{X}$, which is any set involved in the problem.

If we assume that

(i) $\boldsymbol{u}$, $\boldsymbol{\tau}$, $\boldsymbol{\sigma}$, p and $\boldsymbol{f}_a$ are asymptotically expandable, with respect to ε, up to order 1, i.e. we assume there exist smooth fields $\boldsymbol{u}^{(i)}$, $\boldsymbol{\tau}^{(i)}$, $\boldsymbol{\sigma}^{(i)}$, $p^{(i)}$ and $\boldsymbol{f}_a^{(i)}$, $i \in \{0,1\}$, such that

$$\boldsymbol{u} = \boldsymbol{u}^{(0)} + \varepsilon \boldsymbol{u}^{(1)} + \boldsymbol{O}(\varepsilon^2) \qquad \boldsymbol{\tau} = \boldsymbol{\tau}^{(0)} + \varepsilon \boldsymbol{\tau}^{(1)} + \boldsymbol{O}(\varepsilon^2)$$
$$\boldsymbol{\sigma} = \boldsymbol{\sigma}^{(0)} + \varepsilon \boldsymbol{\sigma}^{(1)} + \boldsymbol{O}(\varepsilon^2) \qquad p = p^{(0)} + \varepsilon p^{(1)} + O(\varepsilon^2)$$
$$\boldsymbol{f}_a = \boldsymbol{f}_a^{(0)} + \varepsilon \boldsymbol{f}_a^{(1)} + \boldsymbol{O}(\varepsilon^2);$$

(ii) $\partial_z \widetilde{\boldsymbol{u}}_{\boldsymbol{s}}^{(1)} = \boldsymbol{0}$ on $]0, t_f[\times\Lambda(t)$;

(iii) $\boldsymbol{n} = \begin{pmatrix} \boldsymbol{\nu} & 0 \end{pmatrix}^\top$ (i.e. $n_z = 0$) on $\partial\Omega$, where $\boldsymbol{\nu}$ is the outer unit normal vector to Ω on $\partial\Omega$;

(iv) the flow is laminar, i.e. $Re \ll 1$;

(v) and $\boldsymbol{u}$, $\boldsymbol{\tau}$ and h are solution of the system (1.5.1a)–(1.5.1i)

then the 0^{th} order dimensionless terms satisfy the following coupled system of evolutionary equations:

(P): Find $\overline{\boldsymbol{\tau}}_{\boldsymbol{s}}^{(0)}$, $\overline{\tau}_{zz}^{(0)}$, $\widetilde{\boldsymbol{u}}_{\boldsymbol{s}}^{(0)}$ and $\widetilde{h}$ defined in $]0, t_f[\times\Omega$ such that

$$\begin{cases}
-\mathbf{div}_{\boldsymbol{s}}\left(\widetilde{h}\ \overline{\boldsymbol{\sigma}}_{\boldsymbol{s}}^{(0)}\right) + \alpha \widetilde{\boldsymbol{u}}_{\boldsymbol{s}}^{(0)} - \widetilde{\boldsymbol{f}}_a^{(1)} = \boldsymbol{0} & \text{in }]0, t_f[\times\Omega & \text{(1.5.2a)} \\
\partial_t \widetilde{h} + \mathrm{div}_{\boldsymbol{s}}(\widetilde{h}\widetilde{\boldsymbol{u}}_{\boldsymbol{s}}^{(0)}) = 0 & \text{in }]0, t_f[\times\Omega & \text{(1.5.2b)} \\
\overline{\boldsymbol{\sigma}}_{\boldsymbol{s}}^{(0)} = \left(\overline{\boldsymbol{\tau}}_{\boldsymbol{s}}^{(0)} - \overline{\tau}_{zz}^{(0)}\mathbf{I}\right) + 2(1-\beta)(\boldsymbol{D}_{\boldsymbol{s}}(\widetilde{\boldsymbol{u}}_{\boldsymbol{s}}^{(0)}) + \mathrm{div}_{\boldsymbol{s}}(\widetilde{\boldsymbol{u}}_{\boldsymbol{s}}^{(0)})\mathbf{I}) & \text{in }]0, t_f[\times\Omega & \text{(1.5.2c)} \\
We\ \overset{\widetilde{\nabla}_{\boldsymbol{s}}^{(0)}}{\overline{\boldsymbol{\tau}}_{\boldsymbol{s}}^{(0)}} + \overline{\boldsymbol{\tau}}_{\boldsymbol{s}}^{(0)} - 2\beta\, \boldsymbol{D}_{\boldsymbol{s}}(\widetilde{\boldsymbol{u}}_{\boldsymbol{s}}^{(0)}) = \boldsymbol{0} & \text{in }]0, t_f[\times\Omega & \text{(1.5.2d)} \\
We\left(\widetilde{D}_{t,\boldsymbol{s}}^{(0)}\overline{\tau}_{zz}^{(0)} + 2\mathrm{div}_{\boldsymbol{s}}(\widetilde{\boldsymbol{u}}_{\boldsymbol{s}}^{(0)})\overline{\tau}_{zz}^{(0)}\right) + \overline{\tau}_{zz}^{(0)} + 2\beta \mathrm{div}_{\boldsymbol{s}}\, \widetilde{\boldsymbol{u}}_{\boldsymbol{s}}^{(0)} = 0 & \text{in }]0, t_f[\times\Omega & \text{(1.5.2e)} \\
\widetilde{\boldsymbol{u}}_{\boldsymbol{s}}^{(0)} \cdot \boldsymbol{\nu} = 0 \text{ and } \overline{\boldsymbol{\sigma}}_{\boldsymbol{s},\boldsymbol{\nu t}}^{(0)} = \boldsymbol{0} & \text{on }]0, t_f[\times\partial\Omega & \text{(1.5.2f)} \\
\widetilde{h}(0,\cdot) = \widetilde{h}_0 & \text{in } \Omega & \text{(1.5.2g)} \\
\overline{\boldsymbol{\tau}}_{\boldsymbol{s}}^{(0)}(0,\cdot) = \overline{\boldsymbol{\tau}}_{\boldsymbol{s},0}^{(0)} \text{ and } \overline{\tau}_{zz}^{(0)}(0,\cdot) = \overline{\tau}_{zz,0}^{(0)} & \text{in } \Omega & \text{(1.5.2h)}
\end{cases}$$

where

$$\widetilde{D}^{(0)}_{t,\boldsymbol{s}} = \partial_t + \left(\widetilde{\boldsymbol{u}}^{(0)}_{\boldsymbol{s}} \cdot \nabla_{\boldsymbol{s}}\right) \quad \textit{and} \quad \overset{\widetilde{\nabla}^{(0)}_{\boldsymbol{s}}}{\overline{\boldsymbol{\tau}}^{(0)}_{\boldsymbol{s}}} = \widetilde{D}^{(0)}_{t,\boldsymbol{s}}\overline{\boldsymbol{\tau}}^{(0)}_{\boldsymbol{s}} - (\nabla_{\boldsymbol{s}}\widetilde{\boldsymbol{u}}^{(0)}_{\boldsymbol{s}})\overline{\boldsymbol{\tau}}^{(0)}_{\boldsymbol{s}} - \overline{\boldsymbol{\tau}}^{(0)}_{\boldsymbol{s}}(\nabla_{\boldsymbol{s}}\widetilde{\boldsymbol{u}}^{(0)}_{\boldsymbol{s}})^{\top}$$

are ad hoc notations and

$$\overline{\boldsymbol{\sigma}}^{(0)}_{\boldsymbol{s}} = \frac{1}{\widetilde{h}}\int_0^{\widetilde{h}} \widetilde{\boldsymbol{\sigma}}^{(0)}_{\boldsymbol{s}}\mathrm{d}z, \quad \overline{\boldsymbol{\tau}}^{(0)}_{\boldsymbol{s}} = \frac{1}{\widetilde{h}}\int_0^{\widetilde{h}} \widetilde{\boldsymbol{\tau}}^{(0)}_{\boldsymbol{s}}\mathrm{d}z \quad \textit{and} \quad \overline{\tau}^{(0)}_{zz} = \frac{1}{\widetilde{h}}\int_0^{\widetilde{h}} \widetilde{\tau}^{(0)}_{zz}\mathrm{d}z$$

are depth averages.

Remarks.

1. This model is asymptotic because the smaller ε is, the more accurate it becomes.

2. The 0-th order dimensionless planar velocity is not averaged in depth because it does not depend on $\widetilde{z}$, as shown in the proof (appendix C). It suggests that the cells move as a block, i.e. all the points on a given vertical move at the same velocity. Hypothesis (ii) reinforces this idea. We show that when $\beta \in \{0, 1\}$, the hypothesis is no longer necessary. It is from this observation, and from the physical meaning behind it, that we allow ourselves to assume it.

3. ζ is assumed to be of the same order of magnitude as ε^{-1}, otherwise α could no longer be a physical constant independent of the geometry.

4. It could seem surprising that (1.5.2a) depends on $\widetilde{\boldsymbol{f}}_a^{(1)}$ and not on $\widetilde{\boldsymbol{f}}_a^{(0)}$ – meaning that the latter disappears from the equations. Actually, it is not. In the proof, we show that

$$\widetilde{\boldsymbol{f}}_a^{(0)} = \boldsymbol{0}$$

   which means that $\widetilde{\boldsymbol{f}}_a = \boldsymbol{O}(\varepsilon)$. This here that the hypotheses we made on the friction coefficient ζ and on the characteristic stresses come into play. If we had rather decided that ζ is not of the same order of magnitude as ε, then we would have $\alpha = \zeta U/\Sigma$ and the conservation law (1.5.2a) would have read

$$-\mathbf{div}_{\boldsymbol{s}}\left(\widetilde{h}\ \overline{\boldsymbol{\sigma}}^{(0)}_{\boldsymbol{s}}\right) + \alpha\widetilde{\boldsymbol{u}}^{(1)}_{\boldsymbol{s}} - \widetilde{\boldsymbol{f}}_a^{(1)} = \boldsymbol{0}$$

   We would still have the first-order term of the active force but the friction force wouldn't have to do with the zero-order term of the velocity, but it would have to do with its first-order term. The new coupled system of evolutionary equations would then contain both $\widetilde{\boldsymbol{u}}^{(0)}_{\boldsymbol{s}}$ and $\widetilde{\boldsymbol{u}}^{(1)}_{\boldsymbol{s}}$, which are unknowns. Therefore, it would complicate the resolution of the system too much. On the contrary, if we had wanted to make appear the zero-order term of the active force, we would have make for instance the following hypothesis:

$$\boldsymbol{f}_a = F\widetilde{\boldsymbol{f}}_a$$

   where the characteristic stress F is of the same order of magnitude as ε, and we would have to assume that $\widetilde{\boldsymbol{f}}_a = \boldsymbol{O}(\varepsilon)$, unlike the previous case where this fact is deduced from the assumptions already in place and from the equations. It is difficult to affirm that one hypothesis is better than the other, especially when the result is the same in all cases.

5. With hypothesis (iv), we do not need the initial condition for the velocity anymore: it should be possible to determine $\widetilde{\boldsymbol{u}}_{\boldsymbol{s}}^{(0)}$ entirely from the equations.

6. Whenever $\beta = 1$, we show that
$$\tau_{zz}^{(0)} = p^{(0)}$$

Idea of proof, complete proof in appendix C. The proof was made for the first time in Chakraborty [2019]. We have added in our version the asymptotic expansion of the boundary conditions on Γ. The proof consists mainly in four steps. Since we would like to reduce our point of view to the plane of the substrate, we will first distinguish the roles of the planar and vertical components (subsection C.1). Then, we will nondimensionalize the obtained equations so that the dependencies on physical parameters are simplified (subsection C.2). The core idea of asymptotic expansion is to approximate the variables of the problem with respect to ε in order to only keep the more significant ones (typically the order 0 terms and the first-order terms). This key step (subsection C.3) allows to make appear the new form of the system. Finally, by combining the obtained equations together, we are able, in a sense, to project the result onto the $(0, x, y)$-plane, by integrating in the depth (i.e. with respect to the variable z) of the three-dimensional domain $\Lambda(t)$ (subsection C.4). The complete proof is not presented here – it is way too long! refer to appendix C if you are interested Rather, we prefer to give an idea of the main steps by focusing on a specific equation: the conservation of linear momentum.

Splitting planar and vertical components By simple identification, we have in $]0, t_f[\times\Lambda(t)$

$$\rho\left(\partial_t \boldsymbol{u}_{\boldsymbol{s}} + (\boldsymbol{u}_{\boldsymbol{s}}\cdot\nabla_s)\boldsymbol{u}_{\boldsymbol{s}}\right) - \mathbf{div}_s(\boldsymbol{\sigma}_{\boldsymbol{s}}) - \partial_z \boldsymbol{\sigma}_{\boldsymbol{sz}} = \mathbf{0} \tag{1.5.3a}$$
$$\rho\left(\partial_t u_z + (\boldsymbol{u}_{\boldsymbol{s}}\cdot\nabla_s)u_z\right) - \mathrm{div}_s(\boldsymbol{\sigma}_{\boldsymbol{sz}}) - \partial_z \sigma_{zz} = 0 \tag{1.5.3b}$$

Dimensional Analysis By applying the changes of variable, the previous equations become

$$\rho\left(\frac{U}{T}\partial_t \widetilde{\boldsymbol{u}}_{\boldsymbol{s}} + \frac{U^2}{L}(\widetilde{\boldsymbol{u}}_{\boldsymbol{s}}\cdot\nabla_s)\widetilde{\boldsymbol{u}}_{\boldsymbol{s}} + \frac{VU}{H}\widetilde{u}_z\partial_z\widetilde{\boldsymbol{u}}_{\boldsymbol{s}}\right) - \frac{\Sigma}{L}\mathbf{div}_s(\widetilde{\boldsymbol{\sigma}}_{\boldsymbol{s}}) - \frac{\Sigma}{H}\partial_z\widetilde{\boldsymbol{\sigma}}_{\boldsymbol{sz}} = \mathbf{0}$$
$$\rho\left(\frac{V}{T}\partial_t \widetilde{u}_z + \frac{UV}{L}(\widetilde{\boldsymbol{u}}_{\boldsymbol{s}}\cdot\nabla_s)\widetilde{u}_z + \frac{V^2}{H}\widetilde{u}_z\partial_z\widetilde{u}_z\right) - \frac{\Sigma}{L}\mathrm{div}_s(\widetilde{\boldsymbol{\sigma}}_{\boldsymbol{sz}}) - \frac{\Sigma}{H}\partial_z\widetilde{\sigma}_{zz} = 0$$

in $]0, \widetilde{t}_f[\times\widetilde{\Lambda}(t)$.

By expressing everything in terms of U, L, ε and η, we end up with

$$\rho\left(\frac{U^2}{L}\partial_t \widetilde{\boldsymbol{u}}_{\boldsymbol{s}} + \frac{U^2}{L}(\widetilde{\boldsymbol{u}}_{\boldsymbol{s}}\cdot\nabla_s)\widetilde{\boldsymbol{u}}_{\boldsymbol{s}} + \frac{U^2}{L}\widetilde{u}_z\partial_z\widetilde{\boldsymbol{u}}_{\boldsymbol{s}}\right) - \frac{\eta U}{L^2}\mathbf{div}_s(\widetilde{\boldsymbol{\sigma}}_{\boldsymbol{s}}) - \frac{\eta U}{\varepsilon L^2}\partial_z\widetilde{\boldsymbol{\sigma}}_{\boldsymbol{sz}} = \mathbf{0}$$
$$\rho\left(\frac{\varepsilon U^2}{L}\partial_t \widetilde{u}_z + \frac{\varepsilon U^2}{L}(\widetilde{\boldsymbol{u}}_{\boldsymbol{s}}\cdot\nabla_s)\widetilde{u}_z + \frac{\varepsilon U^2}{L}\widetilde{u}_z\partial_z\widetilde{u}_z\right) - \frac{\eta U}{L^2}\mathrm{div}_s(\widetilde{\boldsymbol{\sigma}}_{\boldsymbol{sz}}) - \frac{\eta U}{\varepsilon L^2}\partial_z\widetilde{\sigma}_{zz} = 0$$

By multiplying both sides in each equation by $\varepsilon\frac{L^2}{U\eta}$, we finally get

$$\varepsilon Re\left(\partial_t \widetilde{\boldsymbol{u}}_{\boldsymbol{s}} + (\widetilde{\boldsymbol{u}}_{\boldsymbol{s}}\cdot\nabla_s)\widetilde{\boldsymbol{u}}_{\boldsymbol{s}} + \widetilde{u}_z\partial_z\widetilde{\boldsymbol{u}}_{\boldsymbol{s}}\right) - \varepsilon\mathbf{div}_s(\widetilde{\boldsymbol{\sigma}}_{\boldsymbol{s}}) - \partial_z\widetilde{\boldsymbol{\sigma}}_{\boldsymbol{sz}} = \mathbf{0} \tag{1.5.4a}$$
$$\varepsilon^2 Re\left(\partial_t \widetilde{u}_z + (\widetilde{\boldsymbol{u}}_{\boldsymbol{s}}\cdot\nabla_s)\widetilde{u}_z + \widetilde{u}_z\partial_z\widetilde{u}_z\right) - \varepsilon\mathrm{div}_s(\widetilde{\boldsymbol{\sigma}}_{\boldsymbol{sz}}) - \partial_z\widetilde{\sigma}_{zz} = 0 \tag{1.5.4b}$$

Asymptotic expansion By using hypothesis (i) and the linearity of the differential operators, by remarking that any differential operator in time or space applied on a $O(\varepsilon^2)$ remains a $O(\varepsilon^2)$ and by considering the previous equality as a polynomial equality in ε, we obtain the following system of equations, valid in $]0,\widetilde{t}_f[\times\widetilde{\Lambda}(t)$:

$$\partial_z \widetilde{\boldsymbol{\sigma}}_{sz}^{(0)} = \mathbf{0} \tag{1.5.5a}$$

$$Re\left(\partial_t \widetilde{\boldsymbol{u}}_s^{(0)} + (\widetilde{\boldsymbol{u}}_s^{(0)} \cdot \nabla_s)\widetilde{\boldsymbol{u}}_s^{(0)} + \widetilde{u}_z^{(0)}\partial_z \widetilde{\boldsymbol{u}}_s^{(0)}\right) - \mathbf{div}_s(\widetilde{\boldsymbol{\sigma}}_s^{(0)}) - \partial_z \widetilde{\boldsymbol{\sigma}}_{sz}^{(1)} = \mathbf{0} \tag{1.5.5b}$$

$$\partial_z \widetilde{\sigma}_{zz}^{(0)} = 0 \tag{1.5.5c}$$

$$\mathrm{div}_s\left(\widetilde{\boldsymbol{\sigma}}_{sz}^{(0)}\right) + \partial_z \widetilde{\sigma}_{zz}^{(1)} = 0 \tag{1.5.5d}$$

Reduction In $]0,\widetilde{t}_f[\times\widetilde{\Omega}$, by injecting the independence of $\widetilde{\boldsymbol{u}}_s^{(0)}$ from $\widetilde{z}$ into the momentum conservation law (1.5.5b), we get by integrating over $[0,\widetilde{h}]$

$$Re\int_0^{\widetilde{h}}\left(\partial_t \widetilde{\boldsymbol{u}}_s^{(0)} + (\widetilde{\boldsymbol{u}}_s^{(0)} \cdot \nabla_s)\widetilde{\boldsymbol{u}}_s^{(0)}\right)\mathrm{d}z + Re\int_0^{\widetilde{h}} u_z^{(0)}\underbrace{\partial_z \widetilde{\boldsymbol{u}}_s^{(0)}}_{\to 0}\mathrm{d}z - \int_0^{\widetilde{h}} \mathbf{div}_s(\widetilde{\boldsymbol{\sigma}}_s^{(0)})\mathrm{d}z - \int_0^{\widetilde{h}} \partial_z \widetilde{\boldsymbol{\sigma}}_{sz}^{(1)}\mathrm{d}z = \mathbf{0}$$

$$\widetilde{h}Re\left(\partial_t \widetilde{\boldsymbol{u}}_s^{(0)} + (\widetilde{\boldsymbol{u}}_s^{(0)} \cdot \nabla_s)\widetilde{\boldsymbol{u}}_s^{(0)}\right) - \mathbf{div}_s\int_0^{\widetilde{h}} \widetilde{\boldsymbol{\sigma}}_s^{(0)}\mathrm{d}z + \widetilde{\boldsymbol{\sigma}}_s^{(0)}\big|_{z=\widetilde{h}}\nabla_s\widetilde{h} - \left[\widetilde{\boldsymbol{\sigma}}_{sz}^{(1)}\right]_{z=0}^{z=\widetilde{h}} = \mathbf{0}$$

$$\widetilde{h}Re\left(\partial_t \widetilde{\boldsymbol{u}}_s^{(0)} + (\widetilde{\boldsymbol{u}}_s^{(0)} \cdot \nabla_s)\widetilde{\boldsymbol{u}}_s^{(0)}\right) - \mathbf{div}_s\int_0^{\widetilde{h}} \widetilde{\boldsymbol{\sigma}}_s^{(0)}\mathrm{d}z + \widetilde{\boldsymbol{\sigma}}_s^{(0)}\big|_{z=\widetilde{h}}\nabla_s\widetilde{h} - \widetilde{\boldsymbol{\sigma}}_{sz}^{(1)}\big|_{z=\widetilde{h}} + \widetilde{\boldsymbol{\sigma}}_{sz}^{(1)}\big|_{z=0} = \mathbf{0}$$

where to pass from the first line to the the second one we used the Leibniz's Integral Rule (B.0.9) from corollary B.2.3. In the complete proof, we show with the same three first steps that the following boundary conditions hold:

$$-\widetilde{\boldsymbol{\sigma}}_s^{(0)}(\nabla_s\widetilde{h}) + \widetilde{\boldsymbol{\sigma}}_{sz}^{(1)} = \mathbf{0} \quad \text{on }]0,\widetilde{t}_f[\times\widetilde{\Gamma}_f(t)$$

$$\widetilde{\boldsymbol{\sigma}}_{sz}^{(1)} - \alpha\widetilde{\boldsymbol{u}}_s^{(0)} + \widetilde{\boldsymbol{f}_a}^{(1)} = \mathbf{0} \quad \text{on }]0,\widetilde{t}_f[\times\widetilde{\Gamma}_0$$

Therefore, we obtain in $]0,\widetilde{t}_f[\times\widetilde{\Omega}$

$$\begin{aligned}\widetilde{h}Re\left(\partial_t \widetilde{\boldsymbol{u}}_s^{(0)} + (\widetilde{\boldsymbol{u}}_s^{(0)} \cdot \nabla_s)\widetilde{\boldsymbol{u}}_s^{(0)}\right) - \mathbf{div}_s\left(\widetilde{h}\,\overline{\boldsymbol{\sigma}}_s^{(0)}\right) + \cancel{\widetilde{\boldsymbol{\sigma}}_{sz}^{(1)}\big|_{z=\widetilde{h}}} - \cancel{\widetilde{\boldsymbol{\sigma}}_{sz}^{(1)}\big|_{z=\widetilde{h}}} + \alpha\widetilde{\boldsymbol{u}}_s^{(0)} - \boldsymbol{f}_a^{(1)} = \mathbf{0}\\ \widetilde{h}Re\left(\partial_t \widetilde{\boldsymbol{u}}_s^{(0)} + (\widetilde{\boldsymbol{u}}_s^{(0)} \cdot \nabla_s)\widetilde{\boldsymbol{u}}_s^{(0)}\right) - \mathbf{div}_s\left(\widetilde{h}\,\overline{\boldsymbol{\sigma}}_s^{(0)}\right) + \alpha\widetilde{\boldsymbol{u}}_s^{(0)} - \boldsymbol{f}_a^{(1)} = \mathbf{0}\end{aligned} \tag{1.5.6}$$

Finally, the very last equation combined with hypothesis (iv) gives us (1.5.2a).

□

In the rest of this document, we will drop orders (0) and (1), subscripts s and bars and tildes, for notation convenience.

1.5.2 To sum up

Thin-layer approximation allowed us to transform our initial system of equations into a simpler one, valid asymptotically, i.e. when the aspect ratio of the geometry $\varepsilon = H/L$ tends to 0.

(P): Find $\boldsymbol{\tau}$, τ_{zz}, $\boldsymbol{u}$ and h defined in $]0,t_f[\times\Omega$ such that

$$\begin{cases} -\mathbf{div}(h\ \boldsymbol{\sigma}) + \alpha\boldsymbol{u} - \boldsymbol{f}_a = \mathbf{0} & \text{in }]0,t_f[\times\Omega & (1.5.7a)\\ \partial_t h + \mathrm{div}(h\boldsymbol{u}) = 0 & \text{in }]0,t_f[\times\Omega & (1.5.7b)\\ \boldsymbol{\sigma} = (\boldsymbol{\tau} - \tau_{zz}\mathbf{I}) + 2(1-\beta)(\boldsymbol{D}(\boldsymbol{u}) + \mathrm{div}(\boldsymbol{u})\mathbf{I}) & \text{in }]0,t_f[\times\Omega & (1.5.7c)\\ We\ \overset{\nabla}{\boldsymbol{\tau}} + \boldsymbol{\tau} - 2\beta\,\boldsymbol{D}(\boldsymbol{u}) = \mathbf{0} & \text{in }]0,t_f[\times\Omega & (1.5.7d)\\ We(D_t\tau_{zz} + 2\mathrm{div}(\boldsymbol{u})\tau_{zz}) + \tau_{zz} + 2\beta\mathrm{div}(\boldsymbol{u}) = 0 & \text{in }]0,t_f[\times\Omega & (1.5.7e)\\ \boldsymbol{u}\cdot\boldsymbol{\nu} = 0 \text{ and } \boldsymbol{\sigma}_{\nu t} = \mathbf{0} & \text{on }]0,t_f[\times\partial\Omega & (1.5.7f)\\ h(0,\cdot) = h_0 & \text{in } \Omega & (1.5.7g)\\ \boldsymbol{\tau}(0,\cdot) = \boldsymbol{\tau}_0 \text{ and } \tau_{zz}(0,\cdot) = \tau_{zz,0} & \text{in } \Omega & (1.5.7h) \end{cases}$$

1.5.3 Slip boundary conditions for obstacles

The proposed regularization in subsubsection 1.4.3 for the obstacle condition is purely numerical. The same steps of proof cannot be applied to it in order to deduce an appropriate thin-layer form. Instead, we propose to apply the same regularization analogously to the boundary conditions obtained after asymptotic expansion. They read:

$$\sigma_{\boldsymbol{\nu}\boldsymbol{\nu}} + \varepsilon_r^{-1}\boldsymbol{u}\cdot\boldsymbol{\nu} = 0 \quad \text{on } \mathbb{R}_+ \times \Omega_{\text{obstacle}} \tag{1.5.8}$$

where $\varepsilon_r > 0$ is the regularization parameter and Ω_{obstacle} is the boundary part representing the obstacle.

1.5.4 Re-scaled system

To allow a better physical interpretation, we redimensionalize the equations, with the same characteristic quantities. At the end of the process, only the linear momentum conservation law is going to change to become

$$\rho\ D_t\boldsymbol{u} - \mathrm{div}(h\boldsymbol{\sigma}) + \zeta\boldsymbol{u} - \varepsilon\boldsymbol{f}_a = \mathbf{0} \tag{1.5.9}$$

We note that the low aspect ratio ε appeared in front of the active force and this is the unique and major difference compared to the equation we had before.

2 Numerical resolution in pure viscous case

To start with, it is interesting to look at the case where the tissue is modeled as a Newtonian fluid, namely when $We = 0$ – i.e. $\lambda = 0$, $\beta = 0$, $\eta_m = 0$ and $\eta = \eta_s$. This has the advantage that we do not have to face all the intrinsic difficulties of the problem from the outset; in particular, we will not have to deal with tensor transport terms; the case $We > 0$ is therefore left for perspective, as said in introduction. It leads to the following Stokes problem for a thin layer approximation:

(P): Find $\boldsymbol{u}$ and h defined in $]0, t_f[\times\Omega$ such that

$$\begin{cases} -\mathbf{div}(2h(\boldsymbol{D}(\boldsymbol{u}) + \mathrm{div}(\boldsymbol{u})\mathbf{I})) + \alpha\boldsymbol{u} + \gamma\mathbf{div}(\ln(h)\boldsymbol{I})\mathbb{1}_{\Omega_c(t)} = \mathbf{0} & \text{in }]0, t_f[\times\Omega & \text{(2.0.1a)} \\ \partial_t h + \mathrm{div}(h\boldsymbol{u}) = 0 & \text{in }]0, t_f[\times\Omega & \text{(2.0.1b)} \\ \boldsymbol{u}\cdot\boldsymbol{\nu} = 0 \text{ and } \boldsymbol{D}(\boldsymbol{u})_{\boldsymbol{\nu t}} = \mathbf{0} & \text{on }]0, t_f[\times\partial\Omega & \text{(2.0.1c)} \\ h(0,\cdot) = h_0 & \text{in } \Omega & \text{(2.0.1d)} \end{cases}$$

We remark that the system does not *explicitly* depend on the viscosity $\eta = \eta_s$. This fact comes from the nondimensionalization we made in the proof of Theorem 1.1.

2.1 Reformulation of the problem

2.1.1 A log-height reformulation

During numerical computations, the approximate height do not necessarily remains positive, even if its exact counterpart height h is always positive. Indeed, when the initial height h_0 is positive, then, the exact height h remains always positive at any time.

The proof is short and, moreover, suggests a possible remedy. Let us introduce the characteristic curve passing through position $\boldsymbol{x} \in \Omega$ at time $t \in [0, t_f]$.[6] Let $(t, \boldsymbol{x}) \in]0, t_f[\times\Omega$ be fixed and let us define $Z(t, \boldsymbol{x}; s) = h(s, \boldsymbol{X}(t, \boldsymbol{x}; s))$, for every $s \in]0, t_f[$. Then for every $s \in]0, t_f[$, we have

$$\begin{aligned} \partial_s(Z(t, \boldsymbol{x}; \cdot))(s) &= \partial_s h(s, \boldsymbol{X}(t, \boldsymbol{x}; s)) + \partial_s \boldsymbol{X}(t, \boldsymbol{x}; s) \cdot \nabla h(s, \boldsymbol{X}(t, \boldsymbol{x}; s)) \\ &= \partial_s h(s, \boldsymbol{X}(t, \boldsymbol{x}; s)) + \boldsymbol{u}(s, \boldsymbol{X}(t, \boldsymbol{x}; s)) \cdot \nabla h(s, \boldsymbol{X}(t, \boldsymbol{x}; s)) \\ &= -\mathrm{div}(\boldsymbol{u})(s, \boldsymbol{X}(t, \boldsymbol{x}; s))\, Z(t, \boldsymbol{x}; s) \end{aligned}$$

Using the relation $Z(0, \boldsymbol{x}; 0) = h_0(\boldsymbol{x})$, coming from the initial condition (2.0.1d), we find that this ordinal differential equation has for solution

$$Z(t, \boldsymbol{x}; s) = h_0(\boldsymbol{x}) \exp\Big(- \int_0^s \mathrm{div}(\boldsymbol{u})(s', \boldsymbol{X}(t, \boldsymbol{x}; s'))\, \mathrm{d}s' \Big) \tag{2.1.1}$$

In particular, for $s = t$, we end up with the relation

$$h(t, \boldsymbol{x}) = h_0(\boldsymbol{x}) \exp\Big(- \int_0^t \mathrm{div}(\boldsymbol{u})(s, \boldsymbol{X}(t, \boldsymbol{x}; s))\, \mathrm{d}s \Big) \tag{2.1.2}$$

Assuming $h_0 > 0$, we get $h > 0$ everywhere at any time. Moreover, the solution is explicit, thanks to an integration along the the trajectories.

[6] See appendix A.0.1 for a definition.

To ensure the positivity property, we consider the change of variable $\xi = \ln h$. The system (2.0.1b) & (2.0.1d) writes equivalently:

$$\begin{cases} \partial_t \xi + (\boldsymbol{u} \cdot \nabla)\xi + \operatorname{div}(\boldsymbol{u}) = 0 & \text{in }]0, t_f[\times\Omega \quad (2.1.3a) \\ \xi(0, \cdot) = \ln h_0 & \text{in } \Omega \quad (2.1.3b) \end{cases}$$

With this change of variable, we are now sure that $h = \exp \xi > 0$, even after discretization. In conclusion, using a log-height formulation at the discrete level should solve the positivity issue.

2.1.2 Time discretization

The time interval $[0, t_f]$ is discretized into sub-intervals of variable length $\Delta t^{(n)}$, $n \in [\![0, n_{\max} - 1]\!]$[7], where $n_{\max} > 0$ is the number of time iterations, satisfying the following rules:

$$\Delta t^{(n)} = \kappa \Delta t^{(n-1)} \qquad \text{if } n \in [\![1, n^\star]\!] \quad (2.1.4)$$

$$\Delta t^{(n)} = \Delta t_{\text{ref}} \qquad \text{if } n \in [\![n^\star + 1, n_{\max} - 1]\!] \quad (2.1.5)$$

$$\Delta t^{(0)} = \min(\Delta t_0, \Delta t_{\text{init}}) \quad (2.1.6)$$

where $n^\star \in [\![1, n_{\max} - 2]\!]$ is the number of adaptations of the time step, Δt_0 is an initial time step assumed to be sufficiently small (it should make the scheme converge), $\Delta t_{\text{init}} = (t_f - t_0)/n_{\max}$ is the canonical time step, Δt_{ref} is the reference time step that we will define below, and $\kappa \geqslant 1$ is a numerical parameter close to 1. The idea is to help the algorithm to start with possible discontinuous initial conditions.

Let us introduce t_n the time at step $n \geqslant 0$. It is defined by the recursive relation

$$t_n = t_{n-1} + \Delta t^{(n-1)}, \ n \in [\![1, n_{\max}]\!] \quad (2.1.7)$$

with $t_0 \in \mathbb{R}_+$ being given (here, $t_0 = 0$). By the definitions of $\Delta t^{(n)}$ and t_n, we find out that, for any $n \in [\![0, n_{\max}]\!]$, we can express t_n as follows:

$$t_n = \begin{cases} \Delta t^{(0)} \dfrac{\kappa^n - 1}{\kappa - 1} + t_0 & \text{if } n \leqslant n^\star \\ (n - n^\star)\Delta t_{\text{ref}} + \Delta t^{(0)} \dfrac{\kappa^{n^\star} - 1}{\kappa - 1} + t_0 & \text{otherwise} \end{cases} \quad (2.1.8)$$

In particular, when $n^\star = 0$, we have $t_n = n\Delta t_{\text{ref}} + t_0$, as expected. We then consider two cases:

- when $\Delta t_{\text{init}} \leqslant \Delta t_0$, we take $n^\star = 0$ and then the time steps are constant, with respect to n, equal to Δt_{ref}, which is taken equal to Δt_{init};
- when $\Delta t_{\text{init}} > \Delta t_0$, we take $n^\star = \lfloor (\log(\Delta t_{\text{init}}) - \log(\Delta t_0))/\log(\kappa) \rceil$ (i.e. $\kappa^{n^\star}\Delta t_0 = \Delta t_{\text{init}}$) and set Δt_{ref} so that $t_{n_{\max}} = t_f$. We assume that $(t_f - t_0)(\kappa - 1) > \Delta t_0(\kappa^{n^\star} - 1)$ and find that
$$\Delta t_{\text{ref}} = \left(t_f - t_0 - \Delta t_0 \frac{\kappa^{n^\star} - 1}{\kappa - 1} \right) \cdot \frac{1}{n_{\max} - n^\star} \approx \frac{t_f - t_0}{n_{\max}} = \Delta t_{\text{init}} \quad (2.1.9)$$
is suitable. Moreover, we have $\Delta t^{(n)} \geqslant \Delta t^{(n-1)}$, for any $n \in [\![1, n_{\max}]\!]$.

[7] The notation $[\![a, b]\!]$, where $a \leqslant b$ are both integers, corresponds to an integer interval, i.e. $[\![a, b]\!] = [a, b] \cap \mathbb{N}$.

The time derivative is approximated by a first order finite difference scheme:

$$\partial_t \xi(t_n, \cdot) = \frac{\xi^{(n)} - \xi^{(n-1)}}{\Delta t^{(n-1)}} + O(\Delta t^{(n-1)}) \tag{2.1.10}$$

for any $n \in [\![1, n_{\max}]\!]$ and where $\xi^{(n)} = \xi(t_n, \cdot)$. In particular, $\xi^{(0)} = \ln h_0 \in \mathrm{L}^\infty(\Omega)$ is known by the initial condition. We will also use the notation $\boldsymbol{u}^{(n)} = \boldsymbol{u}(t_n, \cdot)$.

When $n \geqslant 1$, assume by recurrence that both $\boldsymbol{u}^{(n-1)}$ and $\xi^{(n-1)}$ are known. Then, a possible time-discretized problem at time t_n we should now solve is the following:

(P): Find $\boldsymbol{u}^{(n)}$ and $h^{(n)}$ defined in $]0, t_f[\times\Omega$ such that

$$\begin{cases} -\mathbf{div}\Big(2\,\mathrm{e}^{\xi^{(n-1)}}(\boldsymbol{D}(\boldsymbol{u}^{(n)}) + \mathrm{div}(\boldsymbol{u}^{(n)})\mathbf{I})\Big) + \alpha\boldsymbol{u}^{(n)} \\ \qquad\qquad + \gamma\mathbf{div}(\xi^{(n)}\boldsymbol{I})\mathbb{1}_{\Omega_c(t)} = \mathbf{0} \quad \text{in }]0, t_f[\times\Omega & \text{(2.1.11a)} \\ \dfrac{\xi^{(n)} - \xi^{(n-1)}}{\Delta t^{(n-1)}} + \Big(\boldsymbol{u}^{(n-1)} \cdot \nabla\Big)\xi^{(n-1)} + \mathrm{div}(\boldsymbol{u}^{(n)}) = 0 \quad \text{in }]0, t_f[\times\Omega & \text{(2.1.11b)} \\ \boldsymbol{u}^{(n)} \cdot \boldsymbol{\nu} = 0 \text{ and } \boldsymbol{D}(\boldsymbol{u}^{(n)})_{\boldsymbol{\nu t}} = \mathbf{0} \quad \text{on }]0, t_f[\times\partial\Omega & \text{(2.1.11c)} \end{cases}$$

2.2 Variational formulation

2.2.1 General variational formulation

Since it is difficult to deal with the term $\mathbb{1}_{\Omega_c(t)}$[8], coming from the active force, we propose to divide the algorithm in two parts. First, we will solve the previous problem by omitting this term. Then we will post-process the solutions so that $\boldsymbol{u}(t, \cdot) = \boldsymbol{u}^{(0)}$ and $h(t, \cdot) = h_0$ in $\Omega_c(t)^c$, at any time $t \in]0, t_f[$.

When $n \geqslant 1$, assume by recurrence that $\xi^{(n-1)} \in \mathrm{L}^\infty(\Omega)$ and $\boldsymbol{u}^{(n-1)}$ are known. Then, $\boldsymbol{u}^{(n)}$ and $\xi^{(n)} \in \mathrm{L}^\infty(\Omega)$ are obtained from a variational formulation of the time-discretized problem at time t_n. By using the property[9]

Property 2.1. *For any sufficiently regular vector field $\boldsymbol{v}$ and symmetric tensor field $\boldsymbol{\tau}$, defined in Ω, we have*

$$\int_\Omega \boldsymbol{D}(\boldsymbol{v}) : \boldsymbol{\tau}\,\mathrm{d}\boldsymbol{x} + \int_\Omega \boldsymbol{v} \cdot \mathbf{div}(\boldsymbol{\tau})\,\mathrm{d}\boldsymbol{x} = \int_{\partial\Omega} \boldsymbol{v} \cdot (\boldsymbol{\tau}\boldsymbol{n})\,\mathrm{d}\boldsymbol{s} \tag{2.2.1}$$

combined with the boundary conditions and by remarking that $\boldsymbol{D}(\boldsymbol{v}) : \boldsymbol{I} = \mathrm{div}(\boldsymbol{v})$, for any sufficiently regular vector field $\boldsymbol{v}$, we come up with the following possible variational formulation of this problem:

(VF): Find $\boldsymbol{u}^{(n)} \in V$ and $\xi^{(n)} \in \mathrm{L}^\infty(\Omega)$ such that

$$\begin{cases} \displaystyle\int_\Omega \Big(2\,\mathrm{e}^{\xi^{(n-1)}}\Big[\boldsymbol{D}(\boldsymbol{u}^{(n)}) : \boldsymbol{D}(\boldsymbol{v}) + \mathrm{div}(\boldsymbol{u}^{(n)})\mathrm{div}(\boldsymbol{v})\Big] + \alpha\boldsymbol{u}^{(n)} \cdot \boldsymbol{v}\Big)\,\mathrm{d}\boldsymbol{x} \\ \qquad\qquad - \displaystyle\int_\Omega \mathrm{div}(\boldsymbol{v})\xi^{(n)}\,\mathrm{d}\boldsymbol{x} = 0 \qquad \forall \boldsymbol{v} \in V \\ \displaystyle -\int_\Omega \mathrm{div}(\boldsymbol{u}^{(n)})\zeta\,\mathrm{d}\boldsymbol{x} - \int_\Omega \frac{\xi^{(n)}\zeta}{\Delta t^{(n-1)}}\,\mathrm{d}\boldsymbol{x} = \int_\Omega \left(-\frac{\xi^{(n-1)}}{\Delta t^{(n-1)}} + \boldsymbol{u}^{(n-1)} \cdot \nabla\xi^{(n-1)}\right)\zeta\,\mathrm{d}\boldsymbol{x} \quad \forall \zeta \in \mathrm{L}^\infty(\Omega) \end{cases}$$

[8] We discuss this point in subsubsection 3.3.4.

[9] See Saramito [2016, section 1.8] for a possible proof.

where $V = \{\boldsymbol{v} \in \mathrm{H}^1(\Omega)^2 \ \mid \ \boldsymbol{v}\cdot\boldsymbol{\nu} = 0 \text{ on } \partial\Omega\}$. Let us introduce the following forms

$$\begin{aligned} a(\xi;\boldsymbol{u},\boldsymbol{v}) &= \int_\Omega \Big(2\,\mathrm{e}^{\xi}\,[\boldsymbol{D}(\boldsymbol{u}) : \boldsymbol{D}(\boldsymbol{v}) + \mathrm{div}(\boldsymbol{u})\mathrm{div}(\boldsymbol{v})] + \alpha\boldsymbol{u}\cdot\boldsymbol{v}\Big)\,\mathrm{d}\boldsymbol{x} \\ b_1(\boldsymbol{u},\zeta) &= -\int_\Omega \gamma\mathrm{div}(\boldsymbol{u})\zeta\,\mathrm{d}\boldsymbol{x} \\ b_2(\boldsymbol{u},\zeta) &= -\int_\Omega \mathrm{div}(\boldsymbol{u})\zeta\,\mathrm{d}\boldsymbol{x} \\ c(\xi,\zeta) &= \frac{1}{\Delta t}\int_\Omega \xi\zeta\,\mathrm{d}\boldsymbol{x} \\ \ell(\xi,\boldsymbol{u};\zeta) &= \int_\Omega \left(-\frac{\xi}{\Delta t} + \boldsymbol{u}\cdot\nabla\xi\right)\zeta\,\mathrm{d}\boldsymbol{x} \end{aligned}$$

defined for any $\boldsymbol{u},\boldsymbol{v} \in V$ and any $\xi,\zeta \in L^\infty(\Omega)$. The forms $a(\xi;\cdot,\cdot)$, b_1, b_2 and c are bilinear while the form $\ell(\xi,\boldsymbol{u};\cdot)$ is linear. The form $a(\xi;\cdot,\cdot)$ is also symmetric. Note that b_1 and b_2 are conceptually very close: whenever $\gamma = 1$, then $b_1 = b_2$, in which case the problem is symmetric. Nevertheless, it seems very unlikely that we will be confronted with this case. The previous variational formulation then writes equivalently:

(VF): Find $\boldsymbol{u}^{(n)} \in V$ and $\xi^{(n)} \in \mathrm{L}^\infty(\Omega)$ such that

$$\begin{aligned} a\Big(\xi^{(n-1)};\boldsymbol{u}^{(n)},\boldsymbol{v}\Big) + b_1\Big(\boldsymbol{v},\xi^{(n)}\Big) &= 0 && \forall \boldsymbol{v} \in V \\ b_2\Big(\boldsymbol{u}^{(n)},\zeta\Big) - \ c\Big(\xi^{(n)},\zeta\Big) &= \ell\Big(\xi^{(n-1)},\boldsymbol{u}^{(n-1)};\zeta\Big) && \forall \zeta \in \mathrm{L}^\infty(\Omega) \end{aligned} \tag{2.2.2}$$

2.2.2 No-penetration boundary conditions for obstacles

The introduction of a curved obstacle modifies a little the variational formulation. We change the associated space into $V = \{\boldsymbol{v} \in \mathrm{H}^1(\Omega)^2 \ \mid \ \boldsymbol{v}\cdot\boldsymbol{\nu} = 0 \text{ on } \Omega_{\text{wall}}\}$. From property 2.1, we have for any $\boldsymbol{v} \in V$:

$$-\int_\Omega \boldsymbol{v}\cdot\mathbf{div}(\boldsymbol{\sigma})\,\mathrm{d}\boldsymbol{x} = \int_\Omega \boldsymbol{D}(\boldsymbol{v}) : \boldsymbol{\sigma}\,\mathrm{d}\boldsymbol{x} - \int_{\partial\Omega} \boldsymbol{v}\cdot(\boldsymbol{\sigma}\boldsymbol{\nu})\,\mathrm{d}\boldsymbol{s}$$

where $\boldsymbol{\sigma} = 2h(\boldsymbol{D}(\boldsymbol{u}) + \mathrm{div}(\boldsymbol{u})\boldsymbol{I})$. Then we split the term $\boldsymbol{\sigma}\boldsymbol{n}$ into its tangential and its normal components and apply the Neumann no-grip boundary condition to get

$$-\int_\Omega \boldsymbol{v}\cdot\mathbf{div}(\boldsymbol{\sigma})\,\mathrm{d}\boldsymbol{x} = \int_\Omega \boldsymbol{D}(\boldsymbol{v}) : \boldsymbol{\sigma}\,\mathrm{d}\boldsymbol{x} + \varepsilon_r^{-1}\int_{\Omega_{\text{obstacle}}} (\boldsymbol{u}\cdot\boldsymbol{\nu})(\boldsymbol{v}\cdot\boldsymbol{\nu})\,\mathrm{d}\boldsymbol{s}$$

As a consequence, the form a in the variational formulation (2.2.2) becomes

$$\begin{aligned} a(\xi;\boldsymbol{u},\boldsymbol{v}) = \int_\Omega \Big(\ 2\,\mathrm{e}^{\xi}\,[\boldsymbol{D}(\boldsymbol{u}) : \boldsymbol{D}(\boldsymbol{v}) + \mathrm{div}(\boldsymbol{u})\mathrm{div}(\boldsymbol{v})] + \alpha\boldsymbol{u}\cdot\boldsymbol{v}\ \Big)\,\mathrm{d}\boldsymbol{x} \\ + \varepsilon_r^{-1}\int_{\Omega_{\text{obstacle}}} (\boldsymbol{u}\cdot\boldsymbol{\nu})(\boldsymbol{v}\cdot\boldsymbol{\nu})\,\mathrm{d}\boldsymbol{s} \end{aligned} \tag{2.2.3}$$

defined for any $\boldsymbol{u},\boldsymbol{v} \in V$ and any $\xi \in L^\infty(\Omega)$.

2.2.3 A discretized variational formulation using the discontinuous Galerkin method

For discretization, we may combine continuous and piecewise $\mathcal{P}_{k+1}$–approximation for the velocity and discontinuous and piecewise $\mathcal{P}_k$–approximation for the height, where $k \geqslant 0$ is the discretization order. For instance, when $k = 0$, the velocity would be continuous and piecewise affine while the height would be discontinuous and piecewise constant. However, the gradient has no more sense for discontinuous functions. To counteract this complication, the discontinuous Galerkin method could be used to discretize the transport term $\boldsymbol{u} \cdot \nabla \xi$ involved in the right-hand-side ℓ.

Let $\mathcal{T}_h$ be a finite element mesh, with $N > 0$ elements, of the flow domain Ω. We introduce the following finite dimensional spaces

$$\begin{aligned} X_h &= \{\boldsymbol{v} \in \mathcal{C}^0\left(\overline{\Omega}\right)^2 \ \mid \ \boldsymbol{v}_{/K} \in \mathcal{P}^2_{k+1}, \forall K \in \mathcal{T}_h\} \subset \mathrm{H}^1(\Omega)^2 \\ V_h &= X_h \cap V = \{\boldsymbol{v} \in X_h \ \mid \ \boldsymbol{v} \cdot \boldsymbol{\nu} = 0 \text{ on } \partial\Omega\} \\ Q_h &= \{q \in \mathrm{L}^\infty(\Omega) \ \mid \ q_{/K} \in \mathcal{P}_k, \forall K \in \mathcal{T}_h\} \subset \mathrm{L}^\infty(\Omega) \end{aligned}$$

∇q has, indeed, no more sense when $q \in Q_h$, but has one when q is restricted to any element of the mesh. For this purpose, we will use as a convenient notation the so-called broken gradient ∇_h defined by

$$(\nabla_h q)_{/K} = \nabla(q_{/K}) \quad \forall K \in \mathcal{T}_h \tag{2.2.4}$$

According to Saramito [2016, section 4.10], the discontinuous Galerkin method extends the upwind scheme to the finite element context. It is typically used for problems which involve transport term, as in our case. As a consequence, we will replace the exact linear form $\ell(\xi, \boldsymbol{u}; \cdot)$ by a discretized version expressed as a sum of integrals over each element of the mesh (by splitting the initial integral over them). Formally, we will only need to substitute the gradient by the broken one in the integral over Ω, by definition. In addition, for each of them, we will add an upwind term of the form

$$\ell_K(h, \boldsymbol{u}; q) = \sum_{S \subset \partial K} \int_S \left(\frac{|\boldsymbol{u} \cdot \boldsymbol{\nu}| - \boldsymbol{u} \cdot \boldsymbol{\nu}}{2} \right) (h - h_{\text{ext}}) q \, \mathrm{d}s \tag{2.2.5}$$

where $h \in Q_h$ is the trial function, $q \in Q_h$ is the test function and h_{ext} is the external trace of h in K, whose definition is given in appendix A.0.2. In other words, $\ell(\xi, \boldsymbol{u}; \zeta)$ will be replaced by

$$\ell_h(\xi, \boldsymbol{u}; \zeta) = \sum_{K \in \mathcal{T}_h} \left(\int_K \left(-\frac{\xi}{\Delta t} + \boldsymbol{u} \cdot \nabla \xi \right) \zeta \, \mathrm{d}\boldsymbol{x} + \ell_K(\xi, \boldsymbol{u}; \zeta) \right) \tag{2.2.6}$$

where $\xi, \zeta \in Q_h$ and $\boldsymbol{u} \in V_h$. Let us specifically take a look at the term inside the sum of ℓ_K. When S is a boundary face, i.e. $S \subset \partial\Omega$, then this term is zero because $\boldsymbol{u} \in V_h$. On the other hand, when S is an internal face between two neighbor elements K_- and K_+, it will be counted twice. However, only one of the two possibly terms is non-zero, due to the change of sign of the outer normal when changing of neighbor element. Let $\boldsymbol{\nu}_-$ (resp. $\boldsymbol{\nu}_+$) be the outer unit normal vector on ∂K_- (resp. ∂K_+). We have $\boldsymbol{\nu}_- = -\boldsymbol{\nu}_+$. We arbitrarily choose $\boldsymbol{\nu} = \boldsymbol{\nu}_-$ as the outer unit normal vector of S. $h_\pm$ (resp. $q_\pm$) will be the restriction of h (resp. q) to $K_\pm$. When the

two terms which involve S are summed together, we get

$$\begin{aligned}
&\int_{S\cap\partial K_-}\left(\frac{|\boldsymbol{u}\cdot\boldsymbol{\nu}_-|-\boldsymbol{u}\cdot\boldsymbol{\nu}_-}{2}\right)(h_- - h_+)q_-\,\mathrm{d}s + \int_{S\cap\partial K_+}\left(\frac{|\boldsymbol{u}\cdot\boldsymbol{\nu}_+|-\boldsymbol{u}\cdot\boldsymbol{\nu}_+}{2}\right)(h_+ - h_-)q_+\,\mathrm{d}s\\
&\quad=\int_S\left(\frac{|\boldsymbol{u}\cdot\boldsymbol{\nu}|}{2}(h_- - h_+)(q_- - q_+) - (\boldsymbol{u}\cdot\boldsymbol{\nu})(h_- - h_+)\Big(\frac{q_- + q_+}{2}\Big)\right)\mathrm{d}s\\
&\quad=\int_S [\![h]\!]\left(\frac{|\boldsymbol{u}\cdot\boldsymbol{\nu}|}{2}[\![q]\!] - (\boldsymbol{u}\cdot\boldsymbol{\nu})\{\!\{q\}\!\}\right)\mathrm{d}s
\end{aligned}$$

and then

$$\begin{aligned}
\sum_{K\in\mathcal{T}_h}\ell_K(h,\boldsymbol{u};q) &= \sum_{K\in\mathcal{T}_h}\sum_{S\subset\partial K}\int_S\left(\frac{|\boldsymbol{u}\cdot\boldsymbol{\nu}|-\boldsymbol{u}\cdot\boldsymbol{\nu}}{2}\right)(h-h_{\mathrm{ext}})q\,\mathrm{d}s\\
&= \sum_{S\in\mathscr{S}_h^{(i)}}\int_S [\![h]\!]\left(\frac{|\boldsymbol{u}\cdot\boldsymbol{\nu}|}{2}[\![q]\!] - (\boldsymbol{u}\cdot\boldsymbol{\nu})\{\!\{q\}\!\}\right)\mathrm{d}s
\end{aligned}\tag{2.2.7}$$

where $[\![q]\!] = q_- - q_+$ is the jump of q across the face, $\{\!\{q\}\!\} = (q_- + q_+)/2$ is its average and $\mathscr{S}_h^{(i)}$ is the set of internal faces of the mesh $\mathcal{T}_h$.

Finally, the discretized version of ℓ reads

$$\ell_h(\xi,\boldsymbol{u};\zeta) = \int_\Omega\left(-\frac{\xi}{\Delta t} + \boldsymbol{u}\cdot\nabla_h\xi\right)\zeta\,\mathrm{d}\boldsymbol{x} + \sum_{S\in\mathscr{S}_h^{(i)}}\int_S [\![\xi]\!]\left(\frac{|\boldsymbol{u}\cdot\boldsymbol{\nu}|}{2}[\![\zeta]\!] - (\boldsymbol{u}\cdot\boldsymbol{\nu})\{\!\{\zeta\}\!\}\right)\mathrm{d}s \tag{2.2.8}$$

where $\xi,\zeta\in Q_h$ and $\boldsymbol{u}\in V_h$, and leads to the following discretized variational formulation of the time-discretized problem:

$(VF)_h$: Find $\boldsymbol{u}^{(n)}\in V_h$ and $\xi^{(n)}\in Q_h$ such that

$$\begin{aligned}
a\big(\xi^{(n-1)};\boldsymbol{u}^{(n)},\boldsymbol{v}\big) + b_1\big(\xi^{(n-1)};\boldsymbol{v},\xi^{(n)}\big) &= 0 && \forall\boldsymbol{v}\in V_h\\
b_2\big(\xi^{(n-1)};\boldsymbol{u}^{(n)},\zeta\big) - c\big(\xi^{(n)},\zeta\big) &= \ell_h\big(\xi^{(n-1)},\boldsymbol{u}^{(n-1)};\zeta\big) && \forall\zeta\in Q_h
\end{aligned}\tag{2.2.9}$$

2.2.4 Case of the initial velocity

When $n=0$, $\boldsymbol{u}^{(0)}$ is defined as the solution of the following problem:

(P): Find $\boldsymbol{u}^{(0)}$ defined in $]0,t_f[\times\Omega$ such that

$$\begin{cases}
-\mathbf{div}\left[2h_0\Big(\boldsymbol{D}(\boldsymbol{u}^{(0)}) + \mathrm{div}(\boldsymbol{u}^{(0)})\mathbf{I}\Big)\right] + \alpha\boldsymbol{u}^{(0)} = -\gamma\mathbf{div}(\ln h_0\boldsymbol{I})\mathbb{1}_{\Omega_c(t)} & \text{in }]0,t_f[\times\Omega & \text{(2.2.10a)}\\
-\mathrm{div}(h_0\,\boldsymbol{u}^{(0)}) = 0 & \text{in }]0,t_f[\times\Omega & \text{(2.2.10b)}\\
\boldsymbol{u}^{(0)}\cdot\boldsymbol{\nu} = 0 \text{ and } \boldsymbol{D}(\boldsymbol{u}^{(0)})_{\boldsymbol{\nu t}} = \mathbf{0} & \text{on }]0,t_f[\times\partial\Omega & \text{(2.2.10c)}
\end{cases}$$

In the same way we derived the general variational formulation, we come up with the one associated to the previous problem:

(VF): Find $\boldsymbol{u}^{(0)} \in V$ such that

$$\int_\Omega \Big(2h_0 \left[\boldsymbol{D}(\boldsymbol{u}^{(0)}) : \boldsymbol{D}(\boldsymbol{v}) + \mathrm{div}(\boldsymbol{u}^{(0)})\mathrm{div}(\boldsymbol{v})\right] + \alpha \boldsymbol{u}^{(0)} \cdot \boldsymbol{v}\Big)\,\mathrm{d}\boldsymbol{x} = \int_\Omega \gamma \ln h_0 \,\mathrm{div}(\boldsymbol{v})\,\mathrm{d}\boldsymbol{x} \quad \forall \boldsymbol{v} \in V \tag{2.2.11}$$

Since we might have some troubles when dealing with points where h_0 is zero, because, among others, of the term $\ln h_0$, we propose to add a kind of protection: h_0 is replaced by $\max(h_0, \varepsilon_h)$, where $\varepsilon_h > 0$ is small and we add the term $\mathbb{1}_{[\ln \varepsilon_h, +\infty[}\{\ln[\max(h_0, \varepsilon_h)]\}$ in the right-hand side.

2.3 Fully implicit time scheme

The previous time discretization is a semi-implicit scheme; it is expected to be conditionally stable: Δt should be small enough to make it converge. Unfortunately, we do not known any explicit stability condition in order to choose this time step. Thus, we turn here to a more robust scheme by introducing an inner fixed-point loop, i.e to a fully implicit variant. We slightly modify the previous notations by introducing a new form for ℓ:

$$\ell(\xi^\star, \xi, \boldsymbol{u}; \zeta) = \int_\Omega \left(-\frac{\xi^\star}{\Delta t} + \boldsymbol{u} \cdot \nabla \xi\right)\zeta \,\mathrm{d}\boldsymbol{x} \tag{2.3.1}$$

defined for any $\xi^\star, \xi, \zeta \in L^\infty(\Omega)$ and any $\boldsymbol{u} \in V$. Here, $\xi^\star$ represents the value at the previous time step while ξ corresponds to the current iterate in the inner fixed-point loop that we expect to converge towards a good candidate for the value at the current time step. In addition to the notations already introduced at then end of subsubsection 2.1.2, we will use $\left(\boldsymbol{u}^{(n,k)}, \xi^{(n,k)}\right)$ to denote the k-th iterate in the inner fixed-point loop at the n-th time step. In particular, the fixed point iteration is initialized as follows:

$$\left(\boldsymbol{u}^{(n,0)}, \xi^{(n,0)}\right) = \left(\boldsymbol{u}^{(n-1)}, \xi^{(n-1)}\right) \tag{2.3.2}$$

When the fixed-point converges, we set

$$\left(\boldsymbol{u}^{(n)}, \xi^{(n)}\right) = \lim_{k \to +\infty} \left(\boldsymbol{u}^{(n,k)}, \xi^{(n,k)}\right) \tag{2.3.3}$$

At time step n and iteration k of the inner fixed-point loop, assuming by recurrence that both $\xi^{(n-1)}$ and $\left(\boldsymbol{u}^{(n,k-1)}, \xi^{(n,k-1)}\right)$ are known, the variational formulation of the implicitly time-discretized problem writes

(VF): Find $\boldsymbol{u}^{(n,k)} \in V$ and $\xi^{(n,k)} \in \mathrm{L}^\infty(\Omega)$ such that

$$\begin{aligned} a\left(\xi^{(n,k-1)}; \boldsymbol{u}^{(n,k)}, \boldsymbol{v}\right) + b_1\left(\boldsymbol{v}, \xi^{(n,k)}\right) &= 0 && \forall \boldsymbol{v} \in V \\ b_2\left(\boldsymbol{u}^{(n,k)}, \zeta\right) - \ c\left(\xi^{(n,k)}, \zeta\right) &= \ell\left(\xi^{(n-1)}, \xi^{(n,k-1)}, \boldsymbol{u}^{(n,k-1)}; \zeta\right) && \forall \zeta \in \mathrm{L}^\infty(\Omega) \end{aligned} \tag{2.3.4}$$

Discretization is then straightforward by applying the discontinuous Galerkin method on the form ℓ as we did in subsubsection 2.2.3.

Remarks.

- If the implicit time scheme had been done without an inner fixed-point loop, the problem to be solved would have been nonlinear and then more difficult.
- In practice, the fixed-point inner loop with index k is stopped when

$$\frac{1}{\Delta t^{(n-1)}} \left\| \left(\boldsymbol{u}^{(n,k)}, \xi^{(n,k)} \right) - \left(\boldsymbol{u}^{(n,k-1)}, \xi^{(n,k-1)} \right) \right\|_{\mathrm{L}^2(\Omega)^2 \times \mathrm{L}^\infty(\Omega)} \leqslant \delta \text{ or } k \geqslant k_{\max} \tag{2.3.5}$$

  where $\delta > 0$ represents an error tolerance, $k_{\max} > 0$ is the maximal number of iterations in the inner loop and $\|(\boldsymbol{u}, \xi)\|^2_{\mathrm{L}^2(\Omega)^2 \times \mathrm{L}^\infty(\Omega)} = \|\boldsymbol{u}\|^2_{\mathrm{L}^2(\Omega)^2} + \|\xi\|^2_{\mathrm{L}^\infty(\Omega)}$. When $k_{\max} = 1$, we recognize the previous semi-implicit time scheme.

3 Results

3.1 Numerical settings and visualization

All the simulations we are going to show here were made with the following numerical settings:

- $h_c = 0.3$;
- $h_0(\boldsymbol{x}) = H(-x)$, for any $\boldsymbol{x} = (x, y) \in \Omega$, where H is the Heaviside function;
- $\Delta t_0 = 10^{-7}$;
- $\kappa = 1.1$;
- $\varepsilon_r = 10^{-7}$;
- $k = 0$ (discretization order);
- $\varepsilon_h = 10^{-2}$;
- $\delta = 10^{-5}$;
- $k_{\max} = 100$ but the loop globally converged with less than 10 iterations, depending on the discretization accuracy.

To graphically represent the height profiles, we perform a L^2 orthogonal projection of the piecewise constant height approximation onto the space $Q_h^{(1)} = \{q \in \mathcal{C}^0\left(\bar{\Omega}\right) \mid q_{/K} \in \mathcal{P}_1, \forall K \in \mathcal{T}_h\}$ of continuous and piecewise affine functions. Formally, $h^\star$ is defined as

$$h^\star = \arg\min_{q \in Q_h^{(1)}} \frac{1}{2} \|h - q\|^2_{\mathrm{L}^2(\Omega)} \tag{3.1.1}$$

A weak formulation of this problem would read

(VF): Find $h^\star \in Q_h^{(1)}$ such that

$$\int_\Omega h^\star q \, \mathrm{d}\boldsymbol{x} = \int_\Omega hq \, \mathrm{d}\boldsymbol{x} \quad \forall q \in Q_h^{(1)} \tag{3.1.2}$$

3.2 Numerical convergence

We propose here to show the numerical convergence of our algorithm in 1D. We start from an initial mesh with initial space and time steps. Then, iteratively, we refine the mesh by dividing simultaneously the space and time steps by 2. Let us remark that, at the same time, dividing the initial time step $\Delta t^{(0)}$ by 2 and doubling the number of time steps $n_{\max}$ is sufficient to divide the time steps by 2 at each iteration, even with our time step adaptation. Likewise, dividing the space step by 2 is equivalent to doubling the number of elements N.

We decide to make three iterations of the previous method and for each case, we choose $t_f = 5$ and $\alpha = \gamma = 1$. The first simulation is done with $\mathcal{N}_1 = (N, n_{\max}, \Delta t_0) = (2.50 \cdot 10^3, 2.50 \cdot 10^3, 1.00 \cdot 10^{-5})$, the second one with $\mathcal{N}_2 = (N, n_{\max}, \Delta t_0) = (5.00 \cdot 10^3, 5.00 \cdot 10^3, 5.00 \cdot 10^{-6})$, the third one with $\mathcal{N}_3 = (N, n_{\max}, \Delta t_0) = (1.00 \cdot 10^4, 1.00 \cdot 10^4, 2.50 \cdot 10^{-6})$ and the last one with $\mathcal{N}_4 = (N, n_{\max}, \Delta t_0) = (2.00 \cdot 10^4, 2.00 \cdot 10^4, 1.25 \cdot 10^{-6})$. To give an idea, we have in all cases $n^\star = 56$ and successively, $\Delta t_{\text{ref}} \approx 2.04 \cdot 10^{-3}$, $\Delta t_{\text{ref}} \approx 1.01 \cdot 10^{-3}$, $\Delta t_{\text{ref}} \approx 5.02 \cdot 10^{-4}$ and finally $\Delta t_{\text{ref}} \approx 2.51 \cdot 10^{-4}$. The convergence is shown in figures 3.1 and 3.2 by presenting the resulting log-heights ξ at times $t = 1.5$ and $t = 4$ (not post-processed) and front profiles x_f, defined on $[0, t_f]$ as the position in Ω such that $h(t, x_f(t)) = h_c$, of each simulation.

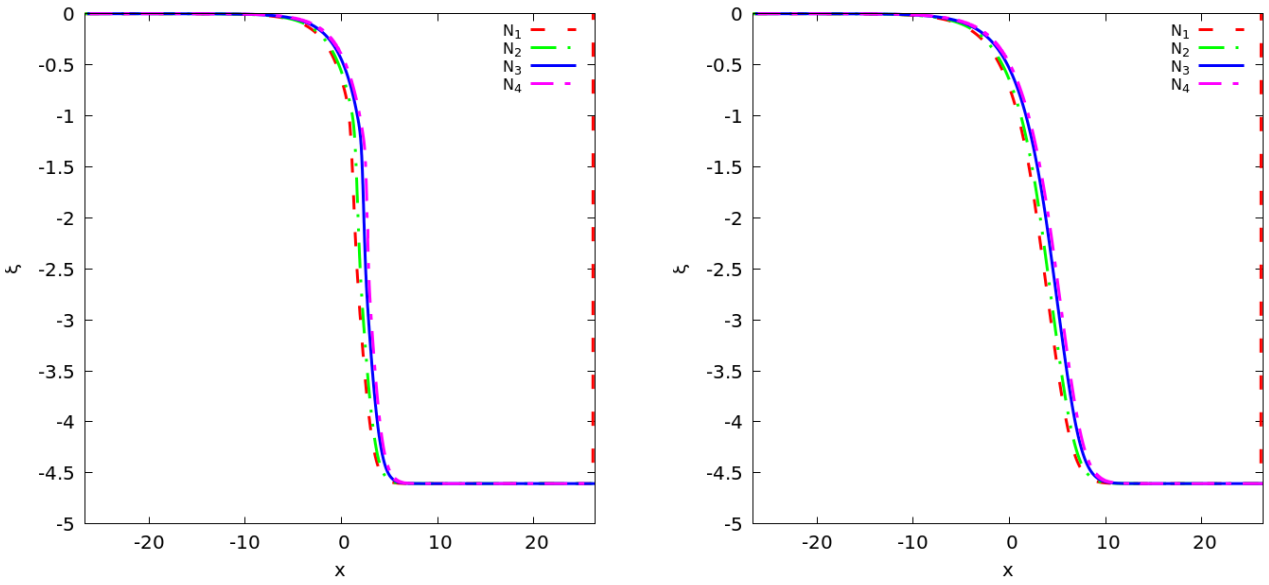

(a) At time $t = 1.5$.

(b) At time $t = 4$.

Figure 3.1: Log-height with the different levels of discretization $(\mathcal{N}_i)_{i\in[\![1,4]\!]}$, both in space and time. From left to right in each plot, the first curve is shifted $1/2$ to the left, the second one $1/4$ to the left, the third one $1/4$ to the right and the last one $1/2$ to the right to allow their distinction, otherwise they would completely overlap.

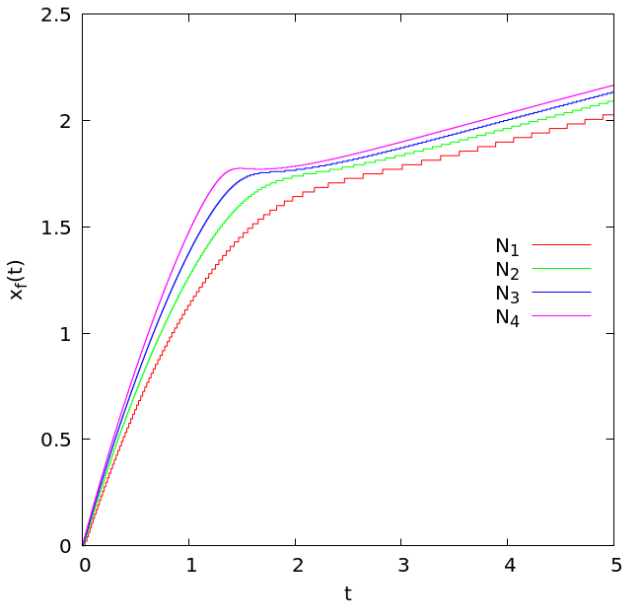

Figure 3.2: Front profile with the different levels of discretization, both in space and time.

3.3 Exploration

3.3.1 Experimental data

As mentioned in introduction, we based our simulations on the data in Tlili et al. [2018b] (oriented 1D) and in Tlili et al. [2018a] (oriented 2D with obstacle). We present here the material we will work with along this section.

The experiences in the first article were done on a 2D domain but the authors averaged in width so that they came up with 1D data, along the x-axis. Indeed, according to Figure 3.3, the velocity field $\boldsymbol{u}$ is globally independent of y. When there is no obstacle, it suggests that 1D simulations are sufficient to describe the cell flow.

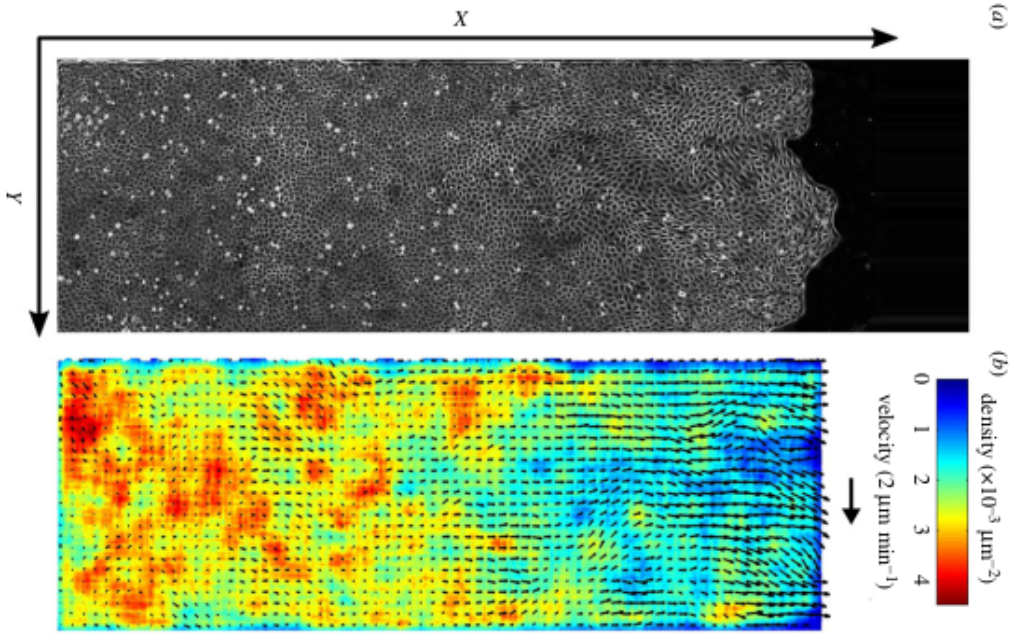

Figure 3.3: Cell migration without obstacle. (a) What is experimentally observed. (b) Corresponding velocity and density. Extracted from Tlili et al. [2018b, Figure 1.].

Still in this article we can find figures 3.4a and 3.4b that show specifically the velocity and the radius profiles against time and position. Here, height, density and radius are closely related. Indeed, the density, or more precisely the mean surface density, denoted d_{mean} is defined by

$$d_{\text{mean}} = \rho\, h, \quad \text{on } [0, t_f] \times \Omega \tag{3.3.1}$$

Then, by assuming that on average, the surface of a cell is nothing but a disc of radius r_{mean} and the mass of a cell $m = \pi r_{\text{mean}}^2 d_{\text{mean}}$ is constant in time and space, we can express the mean radius as a function of the height:

$$r_{\text{mean}} = \sqrt{\frac{m}{\pi\rho}}\, h^{-1/2} \propto h^{-1/2}, \quad \text{on } [0, t_f] \times \Omega \tag{3.3.2}$$

More surprising, Figure 3.4c illustrates the linear relation that exists between the radius and the velocity, on average. This is a very important point we will focus on a bit further in this section.

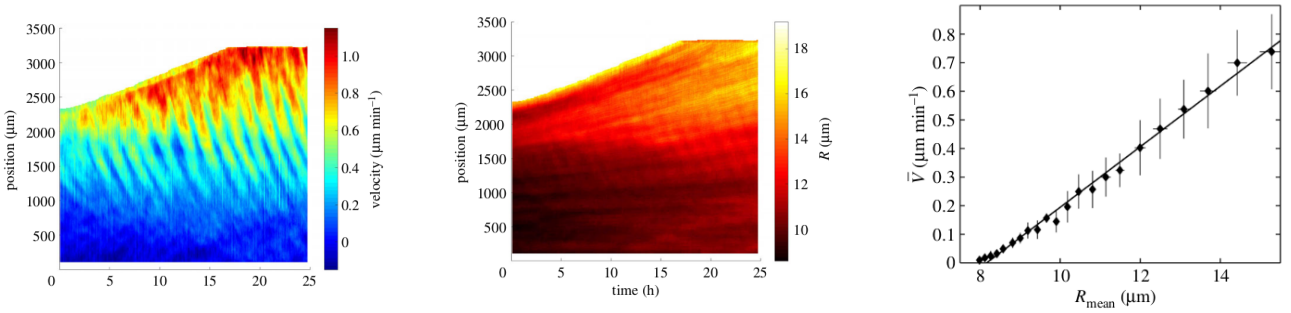

(a) Space-time diagram of cell velocity $\boldsymbol{u}$.

(b) Space-time diagram of effective cell radius r_{mean}.

(c) Cell velocity–cell radius correlation.

Figure 3.4: Experimental radius and velocity diagrams. Extracted from Tlili et al. [2018b]

We are also able to retrieve the position of the tissue front from the mean density, given in the supplemental material. The front x_f is time-dependent function. It is defined on $[0, t_f]$ as the position in Ω such that $h(t, x_f(t)) = h_c$. Figure 3.5 shows some corresponding experimental curves. Assuming ρ is constant, the height h can be obtained by the measurement of d_{mean}, according to equality (3.3.1).

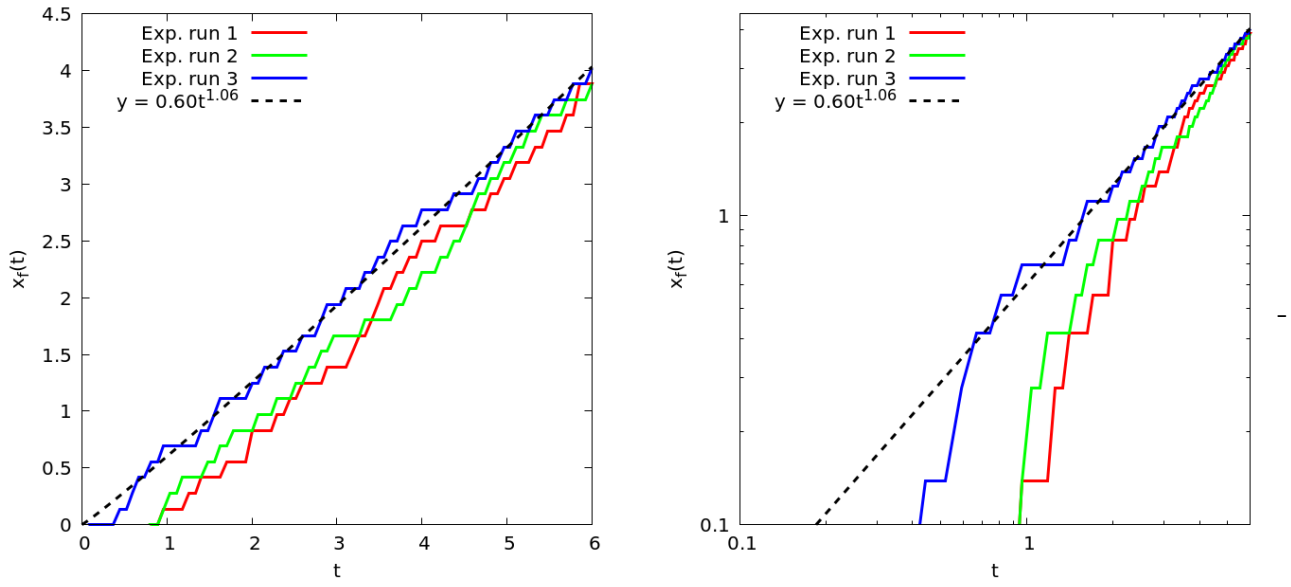

(a)

(b) Log-log scale

Figure 3.5: Experimental front profiles, generated with data from Tlili et al. [2018b]

In Tlili et al. [2018a], the experiences were done on a 2D domain where there is an obstacle, as illustrated in Figure 3.6. The authors performed ten similar experimental runs in order to study the sensibility of the results. Arbitrarily, we choose to base our comparisons on the data associated to the first experimental run.

By extracting the relevant information, we find that the strip length is 4000 μm, the strip width 750 μm, the obstacle diameter 150 μm. We choose the characteristic length to be the obstacle radius, namely $L = 75$ μm. Following the nondimensionalization we made in the proof

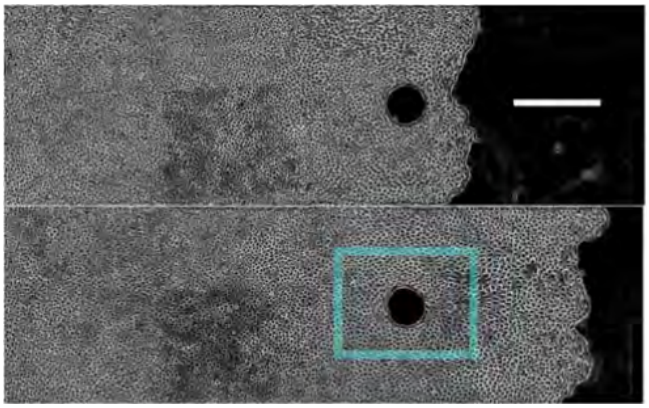

Figure 3.6: Cell migration with obstacle. (a) At $t = 0$ h. (b) At $t = 12$ h. Extracted from Tlili et al. [2018a, Figure 1.].

of Theorem 1.1 and by putting the origin at the center of the domain, the computation domain is then $\Omega = [-80/3, 80/3] \times [0, 5]$, $y = 0$ being an axis of symmetry for both $\boldsymbol{u}$ and h in our model. Still in this paper, we learn that "the typical time for cells to migrate over a distance equivalent to the obstacle diameter of 200 μm is 3 h". It means that the the typical time for cells to migrate over a distance of 75 μm is 1.125 h. As a result, this is the value we choose for the characteristic time, namely $T = 67.5$ min. To give an idea, the characteristic velocity is then $U = L/T = 10/9\ \mu\text{m} \cdot \text{min}^{-1}$. Finally, the center of the obstacle coincides with the origin. We choose $t_f = 20/3$ as final dimensionless time. We shall discuss this value in subsubsection 3.3.4. It corresponds to a time of 7.5 h. At the end of this allotted time, the cells should have migrated over a distance of $L/4 = 500$ μm. For the 1D case, we will keep those characteristic quantities and will take as computation domain $\Omega = [-80/3, 80/3]$.

3.3.2 Objective and strategy

Through *qualitative* comparisons with experimental data, we will be able to refine and highlight the limitations of the model in pure viscous case, as we focused on it in section 2. Ideally, the numerical results will provide another perspective on the biophysical mechanisms involved.

For that purpose, we aim at finding the physical parameters α and γ involved in the model that best fit the experimental data. Our first point of entry for the comparison is in the model solutions. Indeed, they directly give the velocity field and the height. Then, we will be able to compare them with the figures presented previously. To go further in the comparison, we will use two additional experimental measures:

- the position of the front with respect to time (Figure 3.5): given the final time we have chosen, we should have $x_f(t_f) = L/4$;
- the local relation between velocity and cell radius: all values gather on a master linear curve (Figure 3.4c).

We will select each couple (α, γ) that will fulfill both conditions. In particular, we will try to highlight the values of α most representative of what can be observed among all the values that this parameter can take. The final couple that will be described as the best will be the one for which the asymptotic behavior of the position of the front or the master curve (which will

not necessarily be linear) will be the closest to what is experimentally observed. Finally, we will propose a 2D simulation and will compare it with what was obtained in Tlili et al. [2018a]. The numerical experiments then conducted in 1D should make it possible to consider only the best case in 2D.

3.3.3 Raw results

Let us make the exploration of the possible couples (α, γ). We run our simulations with $t_f = {}^{20}/_{3}$, $N = 1000$ and $n_{\max} = 5000$. Table 3.1 gives a brief summary of couples that fit the condition $x_f(t_f) = L/4$; they were found by trial and error. Let us take a look at the following representative cases:

- $\alpha = 10$ will represent the class of large α;
- $\alpha = 0$ will represent the class of small α;
- $\alpha = 10^{-1}$ will represent the other ones.

α	0	10^{-2}	10^{-1}	1	10	10^2	10^{99}
γ	$3 \cdot 10^{-2}$	$7 \cdot 10^{-2}$	$7.8 \cdot 10^{-1}$	$1.17 \cdot 10$	$1.175 \cdot 10^2$	$1.175 \cdot 10^3$	$1.175 \cdot 10^{100}$

Table 3.1: Some couples (α, γ) for which $x_f(t_f) \approx L/4$.

Let us begin with $\alpha = 10$. A summary of the obtained results is given by Figure 3.7. In figures (a) and (b), we see that the velocity decreases in intensity at the front over time. More precisely, we first have a ramp with strong growth, localized at the front (short times), which then tends to sag and spread more and more evenly over the tissue domain $\Omega_c(t)$ (longer times). As a result, in figure (c), values $(r_{\text{mean}}(t_n, x_i), u(t_n, x_i))_{n,i}$ indeed gather on a master curve, that seems to be a square root. The tissue height, in figures (d) and (e), on the other hand, sags, i.e. reaches the critical height h_c, quite quickly. Finally, figure (f) shows the front position with respect to time in log-log scale. What we observe in it is actually a square root curve times a constant. It is possible to prove it formally. Indeed, for large α, the viscous effects can be neglected in front of the friction and the active force. If we assume for the moment[10] that h decreases just fast enough not to be affected by the no-penetration condition $\boldsymbol{u} \cdot \boldsymbol{\nu} = 0$ then, according to appendix D, since , $\boldsymbol{u}$ and h are explicit and there exists a constant C_f such that

$$x_f(t) = C_f \left(\frac{\gamma}{\alpha}\right)^{1/2} \sqrt{t} \tag{3.3.3}$$

A summary of the obtained results with $\alpha = 0$ is given by Figure 3.8. In figure (a), the velocity seems to be an increasing linear function in the tissue domain, at any time. On the other hand, there is no great variation in amplitude. As a result, in figure (c), values $(r_{\text{mean}}(t_n, x_i), u(t_n, x_i))_{n,i}$ does not gather on a master curve. On a the contrary, at a given time, the effective cell radius is globally constant. Therefore, the tissue height, in figures (d) and (e), is globally constant in space, it slightly sags only near the front. This last effect and the loss of height over time show the presence of movement. In particular, the time it reaches the critical height h_c must be very large. Finally, figure (f) shows the front position with respect to time in log-log scale. We observe a linear curve close to $y = x$.

[10] More details in subsubsection 3.3.4.

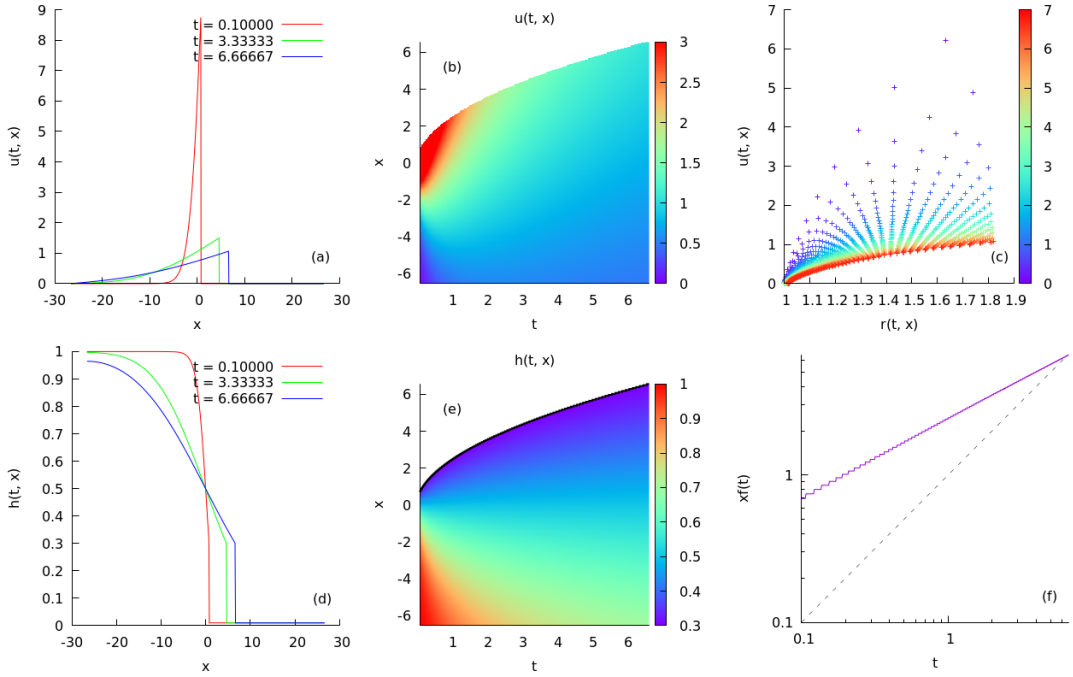

Figure 3.7: Summary of numerical results obtained with $\alpha = 10$ and $\gamma = 1.175 \cdot 10^2$. Figure (c) represents the velocity against the mean radius (expressed as $r_{\text{mean}} = h^{-1/2}$, as we saw in subsubsection 3.3.1) and a color corresponds to a specific time. Figure (f) shows the evolution of the front position over time, in log-log scale.

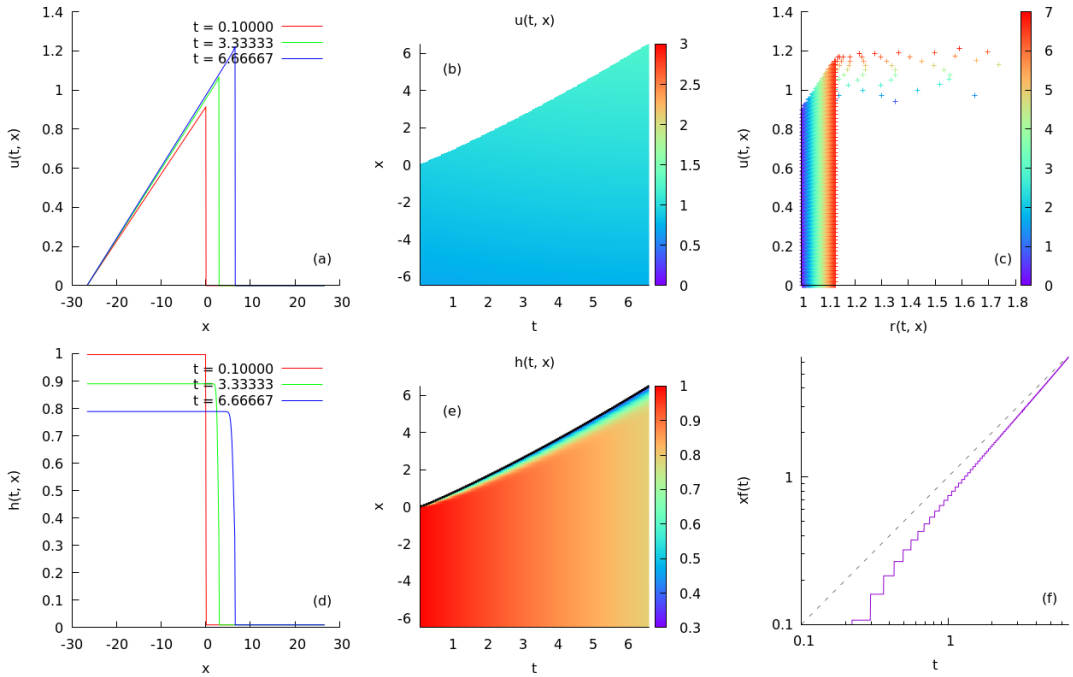

Figure 3.8: Summary of numerical results obtained with $\alpha = 0$ and $\gamma = 0.03$. Figure (c) represents the velocity against the mean radius (expressed as $r_{\text{mean}} = h^{-1/2}$, as we saw in subsubsection 3.3.1) and a color corresponds to a specific time. Figure (f) shows the evolution of the front position over time, in log-log scale.

A summary of the obtained results with $\alpha = 10^{-1}$ is given by Figure 3.9. In figures (a) and (b), we see that the velocity decreases in intensity at the front over time. More precisely, we first have a ramp with little growth (compared to what we had for $\alpha = 10$), localized at the front (short times), which then tends to sag and spread more and more evenly over the tissue domain $\Omega_c(t)$ (longer times). As a result, in figure (c), values $(r_{\text{mean}}(t_n, x_i), u(t_n, x_i))_{n,i}$ indeed gather on a master curve, that seems to be a square root. The tissue height, in figures (d) and (e), on the other hand, sags quickly, but not as much as for $\alpha = 10$. Finally, figure (f) shows the front position with respect to time in log-log scale. It can be seen as a juxtaposition of two curves, a sign of the existence of two regimes for this specific case, as shown in Figure 3.10. In particular, the second regime corresponds to an affine evolution of the front position.

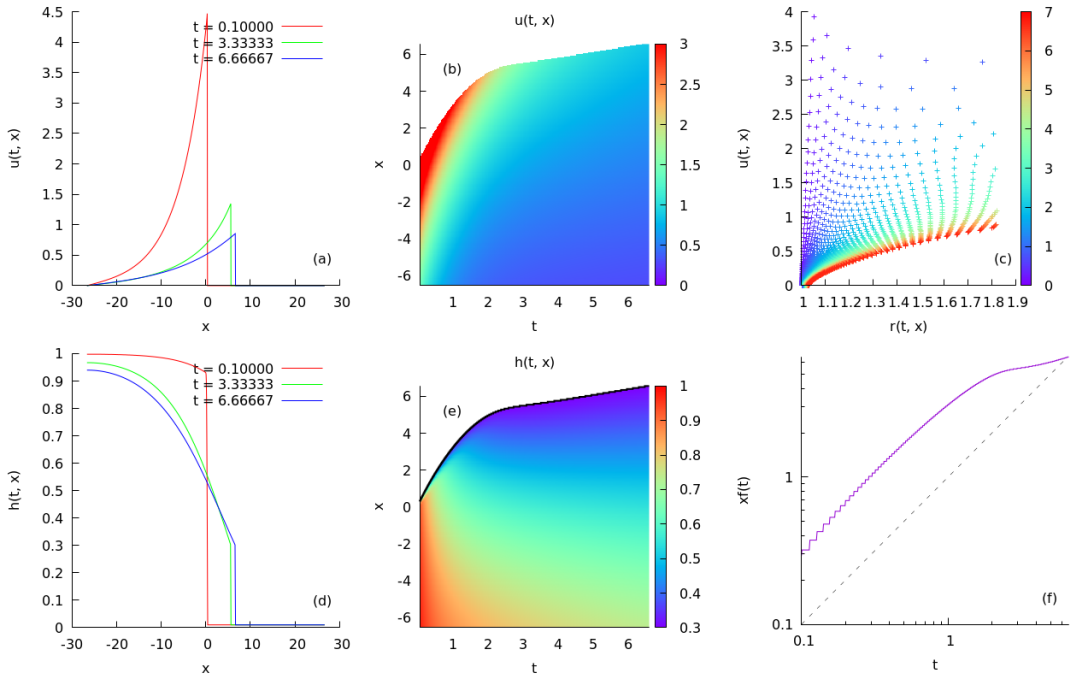

Figure 3.9: Summary of numerical results obtained with $\alpha = 10^{-1}$ and $\gamma = 7.8 \cdot 10^{-1}$. Figure (c) represents the velocity against the mean radius (expressed as $r_{\text{mean}} = h^{-1/2}$, as we saw in subsubsection 3.3.1) and a color corresponds to a specific time. Figure (f) shows the evolution of the front position over time, in log-log scale.

3.3.4 Discussion

Before discussing the solutions selected, we should return to the very validity of these solutions. Indeed, Figure 3.11 shows that the non post-processed height is likely to reach the right boundary of the domain before the end of the simulation. It also shows that if the solution is valid for sufficiently large α, which corresponds to a borderline case for which the dynamics do not change from one α to another, it will also be valid for the others, since the cells spread all the faster the larger α. Even though the $\alpha = 10$ solution sees the right boundary of the domain, this is not very troublesome if we compare to what we obtain with the large α model, presented in the appendix D.

The problem highlighted here is indeed a problem insofar as, as soon as the boundary is reached, the behavior of the solutions changes to satisfy the no-penetration condition. From a

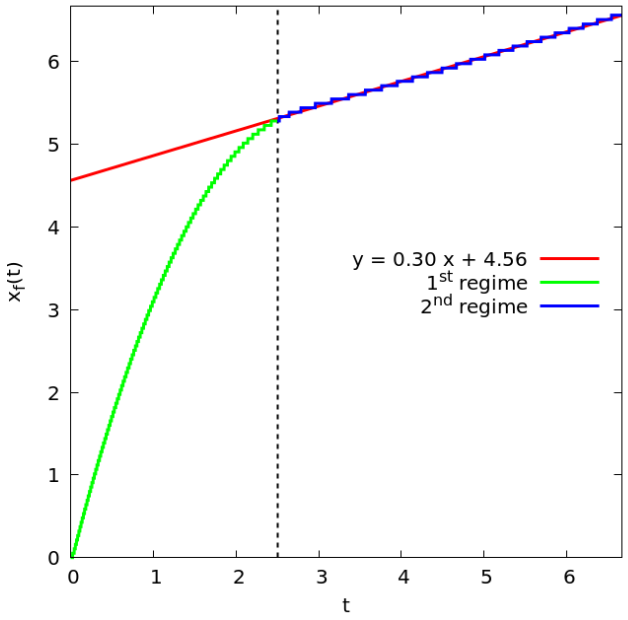

Figure 3.10: Front position with respect to time, obtained with $\alpha = 10^{-1}$ and $\gamma = 7.8 \cdot 10^{-1}$. The vertical dashed line separate the two identified regimes.

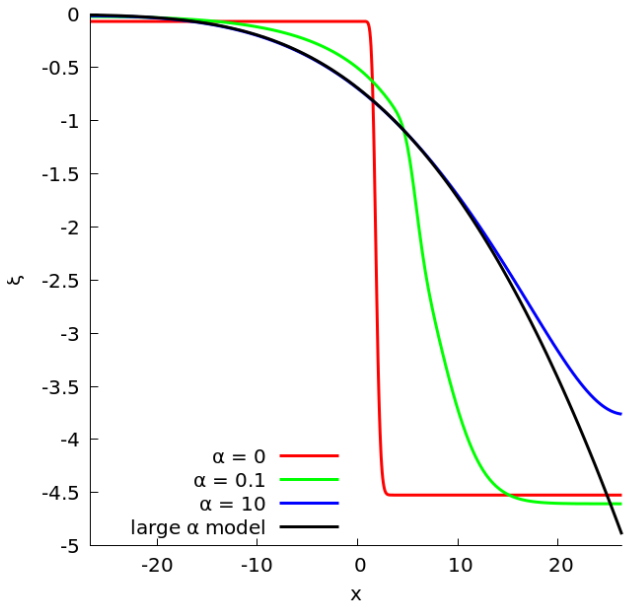

Figure 3.11: Numerical log-height ξ obtained with the three representative α at time $t = 5$. The curve reaches the right boundary of the domain before the end of the simulation and the solution is then influenced by the no-penetration condition. Black curve corresponds to the exact non post-processed height solution of the large α model, presented in appendix D.

physical point of view, this is unsatisfactory: the mechanics of the phenomenon will not change if the cells come critically close to the boundary. There are several possible causes for this effect. First of all, we could think about the critical height. Indeed, if it was directly processed by the numerical resolution, and not in post-processing, the cells would not reach the boundary in the time interval we have chosen. But that would only partially solve the problem. We could also think about the edge condition itself, which is obviously not suitable.

Let us come back to the simulations we made previously. They have highlighted three main types of behavior:

- When α is large, case previously represented by $\alpha = 10$, friction dominates over viscosity and the solutions converge toward the large α model, presented in appendix D. We can write the front position with respect to time as $C_f\sqrt{t}$, where C_f is a nonzero constant. Moreover, points $(r_{\text{mean}}(t_n, x_i), u(t_n, x_i))_{n,i}$ gather on a master curve.

- Conversely, when α is small enough, the friction is negligible with respect to viscosity and the solutions converge toward the limit case $\alpha = 0$. The front has a linear profile over time and no relation between the effective cell radius and the velocity can be deduced.

- Eventually, the hybrid case, previously represented by $\alpha = 10^{-1}$, highlights the existence of two regimes: a relatively short transitional regime and a permanent regime, in which the position of the front depends upon time in an affine way. Like the large α limit, points $(r_{\text{mean}}(t_n, x_i), u(t_n, x_i))_{n,i}$ gather on a master curve.

However, the small α case is not satisfactory as the friction cannot be neglected. The large α case can be ruled out as well. Indeed, Figure 3.12 (see also Figure 3.5) suggests us that, after an initial flow regime, the front position behaves as $x_f(t) = C_f t^a$, with $C_f \approx 0.6$ and $a \geqslant 1$. As a result, we consider the case $\alpha = 10^{-1}$ as the one that best fits the requirements we identified as important in subsubsection 3.3.2.

However, this case is far from perfect. First of all, the requirements are not fully fulfilled. Also, we notice that the velocity decreases in intensity at the front over time, unlike what we observe in Figure 3.4a. Either the active force generates a dynamic forcing the cells to slow down, or the absence of elasticity prevents an increase in this intensity, the two cases not being mutually exclusive. We said in subsubsection 1.4.2 it was convenient not to normalize the gradient of the height. On the other hand, the active force is sensitive to the gradient norm. Thus, except when α is small, although its norm increases as one approaches the front, helping to make speed an increasing function in space, at a fixed position close to the front it decreases due to the spread of the solution. As suggested during an internal discussion, a possible remedy would be to normalize the gradient in order to have a pure direction.

More generally, the model is not robust as shown at the beginning of the discussion. We suggested that we could have directly processed the height in the variational formulation. But this not that simple. Actually, we tried to put the indicator function directly into the form b_1 (see 2.2). For that purpose, we used a regularized Heaviside function. Unfortunately, the solution looked like a step function modeled on the mesh and was too sensitive to how to regulate the Heaviside's function, leading to convergence problems. This is why we have chosen to add a post-processing stage. This solution is not perfect because it induces a loss of height mass (understanding the area under the height curve) over time. For the final time chosen, the losses are not too important, of the order of 10 %, but for longer times, it would be prohibitive. That said, the model is not as bad as it could have been, given its simplicity.

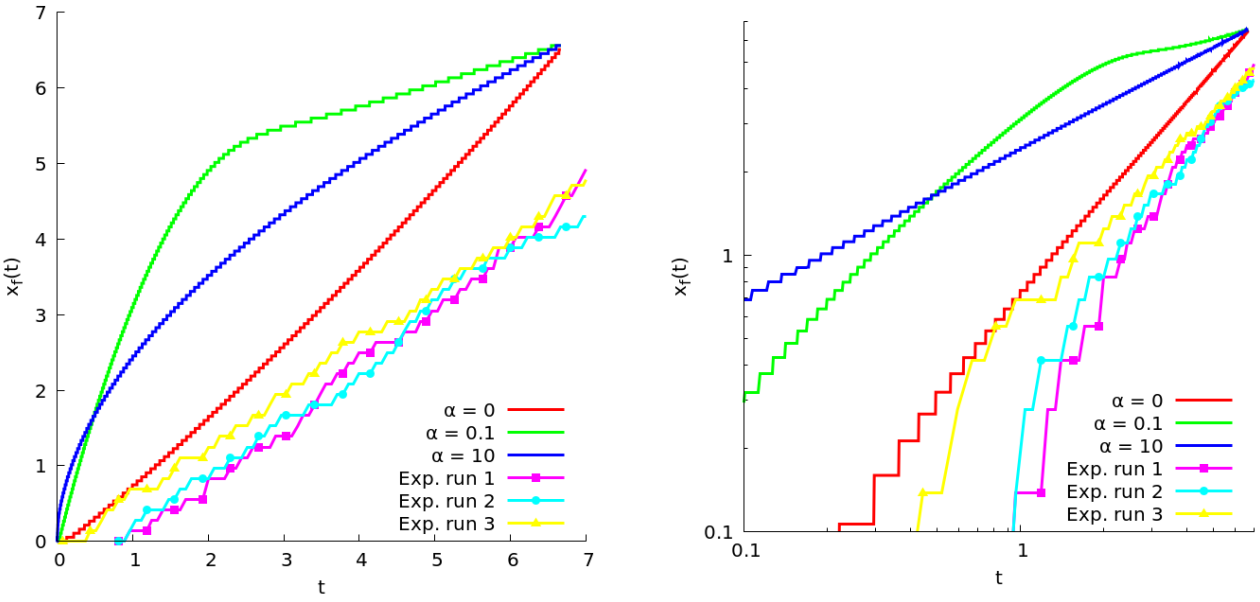

(a) (b) Log-log scale

Figure 3.12: Front positions over time for the different couples (α, γ) we have chosen and from the experimental data.

3.3.5 2D simulation

Since a 2D simulation is costly in computing time, we propose to run only one, with the best couple (α, γ) we identified, namely $\alpha = 10^{-1}$ and $\gamma = 0.78$. The resulting height at final time is presented in Figure 3.13 for the part of the domain where there are variations. It shows an increase in height upwind the obstacle. Probably, this means that the cells compress and get denser as they are slowed down by the obstacle. Finally, 3.14 illustrates the cell flow in 3D .

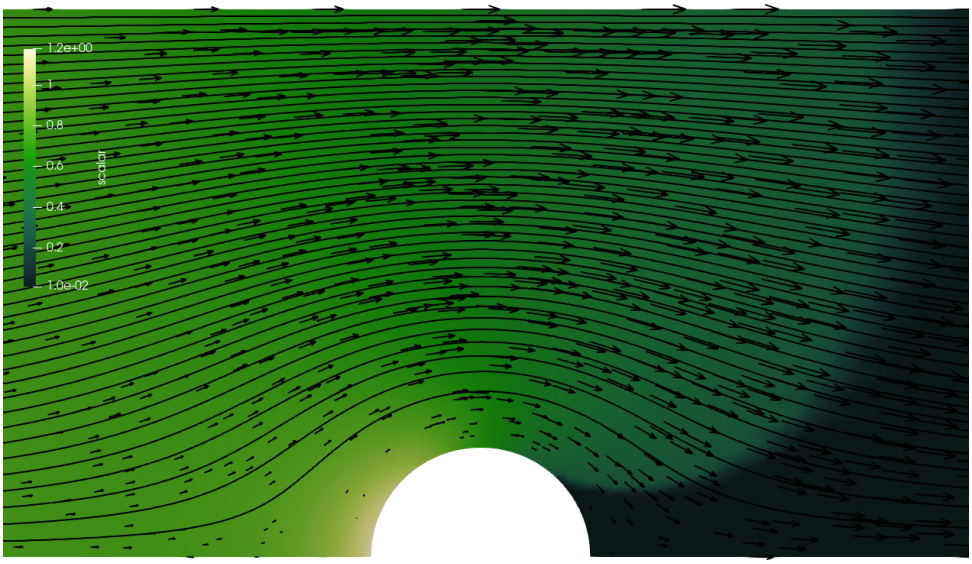

Figure 3.13: Numerical velocity and height around the obstacle at $t \approx t_f = {}^{20}/_{3}$, with $n_{\max} = 5000$ and $N = 5527$. The height is represented by the color gradient and the velocity by the vector field. There are also streamlines to show the flow movement.

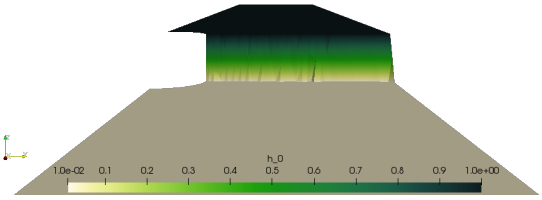

(a) $t = 0$

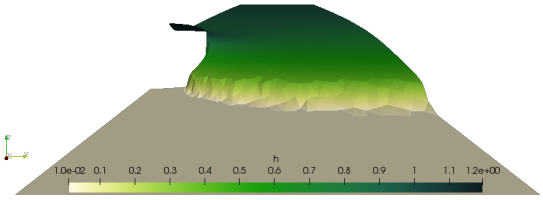

(b) $t \approx 1.24$

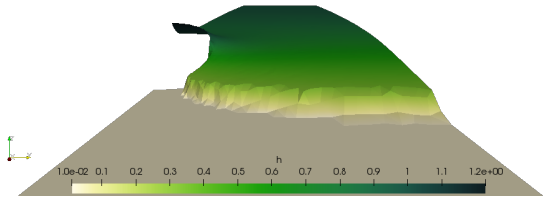

(c) $t \approx 2.59$

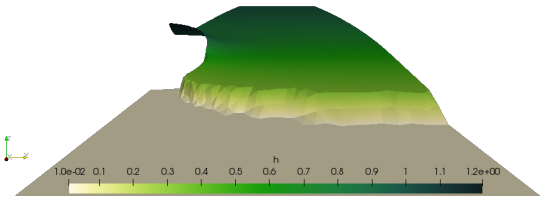

(d) $t \approx 3.95$

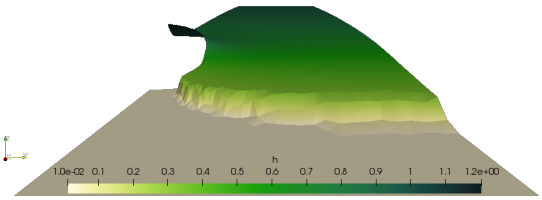

(e) $t \approx 5.31$

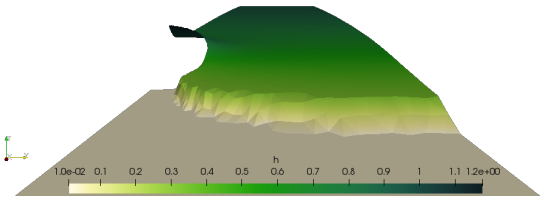

(f) $t \approx 6.67 \approx t_f = 20/3$

Figure 3.14: 3D view of the cell flow with the presence of an obstacle, where $n_{\max} = 5000$ and $N = 5527$.

Conclusion

In section 1, we set out the laws governing the viscoelastic behavior of epithelial tissues (1.2, 1.3 and 1.4). The resulting equations were then asymptotically approximated by a simpler model, invoking the low aspect ratio of the geometry. The numerical resolution of the resulting system was conducted in section 2 for the special case where elastic effects are neglected (i.e. $We = 0$). We discretized the problem in time using a fully implicit upwind scheme with variable time steps, to ensure stability of the latter if the initial condition is not sufficiently smooth (2.1.2 and 2.3). We also changed the variable for the height to ensure its positivity at any stage of the discretization (2.1.1). The space variable was done through a variational formulation of the problem discretized in time (2.2). In order to be able to approach the height by a discontinuous function, we used in particular a discontinuous Galerkin method (2.2.3). We then showed empirically in section 3 the convergence of our algorithm (3.2) before proposing a strategy of 1D comparison of the numerical results with the experimental data (3.3.2). This strategy consisted in using two experimental measurements: the position of the front with respect to time and the local relation between cell radius and cell velocity suggesting an alignment of the values on a master curve. We were then able to identify the set of parameters that best corresponded to the aforementioned constraints, given the experimental curves available to us (3.3.4).

These numerical experiments were able to highlight the limitations of the model and the numerical problems encountered. We have endeavored to cover the entire modelling chain: equation generation, transposition into algorithms and experimental validation. This overview allowed us to identify new perspectives or to clarify existing ones. The developments envisaged therefore affect both the mathematical model and its numerical resolution. As it stands, the model has failed to faithfully reproduce the experimental data, particularly the two points of interest to us. On the one hand, we can regret the lack of elasticity, an effect that requires further development. Working with $We > 0$ would lead to consider a tensor transport term. Numerically, we would come back to using the discontinuous Galerkin method but this is not a foregone conclusion: we would then have the height/elastic stress tensor coupling and, as suggested in Saramito [2020, subsection 5.3], we would surely have to consider a θ-scheme for discretization in time. On the other hand, the active force must greatly influence the dynamics, and its writing cannot be left to intuition alone. It must be chosen and handled with care. If possible, it must avoid the use of post-processing, among other things, so as not to cause a loss of mass over time. But this allowed us to see (3.3.4) that the actual no-penetration condition is unsatisfactory because the cells "see" the boundary coming, which tends to influence the behavior of the solution. A possible remedy would be to consider absorbing boundary conditions. That being said, it is clear that more complex effects must be taken into account in its expression. As mentioned in the introduction, one could think of polarity. Its coupling with the current viscoelastic model is in any case inevitable but remains an open question. Finally, a more in-depth study of migration behavior in the presence of an obstacle or in the context of a more exotic geometry would be beneficial. We have shown results in the particular case of a circular obstacle in a rectangular domain (3.3.5), but the ideal would be to consider any geometry and especially, if possible, complex geometries.

References

R. Alert and X. Trepat. Physical models of collective cell migration. *Annual Review of Condensed Matter Physics*, 11(1):77–101, Mar 2020. ISSN 1947-5462. doi: 10.1146/annurev-conmatphys-031218-013516. URL http://dx.doi.org/10.1146/annurev-conmatphys-031218-013516.

F. Bouchut and S. Boyaval. A new model for shallow viscoelastic fluids. *Mathematical Models and Methods in Applied Sciences*, 23(8):1479–1526, Jan. 2013. doi: 10.1142/S0218202513500140. URL https://hal-enpc.archives-ouvertes.fr/hal-00628651.

S. Chakraborty. Continuous mathematical models of cell migration. Master's thesis, Grenoble INP – Ensimag, 2019.

S. Gérald. *Discontinuous Galerkin method and implicit-explicit time integrations based on a decoupling of degrees of freedom. Applications to the system of Navier-Stokes equations.* Theses, Université Pierre et Marie Curie - Paris VI, Nov. 2013. URL https://tel.archives-ouvertes.fr/tel-00943621. Version internet: annexe G (p. 211-243) modifiée car contenu protégé.

P. Germain and P. Muller. *Introduction à la mécanique des milieux continus*. Masson, 2nd edition, 1995.

E. Maitre. Modèles et calcul d'interfaces, Fall semester 2010. Lecture notes.

P. Saramito. *Complex fluids*, volume 79 of *Mathématiques et Applications*. Springer International Publishing, first edition, 2016.

P. Saramito. Efficient C++ finite element computing with Rheolef. Lecture, Jan. 2020. URL https://cel.archives-ouvertes.fr/cel-00573970.

S. Tlili, M. Durande, C. Gay, B. Ladoux, F. Graner, and H. Delanoë-Ayari. A migrating epithelial monolayer flows like a maxwell viscoelastic liquid, 2018a. URL https://arxiv.org/abs/1811.05001. submitted paper.

S. Tlili, E. Gauquelin, B. Li, O. Cardoso, B. Ladoux, H. Delanoë-Ayari, and F. Graner. Collective cell migration without proliferation: density determines cell velocity and wave velocity. *Royal Society Open Science*, 5(5):172421, 2018b. doi: 10.1098/rsos.172421. URL https://royalsocietypublishing.org/doi/abs/10.1098/rsos.172421.

A Definitions

A.0.1 Characteristic curve

Let Ω be an open set of $\mathbb{R}^d$, $d \in \mathbb{N}^*$.

Definition A.1. The characteristic curve $\boldsymbol{X}(t, \boldsymbol{x}; \cdot)$ passing through position $\boldsymbol{x} \in \Omega$ at time $t \in [0, t_f]$ is the function satisfying the following ordinary differential equation:

$$\begin{cases} \partial_s \boldsymbol{X}(t, \boldsymbol{x}; s) = \boldsymbol{u}(s, \boldsymbol{X}(t, \boldsymbol{x}; s)), \ \forall s \in]0, t_f[\\ \quad \boldsymbol{X}(t, \boldsymbol{x}; t) = \boldsymbol{x} \end{cases} \tag{A.0.1}$$

From the Cauchy-Lipschitz theorem, this problem is well-posed, assuming at least that $\boldsymbol{u}$ is Lipschitzian, therefore the characteristic curve is uniquely defined.

A.0.2 External trace

We will use here the notations introduced in subsubsection 2.2.3.

Definition A.2. Let $q \in Q_h$ and $K \in \mathcal{T}_h$ be an element of the mesh. The external trace of q in K is the function q_{ext} defined on any face $S \subset \partial K$ by

$$\forall \boldsymbol{x}_S \in S, \quad q_{\text{ext}}(\boldsymbol{x}_S) = \begin{cases} \lim\limits_{\boldsymbol{x} \to \boldsymbol{x}_S} q_{/K}(\boldsymbol{x}) & \text{if } S \subset \partial\Omega \\ \lim\limits_{\boldsymbol{x} \to \boldsymbol{x}_S} q_{/K'}(\boldsymbol{x}) & \text{if } S \in \mathscr{S}_h^{(i)} \end{cases} \tag{A.0.2}$$

where $K' \in \mathcal{T}_h$ is the unique neighbor element of K such that $S = \partial K \cap \partial K'$.

This definition is actually an adaptation of the general one to our particular case. Saramito [2016, Section 4.10] proposes another specific definition when the trace of function is imposed by a Dirichlet boundary condition while you can find a more general one in Gérald [2013, § I.2.3.4.1].

B Integral rules

Theorem B.1 (Reynolds transport formulas)**.** *Let Ω be an open set of $\mathbb{R}^d$, $d \in \mathbb{N}^*$ and ω be an open, connected and bounded subset of Ω. Let $\omega(t) = \boldsymbol{X}(0, \omega; t)$, where $\boldsymbol{X}(0, \boldsymbol{x}; \cdot)$ is the characteristic curve passing through position $\boldsymbol{x} \in \omega$ at time $t = 0$ and $\boldsymbol{u}$ be a vector field defined in $\mathbb{R}_+ \times \Omega$. For any differentiable scalar field, vector field or tensor field defined in $\mathbb{R}_+ \times \Omega$, in all cases denoted by f, we have*

$$\frac{\mathrm{d}}{\mathrm{d}t} \int_{\omega(t)} f \, \mathrm{d}\boldsymbol{x} = \int_{\omega(t)} \partial_t f \, \mathrm{d}\boldsymbol{x} + \int_{\partial\omega(t)} (\boldsymbol{u} \cdot \boldsymbol{n}) f \, \mathrm{d}\boldsymbol{x} \tag{B.0.1}$$

In particular, by applying the Green formula, we have

$$\frac{\mathrm{d}}{\mathrm{d}t} \int_{\omega(t)} f \, \mathrm{d}\boldsymbol{x} = \int_{\omega(t)} (\partial_t f + \operatorname{div}(f\boldsymbol{u})) \, \mathrm{d}\boldsymbol{x} \tag{B.0.2}$$

when f is a scalar field and

$$\frac{\mathrm{d}}{\mathrm{d}t} \int_{\omega(t)} f \, \mathrm{d}\boldsymbol{x} = \int_{\omega(t)} (\partial_t f + \operatorname{div}(f \otimes \boldsymbol{u})) \, \mathrm{d}\boldsymbol{x} \tag{B.0.3}$$

when f is a vector field.

Theorem B.2 (Leibniz's Integral Rule)**.** *Let I and Ω be intervals of $\mathbb{R}$. Let $f : I \times \Omega \longrightarrow \mathbb{R}^d$ be a function such that*

- *$\partial_x f$ exists and is defined on $I \times \Omega$;*
- *both f and $\partial_x f$ are continuous on $I \times \Omega$;*
- *there exists an integrable function $g : I \longrightarrow \mathbb{R}_+$ such that for every $(t, x) \in I \times \Omega$,*

$$\left\| \frac{\partial f}{\partial x}(t, x) \right\| \leqslant g(t).$$

Let $a : \Omega \longrightarrow I$ and $b : \Omega \longrightarrow I$ be two differentiable functions on Ω. Then the following parametrized integral function F, defined on Ω by

$$F(x) = \int_{a(x)}^{b(x)} f(t, x) \mathrm{d}t$$

is differentiable and

$$F'(x) = f(b(x), x)b'(x) - f(a(x), x)a'(x) + \int_{a(x)}^{b(x)} \frac{\partial f}{\partial x}(t, x) \mathrm{d}t \tag{B.0.4}$$

Proof. Let $G : \mathbb{R}^3 \longrightarrow \mathbb{R}^d$ be the function defined by

$$G(u, v, x) = \int_u^v f(t, x) \mathrm{d}t$$

We remark that

$$F(x) = G(a(x), b(x), x)$$

Since G is differentiable with respect to each of its variables (thanks to the first fundamental theorem of calculus and the basic form of Leibniz's Integral Rule), F is also differentiable as function composed of differentiable functions. To compute the derivative of F, we thus have to apply the chain rule on G:

$$F'(x) = \frac{\partial G}{\partial u}(a(x), b(x), x)a'(x) + \frac{\partial G}{\partial v}(a(x), b(x), x)b'(x) + \frac{\partial G}{\partial x}(a(x), b(x), x)$$

Let us compute the partial derivatives of G. From the first fundamental theorem of calculus, we have

$$\frac{\partial G}{\partial u}(u, v, x) = -f(u, x)$$
$$\frac{\partial G}{\partial v}(u, v, x) = f(v, x)$$

and by the basic form of Leibniz's Integral Rule

$$\frac{\partial G}{\partial x}(u, v, x) = \int_u^v \frac{\partial f}{\partial x}(t, x) \mathrm{d}t$$

By replacing those quantities in the relation linking F' and the partial derivatives of G, we end up with the result. □

Corollary B.2.1. *Let I be an interval of $\mathbb{R}$, Ω be an interval of $\mathbb{R}$ and P be a rectangle of $\mathbb{R}^2$. Let $\boldsymbol{u} : P \longrightarrow \mathbb{R}^2$ be a vector field and $\varphi : I \times P \longrightarrow \mathbb{R}$ be a scalar field which satisfies all the hypotheses of Leibniz's Integral Rule with respect to both x and y. Let $a : P \longrightarrow I$ and $b : P \longrightarrow I$ be two differentiable functions on P. Then, for any $(x, y) \in P$*

$$(\boldsymbol{u}\cdot\nabla)\int_{a(x,y)}^{b(x,y)}\varphi(t,x,y)\mathrm{d}t = \int_{a(x,y)}^{b(x,y)}(\boldsymbol{u}\cdot\nabla)\varphi(t,x,y)\mathrm{d}t + [(\boldsymbol{u}\cdot\nabla)b(x,y)]\,\varphi(b(x,y),x,y) - [(\boldsymbol{u}\cdot\nabla)a(x,y)]\,\varphi(a(x,y),x,y) \tag{B.0.5}$$

Proof. From Leibniz's Integral Rule B.2 applied to φ, we have

$$u_x\partial_x\int_{a(x,y)}^{b(x,y)}\varphi(t,x,y)\mathrm{d}t = \int_{a(x,y)}^{b(x,y)}u_x\partial_x\varphi(t,x,y)\mathrm{d}t + \varphi(b(x,y),x,y)u_x\partial_x b(x,y) - \varphi(a(x,y),x,y)u_x\partial_x a(x,y)$$

We obtain the same kind of relation by differentiating with respect to y. Summing the two relations in x and y yields the result. □

Corollary B.2.2. *Let I be an interval of $\mathbb{R}$, Ω be an interval of $\mathbb{R}$ and P be a rectangle of $\mathbb{R}^2$. Let $\boldsymbol{u} : P \longrightarrow \mathbb{R}^2$ be a vector field and $\boldsymbol{v} : I \times P \longrightarrow \mathbb{R}^2$ be a vector field which satisfies all the hypotheses of Leibniz's Integral Rule with respect to both x and y. Let $a : P \longrightarrow I$ and $b : P \longrightarrow I$ be two differentiable functions on P. Then, for any $(x, y) \in P$*

$$(\boldsymbol{u}\cdot\nabla)\int_{a(x,y)}^{b(x,y)}\boldsymbol{v}(t,x,y)\mathrm{d}t = \int_{a(x,y)}^{b(x,y)}(\boldsymbol{u}\cdot\nabla)\boldsymbol{v}(t,x,y)\mathrm{d}t + [(\boldsymbol{u}\cdot\nabla)b(x,y)]\,\boldsymbol{v}(b(x,y),x,y) - [(\boldsymbol{u}\cdot\nabla)a(x,y)]\,\boldsymbol{v}(a(x,y),x,y) \tag{B.0.6}$$

$$\mathrm{div}\int_{a(x,y)}^{b(x,y)}\boldsymbol{v}(t,x,y)\mathrm{d}t = \int_{a(x,y)}^{b(x,y)}\mathrm{div}(\boldsymbol{v})(t,x,y)\mathrm{d}t + \boldsymbol{v}(b(x,y),x,y)\cdot\nabla b(x,y) - \boldsymbol{v}(a(x,y),x,y)\cdot\nabla a(x,y) \tag{B.0.7}$$

Proof.

- The first result is directly obtained from the corollary B.2.1 by using as φ any component of $\boldsymbol{v}$ and then summing.
- The second result is directly obtained from the corollary B.2.1 by using first $\varphi = v_x$ and $\boldsymbol{u} = \begin{pmatrix}1 & 0\end{pmatrix}^\top$ then $\varphi = v_y$ and $\boldsymbol{u} = \begin{pmatrix}0 & 1\end{pmatrix}^\top$. Summing the two relations in x and y yields the result.

□

Corollary B.2.3. *Let I be an interval of $\mathbb{R}$, Ω be an interval of $\mathbb{R}$ and P be a rectangle of $\mathbb{R}^2$. Let $\boldsymbol{u} : P \longrightarrow \mathbb{R}^2$ be a vector field and $\boldsymbol{\tau}$ be a second-order tensor defined on $I \times P$ which satisfies all the hypotheses of Leibniz's Integral Rule with respect to both x and y. Let $a : P \longrightarrow I$ and $b : P \longrightarrow I$ be two differentiable functions on P. Then, for any $(x, y) \in P$*

$$(\boldsymbol{u}\cdot\nabla)\int_{a(x,y)}^{b(x,y)}\boldsymbol{\tau}(t,x,y)\mathrm{d}t = \int_{a(x,y)}^{b(x,y)}(\boldsymbol{u}\cdot\nabla)\boldsymbol{\tau}(t,x,y)\mathrm{d}t + [(\boldsymbol{u}\cdot\nabla)b(x,y)]\,\boldsymbol{\tau}(b(x,y),x,y) - [(\boldsymbol{u}\cdot\nabla)a(x,y)]\,\boldsymbol{\tau}(a(x,y),x,y) \tag{B.0.8}$$

$$\mathbf{div}\int_{a(x,y)}^{b(x,y)}\boldsymbol{\tau}(t,x,y)\mathrm{d}t = \int_{a(x,y)}^{b(x,y)}\mathbf{div}(\boldsymbol{\tau})(t,x,y)\mathrm{d}t + \boldsymbol{\tau}(b(x,y),x,y)\cdot\nabla b(x,y) - \boldsymbol{\tau}(a(x,y),x,y)\cdot\nabla a(x,y) \tag{B.0.9}$$

Proof.

- The first result is directly obtained from the relation (B.0.6) of the corollary B.2.2 by using as $\boldsymbol{v}$ any line vector of $\boldsymbol{\tau}$ and then summing.
- The second result is obtained in exactly the same way from relation (B.0.6) of the corollary B.2.2.

□

C Proof of Theorem 1.1 – Thin-layer approximation

In what follows, a will be a generic scalar field, $\boldsymbol{a}$ a generic vector field and $\boldsymbol{\alpha}$ a generic tensor.

This proof leads to *a lot* of equations and it quickly becomes difficult to find their way around. To help the reader, every step distinguishes four types of equation: conservation laws, constitutive equations, boundary conditions and initial conditions. Moreover, there is a pattern – that starts at subsection C.1 and stops at subsection C.4 – in the equation numbering. Globally, an equation is numbered according to this pattern:

(C.<step>.<type_of_equation>x)

where x is a letter used to distinguish equations inside a same category. Here is the correspondence between the categories and the numbers:

Step	Splitting planar and vertical components	Dimensional analysis	Asymptotic expansion
number	1	2	3

Type of eq.	Conservation laws	Constitutive eq.	Boundary cond.	Initial cond.
number	1; 2	3; 4	5; 6; 7	8

C.1 Splitting planar and vertical components

The idea here is to prepare the forthcoming projection[11] of the three-dimensional $\Lambda(t)$ domain onto its two-dimensional counterpart Ω. We would like to find new relations for our variables, viewed as projections of those we have for the initial coupled system of evolutionary equations, i.e. that do not depend on the vertical component z. This will essentially be achieved by first splitting planar and vertical components then by integrating over $[0, h]$ the different equations we will obtain in the next subsections.

C.1.1 Conservation laws

$$\mathrm{div}_{\boldsymbol{s}}(\boldsymbol{u_s}) + \frac{\partial u_z}{\partial z} = 0 \tag{C.1.1}$$

[11] not in a geometrical sense but in a topological sense

$$\rho\left(\frac{\partial \boldsymbol{u_s}}{\partial t} + (\boldsymbol{u_s}\cdot\nabla_s)\boldsymbol{u_s}\right) - \mathbf{div}_s(\boldsymbol{\sigma_s}) - \frac{\partial \boldsymbol{\sigma_{sz}}}{\partial z} = \mathbf{0} \tag{C.1.2a}$$

$$\rho\left(\frac{\partial u_z}{\partial t} + (\boldsymbol{u_s}\cdot\nabla_s)u_z\right) - \mathrm{div}_s(\boldsymbol{\sigma_{sz}}) - \frac{\partial \sigma_{zz}}{\partial z} = 0 \tag{C.1.2b}$$

C.1.2 Constitutive equations

$$\boldsymbol{\sigma_s} = \boldsymbol{\tau_s} + 2\eta_s\,\boldsymbol{D_s}(\boldsymbol{u_s}) - p\mathbf{I_s} \tag{C.1.3a}$$

$$\boldsymbol{\sigma_{sz}} = \boldsymbol{\tau_{sz}} + \eta_s\left(\frac{\partial \boldsymbol{u_s}}{\partial z} + \nabla_s u_z\right) \tag{C.1.3b}$$

$$\sigma_{zz} = \tau_{zz} + 2\eta_s\frac{\partial u_z}{\partial z} - p \tag{C.1.3c}$$

$$\lambda\Bigg[\ \frac{\partial \boldsymbol{\tau_s}}{\partial t} + (\boldsymbol{u_s}\cdot\nabla_s)\boldsymbol{\tau_s} - (\nabla_s\boldsymbol{u_s})\boldsymbol{\tau_s} - \boldsymbol{\tau_s}(\nabla_s\boldsymbol{u_s})^\top - \frac{\partial \boldsymbol{u_s}}{\partial z}\otimes\boldsymbol{\tau_{sz}} - \boldsymbol{\tau_{sz}}\otimes\frac{\partial \boldsymbol{u_s}}{\partial z}\ \Bigg] + \boldsymbol{\tau_s} = 2\eta_m\,\boldsymbol{D_s}(\boldsymbol{u_s}) \tag{C.1.4a}$$

$$\lambda\Bigg[\ \frac{\partial \boldsymbol{\tau_{sz}}}{\partial t} + (\boldsymbol{u_s}\cdot\nabla_s)\boldsymbol{\tau_{sz}} - (\nabla_s\boldsymbol{u_s})\boldsymbol{\tau_{sz}} - \boldsymbol{\tau_s}(\nabla_s u_z) - \frac{\partial \boldsymbol{u_s}}{\partial z}\tau_{zz} - \boldsymbol{\tau_{sz}}\frac{\partial u_z}{\partial z}\ \Bigg] + \boldsymbol{\tau_{sz}} = \eta_m\left(\frac{\partial \boldsymbol{u_s}}{\partial z} + \nabla_s u_z\right) \tag{C.1.4b}$$

$$\lambda\left[\ \frac{\partial \tau_{zz}}{\partial t} + (\boldsymbol{u_s}\cdot\nabla_s)\tau_{zz} - 2\nabla_s u_z\cdot\boldsymbol{\tau_{sz}} - 2\frac{\partial u_z}{\partial z}\tau_{zz}\ \right] + \tau_{zz} = 2\eta_m\frac{\partial u_z}{\partial z} \tag{C.1.4c}$$

C.1.3 Boundary conditions

On $]0,t_f[\times\Gamma_f(t)$:

$$\frac{\partial h}{\partial t} + (\boldsymbol{u_s}\cdot\nabla_s)h - u_z = 0 \tag{C.1.5a}$$

$$-\boldsymbol{\sigma_s}(\nabla_s h) + \boldsymbol{\sigma_{sz}} = \mathbf{0} \tag{C.1.5b}$$

$$-\boldsymbol{\sigma_{sz}}\cdot\nabla_s h + \sigma_{zz} = 0 \tag{C.1.5c}$$

On $]0,t_f[\times\Gamma_0$:

$$-u_z = 0 \tag{C.1.6a}$$

$$-\boldsymbol{\sigma_{sz}} + \zeta\boldsymbol{u_s} = \boldsymbol{f}_a \tag{C.1.6b}$$

On $]0,t_f[\times\Gamma(t)$:

$$(\boldsymbol{\sigma}_s\boldsymbol{n}_s)_{t,s} + ((\boldsymbol{\sigma}_{sz})_{t,s} - (\boldsymbol{\sigma}_{sz}\cdot\boldsymbol{n}_s)\boldsymbol{n}_s - \sigma_{zz}n_z\boldsymbol{n}_s)n_z = \mathbf{0}$$
$$\boldsymbol{\sigma}_{sz}\cdot\boldsymbol{n}_s + (\sigma_{zz} - (\boldsymbol{\sigma}_s\boldsymbol{n}_s)\cdot\boldsymbol{n}_s)n_z + (\sigma_{zz}n_z - 2\boldsymbol{\sigma}_{sz}\cdot\boldsymbol{n}_s)n_z^2 = 0$$

If $\Gamma(t)$ is regular enough, then $\boldsymbol{n}$ is collinear to $\begin{pmatrix}\boldsymbol{\nu} & 0\end{pmatrix}^\top$, where $\boldsymbol{\nu}$ is the outer unit normal vector to Ω on $\partial\Omega$. As a consequence, $\boldsymbol{n_s}$ does not depend on z. Then, it exists a scalar field $C > 0$ such that

$$\boldsymbol{n_s} = C\boldsymbol{\nu}$$

Actually, we can give an explicit form to C. Indeed, since $\|\boldsymbol{n}\|_2 = \|\boldsymbol{\nu}\|_2 = 1$, we end up with $C^2 + n_z^2 = 1$ then $C = \sqrt{1-n_z^2} \in]0,1]$ since $n_z \in [0,1[$. By replacing n_s in the previous relations and adding the boundary condition for the velocity, we obtain

$$\boldsymbol{u_s}\cdot\boldsymbol{\nu} = 0 \tag{C.1.7a}$$
$$C\boldsymbol{\sigma}_s\boldsymbol{\nu} - C^3((\boldsymbol{\sigma}_s\boldsymbol{\nu})\cdot\boldsymbol{\nu})\boldsymbol{\nu} + \Big(\boldsymbol{\sigma}_{sz} - 2C^2(\boldsymbol{\sigma}_{sz}\cdot\boldsymbol{\nu})\boldsymbol{\nu} - C\sigma_{zz}n_z\boldsymbol{\nu}\Big)n_z = \mathbf{0} \tag{C.1.7b}$$
$$C\boldsymbol{\sigma}_{sz}\cdot\boldsymbol{\nu} + (\sigma_{zz} - C^2(\boldsymbol{\sigma}_s\boldsymbol{\nu})\cdot\boldsymbol{\nu})n_z + (\sigma_{zz}n_z - 2C\boldsymbol{\sigma}_{sz}\cdot\boldsymbol{\nu})n_z^2 = 0 \tag{C.1.7c}$$

C.1.4 Initial conditions

On Γ_0 :

$$h(0,\cdot) = h_0 \tag{C.1.8a}$$

In $\Lambda(0)$:

$$\boldsymbol{u_s}(0,\cdot) = \boldsymbol{u}_{0,s} \tag{C.1.8b}$$
$$u_z(0,\cdot) = u_{0,z} \tag{C.1.8c}$$

In $\Lambda(0)$:

$$\boldsymbol{\tau_s}(0,\cdot) = \boldsymbol{\tau}_{0,s} \tag{C.1.8d}$$
$$\boldsymbol{\tau}_{sz}(0,\cdot) = \boldsymbol{\tau}_{0,sz} \tag{C.1.8e}$$
$$\tau_{zz}(0,\cdot) = \tau_{0,zz} \tag{C.1.8f}$$

C.2 Dimensional Analysis

For notation convenience, we will drop the tilde in what follows. The following table shows how we proceed the nondimensionalization of the equations in practice:

With dimension	Without dimension
a	$A\,a$
$\partial_t a$	${}^{A}/_{T}\;\partial_t a$
$\partial_z a$	${}^{A}/_{H}\;\partial_z a$
$\nabla_s a$	${}^{1}/_{L}\;\nabla_s a$
$\mathrm{div}_s\boldsymbol{a}$	${}^{1}/_{L}\;\mathrm{div}_s\boldsymbol{a}$

where A is the characteristic quantity associated with the scalar field a. These relations can be easily generalized for a vector field or a tensor.

C.2.1 Conservation laws

$$\mathrm{div}_s(\boldsymbol{u_s}) + \frac{\partial u_z}{\partial z} = 0 \tag{C.2.1}$$

$$\rho\left(\frac{U}{T}\frac{\partial \boldsymbol{u_s}}{\partial t}+\frac{U^2}{L}(\boldsymbol{u_s}\cdot\nabla_s)\boldsymbol{u_s}+\frac{VU}{H}u_z\frac{\partial \boldsymbol{u_s}}{\partial z}\right)-\frac{\Sigma}{L}\mathbf{div}_s(\boldsymbol{\sigma_s})-\frac{\Sigma}{H}\frac{\partial \boldsymbol{\sigma}_{sz}}{\partial z}=\mathbf{0}$$
$$\rho\left(\frac{V}{T}\frac{\partial u_z}{\partial t}+\frac{UV}{L}(\boldsymbol{u_s}\cdot\nabla_s)u_z+\frac{V^2}{H}u_z\frac{\partial u_z}{\partial z}\right)-\frac{\Sigma}{L}\mathrm{div}_s(\boldsymbol{\sigma}_{sz})-\frac{\Sigma}{H}\frac{\partial \sigma_{zz}}{\partial z}=0$$

By expressing everything in terms of U, L, ε and η, we end up with

$$\rho\left(\frac{U^2}{L}\frac{\partial \boldsymbol{u_s}}{\partial t}+\frac{U^2}{L}(\boldsymbol{u_s}\cdot\nabla_s)\boldsymbol{u_s}+\frac{U^2}{L}u_z\frac{\partial \boldsymbol{u_s}}{\partial z}\right)-\frac{\eta U}{L^2}\mathbf{div}_s(\boldsymbol{\sigma_s})-\frac{\eta U}{\varepsilon L^2}\frac{\partial \boldsymbol{\sigma}_{sz}}{\partial z}=\mathbf{0}$$
$$\rho\left(\frac{\varepsilon U^2}{L}\frac{\partial u_z}{\partial t}+\frac{\varepsilon U^2}{L}(\boldsymbol{u_s}\cdot\nabla_s)u_z+\frac{\varepsilon U^2}{L}u_z\frac{\partial u_z}{\partial z}\right)-\frac{\eta U}{L^2}\mathrm{div}_s(\boldsymbol{\sigma}_{sz})-\frac{\eta U}{\varepsilon L^2}\frac{\partial \sigma_{zz}}{\partial z}=0$$

By multiplying both sides in each equation by $\varepsilon\frac{L^2}{U\eta}$, we finally get

$$\varepsilon Re\left(\frac{\partial \boldsymbol{u_s}}{\partial t}+(\boldsymbol{u_s}\cdot\nabla_s)\boldsymbol{u_s}+u_z\frac{\partial \boldsymbol{u_s}}{\partial z}\right)-\varepsilon\mathbf{div}_s(\boldsymbol{\sigma_s})-\frac{\partial \boldsymbol{\sigma}_{sz}}{\partial z}=\mathbf{0} \tag{C.2.2a}$$
$$\varepsilon^2 Re\left(\frac{\partial u_z}{\partial t}+(\boldsymbol{u_s}\cdot\nabla_s)u_z+u_z\frac{\partial u_z}{\partial z}\right)-\varepsilon\mathrm{div}_s(\boldsymbol{\sigma}_{sz})-\frac{\partial \sigma_{zz}}{\partial z}=0 \tag{C.2.2b}$$

C.2.2 Constitutive equations

$$\boldsymbol{\sigma_s}=\boldsymbol{\tau_s}+2(1-\beta)\,\boldsymbol{D_s}(\boldsymbol{u_s})-p\mathbf{I_s} \tag{C.2.3a}$$
$$\varepsilon\boldsymbol{\sigma}_{sz}=\varepsilon\boldsymbol{\tau}_{sz}+(1-\beta)\left(\frac{\partial \boldsymbol{u_s}}{\partial z}+\varepsilon^2\nabla_s u_z\right) \tag{C.2.3b}$$
$$\sigma_{zz}=\tau_{zz}+2(1-\beta)\frac{\partial u_z}{\partial z}-p \tag{C.2.3c}$$

$$\begin{aligned}\varepsilon We\Big[\frac{\partial \boldsymbol{\tau_s}}{\partial t}&+(\boldsymbol{u_s}\cdot\nabla_s)\boldsymbol{\tau_s}\\ &-(\nabla_s\boldsymbol{u_s})\boldsymbol{\tau_s}-\boldsymbol{\tau_s}(\nabla_s\boldsymbol{u_s})^\top\Big]-We\left(\frac{\partial \boldsymbol{u_s}}{\partial z}\otimes\boldsymbol{\tau}_{sz}+\boldsymbol{\tau}_{sz}\otimes\frac{\partial \boldsymbol{u_s}}{\partial z}\right)\\ &+\varepsilon\boldsymbol{\tau_s}=2\varepsilon\beta\,\boldsymbol{D_s}(\boldsymbol{u_s})\end{aligned} \tag{C.2.4a}$$

$$\begin{aligned}\varepsilon We\Big[\frac{\partial \boldsymbol{\tau}_{sz}}{\partial t}&+(\boldsymbol{u_s}\cdot\nabla_s)\boldsymbol{\tau}_{sz}\\ &-\left(\nabla_s\boldsymbol{u_s}+\frac{\partial u_z}{\partial z}\mathbf{I_s}\right)\boldsymbol{\tau}_{sz}-\varepsilon\boldsymbol{\tau_s}(\nabla_s u_z)\Big]-We\frac{\partial \boldsymbol{u_s}}{\partial z}\tau_{zz}\\ &+\varepsilon\boldsymbol{\tau}_{sz}=\beta\left(\frac{\partial \boldsymbol{u_s}}{\partial z}+\varepsilon^2\nabla_s u_z\right)\end{aligned} \tag{C.2.4b}$$

$$We\left[\frac{\partial \tau_{zz}}{\partial t}+(\boldsymbol{u_s}\cdot\nabla_s)\tau_{zz}-2\varepsilon\nabla_s u_z\cdot\boldsymbol{\tau}_{sz}-2\frac{\partial u_z}{\partial z}\tau_{zz}\right]+\tau_{zz}=2\beta\frac{\partial u_z}{\partial z} \tag{C.2.4c}$$

C.2.3 Boundary conditions

On $]0, t_f[\times\Gamma_f(t)$:

$$\frac{\partial h}{\partial t} + (\boldsymbol{u_s}\cdot\nabla_{\boldsymbol{s}})h - u_z = 0 \tag{C.2.5a}$$
$$-\varepsilon\boldsymbol{\sigma_s}(\nabla_{\boldsymbol{s}}h) + \boldsymbol{\sigma_{sz}} = \boldsymbol{0} \tag{C.2.5b}$$
$$-\varepsilon\boldsymbol{\sigma_{sz}}\cdot\nabla_{\boldsymbol{s}}h + \sigma_{zz} = 0 \tag{C.2.5c}$$

On $]0, t_f[\times\Gamma_0$:

$$-u_z = 0 \tag{C.2.6a}$$
$$-\boldsymbol{\sigma_{sz}} + \varepsilon\alpha\boldsymbol{u_s} = \boldsymbol{f}_a \tag{C.2.6b}$$

On $]0, t_f[\times\Gamma(t)$:

$$\boldsymbol{u_s}\cdot\boldsymbol{\nu} = 0 \tag{C.2.7a}$$
$$C\boldsymbol{\sigma_s}\boldsymbol{\nu} - C^3((\boldsymbol{\sigma_s}\boldsymbol{\nu})\cdot\boldsymbol{\nu})\boldsymbol{\nu} + \Big(\boldsymbol{\sigma_{sz}} - 2C^2(\boldsymbol{\sigma_{sz}}\cdot\boldsymbol{\nu})\boldsymbol{\nu} - C\sigma_{zz}n_z\boldsymbol{\nu}\Big)n_z = \boldsymbol{0} \tag{C.2.7b}$$
$$C\boldsymbol{\sigma_{sz}}\cdot\boldsymbol{\nu} + (\sigma_{zz} - C^2(\boldsymbol{\sigma_s}\boldsymbol{\nu})\cdot\boldsymbol{\nu})n_z + (\sigma_{zz}n_z - 2C\boldsymbol{\sigma_{sz}}\cdot\boldsymbol{\nu})n_z^2 = 0 \tag{C.2.7c}$$

C.2.4 Initial conditions

On Γ_0 :

$$h(0,\cdot) = h_0 \tag{C.2.8a}$$

In $\Lambda(0)$:

$$\boldsymbol{u_s}(0,\cdot) = \boldsymbol{u}_{0,s} \tag{C.2.8b}$$
$$u_z(0,\cdot) = u_{0,z} \tag{C.2.8c}$$

In $\Lambda(0)$:

$$\boldsymbol{\tau_s}(0,\cdot) = \boldsymbol{\tau}_{0,s} \tag{C.2.8d}$$
$$\boldsymbol{\tau_{sz}}(0,\cdot) = \boldsymbol{\tau}_{0,sz} \tag{C.2.8e}$$
$$\tau_{zz}(0,\cdot) = \tau_{0,zz} \tag{C.2.8f}$$

C.3 Asymptotic expansion

C.3.1 Conservation laws

$$\mathrm{div}_{\boldsymbol{s}}(\boldsymbol{u_s}^{(0)} + \varepsilon\boldsymbol{u_s}^{(1)} + \boldsymbol{O}(\varepsilon^2)) + \frac{\partial\Big(u_z^{(0)} + \varepsilon u_z^{(1)} + O(\varepsilon^2)\Big)}{\partial z} = 0$$

By using hypothesis (i) and the linearity of the differential operators, by remarking that any differential operator in time or space applied on a $O(\varepsilon^2)$ remains a $O(\varepsilon^2)$ and by considering the previous equality as a polynomial equality whose variable is ε, we obtain the system of equations

$$\mathrm{div}_{\boldsymbol{s}}(\boldsymbol{u_s}^{(0)}) + \frac{\partial u_z^{(0)}}{\partial z} = 0 \tag{C.3.1a}$$
$$\mathrm{div}_{\boldsymbol{s}}(\boldsymbol{u_s}^{(1)}) + \frac{\partial u_z^{(1)}}{\partial z} = 0 \tag{C.3.1b}$$

$$\frac{\partial \boldsymbol{\sigma}_{\boldsymbol{s}z}^{(0)}}{\partial z} = \mathbf{0} \tag{C.3.2a}$$

$$Re\left(\frac{\partial \boldsymbol{u}_{\boldsymbol{s}}^{(0)}}{\partial t} + (\boldsymbol{u}_{\boldsymbol{s}}^{(0)} \cdot \nabla_{\boldsymbol{s}})\boldsymbol{u}_{\boldsymbol{s}}^{(0)} + u_z^{(0)}\frac{\partial \boldsymbol{u}_{\boldsymbol{s}}^{(0)}}{\partial z}\right) - \mathbf{div}_{\boldsymbol{s}}(\boldsymbol{\sigma}_{\boldsymbol{s}}^{(0)}) - \frac{\partial \boldsymbol{\sigma}_{\boldsymbol{s}z}^{(1)}}{\partial z} = \mathbf{0} \tag{C.3.2b}$$

$$\frac{\partial \sigma_{zz}^{(0)}}{\partial z} = 0 \tag{C.3.2c}$$

$$\mathrm{div}_{\boldsymbol{s}}\left(\boldsymbol{\sigma}_{\boldsymbol{s}z}^{(0)}\right) + \frac{\partial \sigma_{zz}^{(1)}}{\partial z} = 0 \tag{C.3.2d}$$

C.3.2 Constitutive equations

$$\boldsymbol{\sigma}_{\boldsymbol{s}}^{(0)} - \boldsymbol{\tau}_{\boldsymbol{s}}^{(0)} - 2(1-\beta)\,\boldsymbol{D}_{\boldsymbol{s}}(\boldsymbol{u}_{\boldsymbol{s}}^{(0)}) + p^{(0)}\mathbf{I}_{\boldsymbol{s}} = \mathbf{0} \tag{C.3.3a}$$

$$\boldsymbol{\sigma}_{\boldsymbol{s}}^{(1)} - \boldsymbol{\tau}_{\boldsymbol{s}}^{(1)} - 2(1-\beta)\,\boldsymbol{D}_{\boldsymbol{s}}(\boldsymbol{u}_{\boldsymbol{s}}^{(1)}) + p^{(1)}\mathbf{I}_{\boldsymbol{s}} = \mathbf{0} \tag{C.3.3b}$$

$$(1-\beta)\frac{\partial \boldsymbol{u}_{\boldsymbol{s}}^{(0)}}{\partial z} = \mathbf{0} \tag{C.3.3c}$$

$$\boldsymbol{\sigma}_{\boldsymbol{s}z}^{(0)} - \boldsymbol{\tau}_{\boldsymbol{s}z}^{(0)} - (1-\beta)\frac{\partial \boldsymbol{u}_{\boldsymbol{s}}^{(1)}}{\partial z} = \mathbf{0} \tag{C.3.3d}$$

$$\sigma_{zz}^{(0)} - \tau_{zz}^{(0)} - 2(1-\beta)\frac{\partial u_z^{(0)}}{\partial z} + p^{(0)} = 0 \tag{C.3.3e}$$

$$\sigma_{zz}^{(1)} - \tau_{zz}^{(1)} - 2(1-\beta)\frac{\partial u_z^{(1)}}{\partial z} + p^{(1)} = 0 \tag{C.3.3f}$$

$$-We\left(\frac{\partial \boldsymbol{u}_s^{(0)}}{\partial z}\otimes\boldsymbol{\tau}_{sz}^{(0)}+\boldsymbol{\tau}_{sz}^{(0)}\otimes\frac{\partial \boldsymbol{u}_s^{(0)}}{\partial z}\right)=\mathbf{0} \tag{C.3.4a}$$

$$\begin{aligned}We\left[\frac{\partial\boldsymbol{\tau}_s^{(0)}}{\partial t}+\left(\boldsymbol{u}_s^{(0)}\cdot\nabla_s+u_z^{(0)}\frac{\partial}{\partial z}\right)\boldsymbol{\tau}_s^{(0)}-(\nabla_s\boldsymbol{u}_s^{(0)})\boldsymbol{\tau}_s^{(0)}-\boldsymbol{\tau}_s^{(0)}(\nabla_s\boldsymbol{u}_s^{(0)})^\top\right]\\ -We\left(\frac{\partial \boldsymbol{u}_s^{(1)}}{\partial z}\otimes\boldsymbol{\tau}_{sz}^{(0)}+\frac{\partial \boldsymbol{u}_s^{(0)}}{\partial z}\otimes\boldsymbol{\tau}_{sz}^{(1)}+\boldsymbol{\tau}_{sz}^{(1)}\otimes\frac{\partial \boldsymbol{u}_s^{(0)}}{\partial z}+\boldsymbol{\tau}_{sz}^{(0)}\otimes\frac{\partial \boldsymbol{u}_s^{(1)}}{\partial z}\right)\\ +\boldsymbol{\tau}_s^{(0)}-2\beta\,\boldsymbol{D}_s(\boldsymbol{u}_s^{(0)})=\mathbf{0}\end{aligned} \tag{C.3.4b}$$

$$-We\frac{\partial \boldsymbol{u}_s^{(0)}}{\partial z}\tau_{zz}^{(0)}-\beta\frac{\partial \boldsymbol{u}_s^{(0)}}{\partial z}=\mathbf{0} \tag{C.3.4c}$$

$$\begin{aligned}We\left[\frac{\partial\boldsymbol{\tau}_{sz}^{(0)}}{\partial t}+\left(\boldsymbol{u}_s^{(0)}\cdot\nabla_s+u_z^{(0)}\frac{\partial}{\partial z}\right)\boldsymbol{\tau}_{sz}^{(0)}-\left(\nabla_s\boldsymbol{u}_s^{(0)}+\frac{\partial u_z^{(0)}}{\partial z}\mathbf{I}_s\right)\boldsymbol{\tau}_{sz}^{(0)}\right]\\ -We\left(\frac{\partial \boldsymbol{u}_s^{(1)}}{\partial z}\tau_{zz}^{(0)}+\frac{\partial \boldsymbol{u}_s^{(0)}}{\partial z}\tau_{zz}^{(1)}\right)+\boldsymbol{\tau}_{sz}^{(0)}-\beta\frac{\partial \boldsymbol{u}_s^{(1)}}{\partial z}=\mathbf{0}\end{aligned} \tag{C.3.4d}$$

$$We\left[\frac{\partial\tau_{zz}^{(0)}}{\partial t}+\left(\boldsymbol{u}_s^{(0)}\cdot\nabla_s+u_z^{(0)}\frac{\partial}{\partial z}\right)\tau_{zz}^{(0)}-2\frac{\partial u_z^{(0)}}{\partial z}\tau_{zz}^{(0)}\right]+\tau_{zz}^{(0)}-2\beta\frac{\partial u_z^{(0)}}{\partial z}=0 \tag{C.3.4e}$$

$$\begin{aligned}We\left[\frac{\partial\tau_{zz}^{(1)}}{\partial t}+\left(\boldsymbol{u}_s^{(1)}\cdot\nabla_s+u_z^{(1)}\frac{\partial}{\partial z}\right)\tau_{zz}^{(0)}\right.\\ +\left(\boldsymbol{u}_s^{(0)}\cdot\nabla_s+u_z^{(0)}\frac{\partial}{\partial z}\right)\tau_{zz}^{(1)}-2\nabla_s u_z^{(0)}\cdot\boldsymbol{\tau}_{sz}^{(0)}\\ \left.-2\frac{\partial u_z^{(1)}}{\partial z}\tau_{zz}^{(0)}-2\frac{\partial u_z^{(0)}}{\partial z}\tau_{zz}^{(1)}\right]-\tau_{zz}^{(1)}-2\beta\frac{\partial u_z^{(1)}}{\partial z}=0\end{aligned} \tag{C.3.4f}$$

C.3.3 Boundary conditions

On $]0,t_f[\times\Gamma_f(t)$:

$$\frac{\partial h}{\partial t}+(\boldsymbol{u}_s^{(0)}\cdot\nabla_s)h-u_z^{(0)}=0 \tag{C.3.5a}$$

$$\boldsymbol{\sigma}_{sz}^{(0)}=\mathbf{0} \tag{C.3.5b}$$

$$-\boldsymbol{\sigma}_s^{(0)}(\nabla_s h)+\boldsymbol{\sigma}_{sz}^{(1)}=\mathbf{0} \tag{C.3.5c}$$

$$\sigma_{zz}^{(0)}=0 \tag{C.3.5d}$$

$$-\boldsymbol{\sigma}_{sz}^{(0)}\cdot\nabla_s h+\sigma_{zz}^{(1)}=0 \tag{C.3.5e}$$

On $]0, t_f[\times\Gamma_0$:

$$-u_z^{(0)} = 0 \tag{C.3.6a}$$
$$-u_z^{(1)} = 0 \tag{C.3.6b}$$
$$\boldsymbol{\sigma}_{sz}^{(0)} + \boldsymbol{f}_a^{(0)} = \mathbf{0} \tag{C.3.6c}$$
$$\boldsymbol{\sigma}_{sz}^{(1)} - \alpha \boldsymbol{u}_s^{(0)} + \boldsymbol{f}_a^{(1)} = \mathbf{0} \tag{C.3.6d}$$

On $]0, t_f[\times\Gamma(t)$:

$$\boldsymbol{u}_s^{(0)} \cdot \boldsymbol{\nu} = 0 \tag{C.3.7a}$$
$$\boldsymbol{u}_s^{(1)} \cdot \boldsymbol{\nu} = 0 \tag{C.3.7b}$$
$$C\boldsymbol{\sigma}_s^{(0)}\boldsymbol{\nu} - C^3((\boldsymbol{\sigma}_s^{(0)}\boldsymbol{\nu})\cdot\boldsymbol{\nu})\boldsymbol{\nu} + \left(\boldsymbol{\sigma}_{sz}^{(0)} - 2C^2(\boldsymbol{\sigma}_{sz}^{(0)}\cdot\boldsymbol{\nu})\boldsymbol{\nu} - C\sigma_{zz}^{(0)} n_z \boldsymbol{\nu}\right) n_z = \mathbf{0} \tag{C.3.7c}$$
$$C\boldsymbol{\sigma}_{sz}^{(0)}\cdot\boldsymbol{\nu} + (\sigma_{zz}^{(0)} - C^2(\boldsymbol{\sigma}_s^{(0)}\boldsymbol{\nu})\cdot\boldsymbol{\nu})n_z + (\sigma_{zz}^{(0)} n_z - 2C\boldsymbol{\sigma}_{sz}^{(0)}\cdot\boldsymbol{\nu})n_z^2 = 0 \tag{C.3.7d}$$

C.3.4 Initial conditions

On Γ_0 :

$$h(0,\cdot) = h_0 \tag{C.3.8a}$$

In $\Lambda(0)$:

$$\boldsymbol{u}_s^{(0)}(0,\cdot) = \boldsymbol{u}_{0,s}^{(0)} \tag{C.3.8b}$$
$$\boldsymbol{u}_s^{(1)}(0,\cdot) = \boldsymbol{u}_{0,s}^{(1)} \tag{C.3.8c}$$
$$u_z^{(0)}(0,\cdot) = u_{0,z}^{(0)} \tag{C.3.8d}$$
$$u_z^{(1)}(0,\cdot) = u_{0,z}^{(1)} \tag{C.3.8e}$$

In $\Lambda(0)$:

$$\boldsymbol{\tau}_s^{(0)}(0,\cdot) = \boldsymbol{\tau}_{0,s}^{(0)} \tag{C.3.8f}$$
$$\boldsymbol{\tau}_s^{(1)}(0,\cdot) = \boldsymbol{\tau}_{0,s}^{(1)} \tag{C.3.8g}$$
$$\boldsymbol{\tau}_{sz}^{(0)}(0,\cdot) = \boldsymbol{\tau}_{0,sz}^{(0)} \tag{C.3.8h}$$
$$\boldsymbol{\tau}_{sz}^{(1)}(0,\cdot) = \boldsymbol{\tau}_{0,sz}^{(1)} \tag{C.3.8i}$$
$$\tau_{zz}^{(0)}(0,\cdot) = \tau_{0,zz}^{(0)} \tag{C.3.8j}$$
$$\tau_{zz}^{(1)}(0,\cdot) = \tau_{0,zz}^{(1)} \tag{C.3.8k}$$

C.4 Reduction

As said in subsection C.1, the idea is now to find new relations for our variables by combining and integrating over $[0, h]$ the different equations we obtained in the previous subsection.

From the constitutive equation (C.3.3c), whenever $\beta \neq 1$, we have

$$\frac{\partial \boldsymbol{u}_s^{(0)}}{\partial z} = \mathbf{0} \tag{C.4.1}$$

which means $u_s^{(0)}$ is independent on z. Whenever $\beta = 1$, we retrieve this result from equation (C.3.4c) as $We(\tau_{zz}^{(0)} + \beta) \neq 0$ whenever $\beta \neq 0$. Indeed, if we assume the opposite, equation (C.3.4e) tells us that $\tau_{zz}^{(0)} = -\beta/We = 0$, which is absurd since we have assumed that $\beta \neq 0$. Thus, by integrating over $[0, h]$ the mass conservation law (C.3.1a) and by using the boundary condition (C.3.6a), we obtain the relation

$$u_z^{(0)}\big|_{z=h} = -h \ \mathrm{div}_s(\boldsymbol{u}_s^{(0)}) \tag{C.4.2}$$

which is valid in the whole domain Ω.

Remark. Equality (C.4.1) suggests that the cells move as a block, i.e. all the points on a given vertical move at the same velocity.

From the momentum conservation laws (C.3.2a) and (C.3.2c) and from the boundary conditions (C.3.5b) and (C.3.5d), we deduce that in $]0, t_f[\times\Lambda(t)$,

$$\boldsymbol{\sigma}_{sz}^{(0)} = \mathbf{0} \tag{C.4.3}$$

$$\sigma_{zz}^{(0)} = 0 \tag{C.4.4}$$

By plugging (C.4.3) in the momentum conservation law (C.3.2d) and in the boundary condition (C.3.5e), we deduce

$$\sigma_{zz}^{(1)} = 0 \tag{C.4.5}$$

Remark. Equations (C.4.4) and (C.4.5) show that $\sigma_{zz} = O(\varepsilon^2)$. Thus, approximately, the cell monolayer is not subject to any tension or compression in the vertical direction. From the equation (C.4.3), we could also say that the cells are subject to a vertical shear that is of the same order as ε. And indeed the boundary condition (C.3.6d) shows that the first-order term is non-negligible.

C.4.1 Conservation laws

From equation (C.4.2) and from the free surface kinematic condition (C.3.5a) we deduce that in $]0, t_f[\times\Omega$

$$\begin{aligned}
\frac{\partial h}{\partial t} + (\boldsymbol{u}_s^{(0)} \cdot \nabla_s) h + h \ \mathrm{div}_s(\boldsymbol{u}_s^{(0)}) &= 0 \\
\frac{\partial h}{\partial t} + \boldsymbol{u}_s^{(0)} \cdot \nabla_s h + h \ \mathrm{div}_s(\boldsymbol{u}_s^{(0)}) &= 0 \\
\frac{\partial h}{\partial t} + \mathrm{div}_s(h\boldsymbol{u}_s^{(0)}) &= 0
\end{aligned} \tag{C.4.6}$$

By injecting the relation (C.4.1) into the momentum conservation law (C.3.2b), we get by integrating over $[0, h]$

$$\begin{aligned}
Re \int_0^h \left(\frac{\partial \boldsymbol{u}_s^{(0)}}{\partial t} + (\boldsymbol{u}_s^{(0)} \cdot \nabla_s)\boldsymbol{u}_s^{(0)} \right) \mathrm{d}z + Re \int_0^h u_z^{(0)} \cancelto{0}{\frac{\partial \boldsymbol{u}_s^{(0)}}{\partial z}} \mathrm{d}z - \int_0^h \mathbf{div}_s(\boldsymbol{\sigma}_s^{(0)}) \mathrm{d}z - \int_0^h \frac{\partial \boldsymbol{\sigma}_{sz}^{(1)}}{\partial z} \mathrm{d}z &= \mathbf{0} \\
hRe \left(\frac{\partial \boldsymbol{u}_s^{(0)}}{\partial t} + (\boldsymbol{u}_s^{(0)} \cdot \nabla_s)\boldsymbol{u}_s^{(0)} \right) - \mathbf{div}_s \int_0^h \boldsymbol{\sigma}_s^{(0)} \mathrm{d}z + \boldsymbol{\sigma}_s^{(0)}\big|_{z=h} \nabla_s h - \left[\boldsymbol{\sigma}_{sz}^{(1)} \right]_{z=0}^{z=h} &= \mathbf{0} \\
hRe \left(\frac{\partial \boldsymbol{u}_s^{(0)}}{\partial t} + (\boldsymbol{u}_s^{(0)} \cdot \nabla_s)\boldsymbol{u}_s^{(0)} \right) - \mathbf{div}_s \int_0^h \boldsymbol{\sigma}_s^{(0)} \mathrm{d}z + \boldsymbol{\sigma}_s^{(0)}\big|_{z=h} \nabla_s h - \boldsymbol{\sigma}_{sz}^{(1)}\big|_{z=h} + \boldsymbol{\sigma}_{sz}^{(1)}\big|_{z=0} &= \mathbf{0}
\end{aligned}$$

where to pass from the first line to the the second one we used the Leibniz's Integral Rule (B.0.9) from corollary B.2.3. Now, by using the boundary conditions (C.3.5c) and (C.3.6d), we obtain

$$\begin{aligned}
hRe \left(\frac{\partial \boldsymbol{u}_s^{(0)}}{\partial t} + (\boldsymbol{u}_s^{(0)} \cdot \nabla_s)\boldsymbol{u}_s^{(0)} \right) - \mathbf{div}_s\left(h\, \overline{\boldsymbol{\sigma}}_s^{(0)} \right) + \cancel{\boldsymbol{\sigma}_{sz}^{(1)}\big|_{z=h}} - \cancel{\boldsymbol{\sigma}_{sz}^{(1)}\big|_{z=h}} + \alpha \boldsymbol{u}_s^{(0)} - \boldsymbol{f}_a^{(1)} &= \mathbf{0} \\
hRe \left(\frac{\partial \boldsymbol{u}_s^{(0)}}{\partial t} + (\boldsymbol{u}_s^{(0)} \cdot \nabla_s)\boldsymbol{u}_s^{(0)} \right) - \mathbf{div}_s\left(h\, \overline{\boldsymbol{\sigma}}_s^{(0)} \right) + \alpha \boldsymbol{u}_s^{(0)} - \boldsymbol{f}_a^{(1)} &= \mathbf{0}
\end{aligned} \tag{C.4.7}$$

It could seem surprising that this relation depends on $\boldsymbol{f}_a^{(1)}$ and not on $\boldsymbol{f}_a^{(0)}$ – meaning that the latter disappears from the equations. Actually, it is not. From the equation (C.4.3) and from the boundary condition (C.3.6c), we remark that

$$\boldsymbol{f}_a^{(0)} = \mathbf{0} \tag{C.4.8}$$

which means that $\boldsymbol{f}_a = \boldsymbol{O}(\varepsilon)$: the active force is of the same order as the aspect ratio of the geometry. This is at this stage that the hypotheses we made on the friction coefficient ζ and on the characteristic stresses come into play. If we had rather decided that ζ is of the same order of magnitude as ε^0, then we would have $\alpha = \zeta U/\Sigma$ and the conservation law (C.4.7) would have read

$$hRe\left(\frac{\partial \boldsymbol{u}_s^{(0)}}{\partial t} + (\boldsymbol{u}_s^{(0)} \cdot \nabla_s)\boldsymbol{u}_s^{(0)}\right) - \mathbf{div}_s\Big(h\,\overline{\boldsymbol{\sigma}}_s^{(0)}\Big) + \alpha \boldsymbol{u}_s^{(1)} - \boldsymbol{f}_a^{(1)} = \mathbf{0}$$

We would still have the first-order term of the active force but the friction force wouldn't have to do with the zero-order term of the velocity, but it would have to do with its first-order term. The new coupled system of evolutionary equations would then contain both $\boldsymbol{u}_s^{(0)}$ and $\boldsymbol{u}_s^{(1)}$, which are unknowns. Therefore, it would complicate the resolution of the system too much. On the contrary, if we had wanted to make appear the zero-order term of the active force, we would have make for instance the following hypothesis:

$$\boldsymbol{f}_a = F\widetilde{\boldsymbol{f}_a}$$

where F is of the same order of magnitude as ε, and we would have the following boundary condition on $]0, t_f[\times\Gamma_0$:

$$\begin{aligned} \boldsymbol{\sigma}_{sz}^{(0)} &= \mathbf{0} \\ \boldsymbol{\sigma}_{sz}^{(1)} - \alpha \boldsymbol{u}_s^{(0)} + \boldsymbol{f}_a^{(0)} &= \mathbf{0} \end{aligned}$$

In this case, we therefore assume that $\boldsymbol{f}_a = \boldsymbol{O}(\varepsilon)$, unlike the previous case where this fact is deduced from the assumptions already in place and from the equations. It is difficult to affirm that one hypothesis is better than the other, especially when the result is the same in all cases.

C.4.2 Constitutive equations

By plugging the relations (C.4.4) and (C.4.5) in the constitutive equations (C.3.3e) and (C.3.3f), we can express the pressure in terms of the elastic stress tensor and the velocity field:

$$p^{(0)} = \tau_{zz}^{(0)} + 2(1-\beta)\frac{\partial u_z^{(0)}}{\partial z} \tag{C.4.9}$$

$$p^{(1)} = \tau_{zz}^{(1)} + 2(1-\beta)\frac{\partial u_z^{(1)}}{\partial z} \tag{C.4.10}$$

Combining the constitutive equation (C.3.3a) and the above first relation, we get

$$\boldsymbol{\sigma}_s^{(0)} = \boldsymbol{\tau}_s^{(0)} + 2(1-\beta)\,\boldsymbol{D}_s(\boldsymbol{u}_s^{(0)}) - \left(\tau_{zz}^{(0)} + 2(1-\beta)\frac{\partial u_z^{(0)}}{\partial z}\right)\mathbf{I}_s$$

and finally thanks to (C.4.1) and (C.4.2)

$$\overline{\boldsymbol{\sigma}}_s^{(0)} = \Big(\overline{\boldsymbol{\tau}}_s^{(0)} - \overline{\tau}_{zz}^{(0)}\mathbf{I}_s\Big) + 2(1-\beta)\Big(\boldsymbol{D}_s(\boldsymbol{u}_s^{(0)}) + \mathrm{div}_s(\boldsymbol{u}_s^{(0)})\mathbf{I}_s\Big) \tag{C.4.11}$$

Remark. Whenever $\beta = 1$, we get from the pressure relation (C.4.9) the following equality:

$$\tau_{zz}^{(0)} = p^{(0)} \tag{C.4.12}$$

Looking first at the constitutive equation (C.3.4b), we remark for instance the coupled terms $\partial_z \boldsymbol{u}_s^{(1)} \otimes \boldsymbol{\tau}_{sz}^{(0)}$. It will make us struggle when we will average on height the constitutive equation because a priori we do not know any handful information (specifically to this case) about those terms[12], except the constitutive equation (C.3.3d). When $\beta = 0$, i.e. when $\eta_m = 0$, it automatically results in $We = 0$ since it is proportional to λ which is itself proportional to η_m. Then we conclude from the constitutive equations that $\boldsymbol{\tau}_s^{(0)} = \mathbf{0}$, $\boldsymbol{\tau}_{sz}^{(0)} = \mathbf{0}$ and $\tau_{zz}^{(0)} = \tau_{zz}^{(1)} = 0$. Thus, the computations we are doing here do not concern the specific case $\beta \neq 0$.

By using the equality (C.4.3), we deduce from (C.3.3d)

$$\boldsymbol{\tau}_{sz}^{(0)} = -(1-\beta)\frac{\partial \boldsymbol{u}_s^{(1)}}{\partial z}$$

Let us take a look at the case $\beta = 1$. From the above equation, we have automatically $\boldsymbol{\tau}_{sz}^{(0)} = \mathbf{0}$. Thus from equation (C.4.1) and from the constitutive equation (C.3.4d), we have

$$\underbrace{\left(We\ \tau_{zz}^{(0)} + 1\right)}_{\neq 0} \frac{\partial \boldsymbol{u}_s^{(1)}}{\partial z} = \mathbf{0}$$

hence

$$\frac{\partial \boldsymbol{u}_s^{(1)}}{\partial z} = \mathbf{0}$$

Now, let us come back to the case $\beta \notin \{0, 1\}$. By hypothesis (ii), that we can justify either by mimicry or to make the computations more convenient, we have

$$\frac{\partial \boldsymbol{u}_s^{(1)}}{\partial z} = \mathbf{0} \tag{C.4.13}$$

then we get

$$\boldsymbol{\tau}_{sz}^{(0)} = \mathbf{0} \tag{C.4.14}$$

By plugging those relations and the relation (C.4.1) in the constitutive equation (C.3.4b), we come up with (even in the case $\beta = 1$ so)

$$We\left[\frac{\partial \boldsymbol{\tau}_s^{(0)}}{\partial t} + \left(\boldsymbol{u}_s^{(0)} \cdot \nabla_s + u_z^{(0)}\frac{\partial}{\partial z}\right)\boldsymbol{\tau}_s^{(0)} - (\nabla_s \boldsymbol{u}_s^{(0)})\boldsymbol{\tau}_s^{(0)} - \boldsymbol{\tau}_s^{(0)}(\nabla_s \boldsymbol{u}_s^{(0)})^\top\right]$$
$$-We\left(\cancelto{\mathbf{0}}{\frac{\partial \boldsymbol{u}_s^{(1)}}{\partial z} \otimes \boldsymbol{\tau}_{sz}^{(0)}} + \cancelto{\mathbf{0}}{\frac{\partial \boldsymbol{u}_s^{(0)}}{\partial z} \otimes \boldsymbol{\tau}_{sz}^{(1)}} + \cancelto{\mathbf{0}}{\boldsymbol{\tau}_{sz}^{(1)} \otimes \frac{\partial \boldsymbol{u}_s^{(0)}}{\partial z}} + \cancelto{\mathbf{0}}{\boldsymbol{\tau}_{sz}^{(0)} \otimes \frac{\partial \boldsymbol{u}_s^{(1)}}{\partial z}}\right)$$
$$+ \boldsymbol{\tau}_s^{(0)} - 2\beta\, \boldsymbol{D}_s(\boldsymbol{u}_s^{(0)}) = \mathbf{0}$$

[12] Even if we had considered higher order terms.

Then, by integrating over $[0, h]$, we have

$$We\left[\int_0^h \frac{\partial \boldsymbol{\tau}_s^{(0)}}{\partial t}\mathrm{d}z + \int_0^h (\boldsymbol{u}_s^{(0)}\cdot\nabla_s)\boldsymbol{\tau}_s^{(0)}\mathrm{d}z + \int_0^h u_z^{(0)}\frac{\partial \boldsymbol{\tau}_s^{(0)}}{\partial z}\mathrm{d}z - \int_0^h (\nabla_s \boldsymbol{u}_s^{(0)})\boldsymbol{\tau}_s^{(0)}\mathrm{d}z - \int_0^h \boldsymbol{\tau}_s^{(0)}(\nabla_s \boldsymbol{u}_s^{(0)})^\top \mathrm{d}z\right] + \int_0^h \boldsymbol{\tau}_s^{(0)}\mathrm{d}z - 2\beta\int_0^h \boldsymbol{D}_s(\boldsymbol{u}_s^{(0)})\mathrm{d}z = \mathbf{0}$$

But since $\boldsymbol{u}_s^{(0)}$ is independent on z (C.4.1), we get after having integrated by part the third term

$$We\left[\int_0^h \frac{\partial \boldsymbol{\tau}_s^{(0)}}{\partial t}\mathrm{d}z + \int_0^h (\boldsymbol{u}_s^{(0)}\cdot\nabla_s)\boldsymbol{\tau}_s^{(0)}\mathrm{d}z + \left[u_z^{(0)}\boldsymbol{\tau}_s^{(0)}\right]_{z=0}^{z=h} - \int_0^h \frac{\partial u_z^{(0)}}{\partial z}\boldsymbol{\tau}_s^{(0)}\mathrm{d}z - (\nabla_s \boldsymbol{u}_s^{(0)})\int_0^h \boldsymbol{\tau}_s^{(0)}\mathrm{d}z - \int_0^h \boldsymbol{\tau}_s^{(0)}\mathrm{d}z\,(\nabla_s \boldsymbol{u}_s^{(0)})^\top\right] + \int_0^h \boldsymbol{\tau}_s^{(0)}\mathrm{d}z - 2\beta h\,\boldsymbol{D}_s(\boldsymbol{u}_s^{(0)}) = \mathbf{0}$$

Now, by using Leibniz's Integral Rule B.2, the boundary condition (C.3.6a), the relation (C.4.2) and once again (C.4.1), we come up with

$$\begin{aligned} We\Bigg[& \frac{\partial}{\partial t}\left(\int_0^h \boldsymbol{\tau}_s^{(0)}\mathrm{d}z\right) - \boldsymbol{\tau}_s^{(0)}\big|_{z=h}\frac{\partial h}{\partial t} \\ & + (\boldsymbol{u}_s^{(0)}\cdot\nabla_s)\int_0^h \boldsymbol{\tau}_s^{(0)}\mathrm{d}z - (\boldsymbol{u}_s^{(0)}\cdot\nabla_s h)\boldsymbol{\tau}_s^{(0)}\big|_{z=h} \\ & - h\ \mathrm{div}_s(\boldsymbol{u}_s^{(0)})\boldsymbol{\tau}_s^{(0)}\big|_{z=h} - \cancel{\left(u_z^{(0)}\boldsymbol{\tau}_s^{(0)}\right)\Big|_{z=0}^{0}} + \mathrm{div}_s(\boldsymbol{u}_s^{(0)})\int_0^h \boldsymbol{\tau}_s^{(0)}\mathrm{d}z \\ & - (\nabla_s \boldsymbol{u}_s^{(0)})\int_0^h \boldsymbol{\tau}_s^{(0)}\mathrm{d}z - \int_0^h \boldsymbol{\tau}_s^{(0)}\mathrm{d}z\,(\nabla_s \boldsymbol{u}_s^{(0)})^\top\Bigg] \\ & + \int_0^h \boldsymbol{\tau}_s^{(0)}\mathrm{d}z - 2\beta h\,\boldsymbol{D}_s(\boldsymbol{u}_s^{(0)}) = \mathbf{0} \end{aligned}$$

then after rearrangement

$$\begin{aligned} We\Bigg[& \left(\frac{\partial}{\partial t} + (\boldsymbol{u}_s^{(0)}\cdot\nabla_s)\right)\left(\int_0^h \boldsymbol{\tau}_s^{(0)}\mathrm{d}z\right) - (\nabla_s \boldsymbol{u}_s^{(0)})\int_0^h \boldsymbol{\tau}_s^{(0)}\mathrm{d}z - \int_0^h \boldsymbol{\tau}_s^{(0)}\mathrm{d}z\,(\nabla_s \boldsymbol{u}_s^{(0)})^\top\Bigg] \\ & + We\ \mathrm{div}_s(\boldsymbol{u}_s^{(0)})\int_0^h \boldsymbol{\tau}_s^{(0)}\mathrm{d}z - \left(\frac{\partial h}{\partial t} + h\ \mathrm{div}_s(\boldsymbol{u}_s^{(0)}) + (\boldsymbol{u}_s^{(0)}\cdot\nabla_s h)\right)\boldsymbol{\tau}_s^{(0)}\big|_{z=h} \\ & + \int_0^h \boldsymbol{\tau}_s^{(0)}\mathrm{d}z - 2\beta h\,\boldsymbol{D}_s(\boldsymbol{u}_s^{(0)}) = \mathbf{0} \end{aligned}$$

From the density conservation law (C.4.6), we get

$$\begin{aligned} We\Bigg[& \left(\frac{\partial}{\partial t} + (\boldsymbol{u}_s^{(0)}\cdot\nabla_s)\right)\left(h\overline{\boldsymbol{\tau}}_s^{(0)}\right) - (\nabla_s \boldsymbol{u}_s^{(0)})\left(h\overline{\boldsymbol{\tau}}_s^{(0)}\right) - \left(h\overline{\boldsymbol{\tau}}_s^{(0)}\right)(\nabla_s \boldsymbol{u}_s^{(0)})^\top\Bigg] \\ & + We\ h\ \mathrm{div}_s(\boldsymbol{u}_s^{(0)})\overline{\boldsymbol{\tau}}_s^{(0)} + h\overline{\boldsymbol{\tau}}_s^{(0)} - 2\beta h\,\boldsymbol{D}_s(\boldsymbol{u}_s^{(0)}) = \mathbf{0} \end{aligned}$$

then

$$We\left[h\left(\frac{\partial}{\partial t}+(\boldsymbol{u}_s^{(0)}\cdot\nabla_s)\right)\overline{\boldsymbol{\tau}}_s^{(0)}-(\nabla_s\boldsymbol{u}_s^{(0)})\left(h\overline{\boldsymbol{\tau}}_s^{(0)}\right)-\left(h\overline{\boldsymbol{\tau}}_s^{(0)}\right)(\nabla_s\boldsymbol{u}_s^{(0)})^\top\right]$$
$$+We\left[\frac{\partial h}{\partial t}+(\boldsymbol{u}_s^{(0)}\cdot\nabla_s)h+h\ \mathrm{div}_s(\boldsymbol{u}_s^{(0)})\right]\overline{\boldsymbol{\tau}}_s^{(0)}$$
$$+h\overline{\boldsymbol{\tau}}_s^{(0)}-2\beta h\,\boldsymbol{D}_s(\boldsymbol{u}_s^{(0)})=\boldsymbol{0}$$

where $\overline{\boldsymbol{\tau}}_s^{(0)}=\frac{1}{h}\int_0^h\boldsymbol{\tau}_s^{(0)}\mathrm{d}z$. We conclude thanks to the density conservation law (C.4.6) and by simplification by $h\neq 0$:

$$We\overset{\nabla_s}{\overline{\boldsymbol{\tau}}}_s^{(0)}+\overline{\boldsymbol{\tau}}_s^{(0)}-2\beta\,\boldsymbol{D}_s(\boldsymbol{u}_s^{(0)})=\boldsymbol{0} \tag{C.4.15}$$

With a similar reasoning, the constitutive equation (C.3.4e) becomes

$$We\left(\frac{\partial\overline{\tau}_{zz}^{(0)}}{\partial t}+\left(\boldsymbol{u}_s^{(0)}\cdot\nabla_s\right)\overline{\tau}_{zz}^{(0)}+2\mathrm{div}_s(\boldsymbol{u}_s^{(0)})\overline{\tau}_{zz}^{(0)}\right)+\overline{\tau}_{zz}^{(0)}+2\beta\mathrm{div}_s(\boldsymbol{u}_s^{(0)})=0$$
$$We\left(\frac{D_s\overline{\tau}_{zz}^{(0)}}{Dt}+2\mathrm{div}_s(\boldsymbol{u}_s^{(0)})\overline{\tau}_{zz}^{(0)}\right)+\overline{\tau}_{zz}^{(0)}+2\beta\mathrm{div}_s(\boldsymbol{u}_s^{(0)})=0 \tag{C.4.16}$$

C.4.3 Boundary conditions

By using the equations (C.4.3) and (C.4.4), we have

$$\boldsymbol{u}_s^{(0)}\cdot\boldsymbol{\nu}=0$$
$$\boldsymbol{\sigma}_s^{(0)}\boldsymbol{\nu}-C^2((\boldsymbol{\sigma}_s^{(0)}\boldsymbol{\nu})\cdot\boldsymbol{\nu})\boldsymbol{\nu}=\boldsymbol{0}$$
$$\sqrt{1-C^2}\,((\boldsymbol{\sigma}_s^{(0)}\boldsymbol{\nu})\cdot\boldsymbol{\nu})=0$$

because $C\neq 0$. By integrating over $[0,h]$ then simplified by $h\neq 0$, we obtain the boundary conditions on $]0,t_f[\times\partial\Omega$:

$$\boldsymbol{u}_s^{(0)}\cdot\boldsymbol{\nu}=0$$
$$\overline{\boldsymbol{\sigma}}_s^{(0)}\boldsymbol{\nu}-\left(\left(\overline{C^2\boldsymbol{\sigma}_s^{(0)}}\boldsymbol{\nu}\right)\cdot\boldsymbol{\nu}\right)\boldsymbol{\nu}=\boldsymbol{0}$$
$$\left(\overline{\sqrt{1-C^2}\ \boldsymbol{\sigma}_s^{(0)}}\boldsymbol{\nu}\right)\cdot\boldsymbol{\nu}=0$$

The simple case $C=1$, imposed by hypothesis (iii), gives the following simplified boundary conditions:

$$\boldsymbol{u}_s^{(0)}\cdot\boldsymbol{\nu}=0 \tag{C.4.17a}$$
$$(\overline{\boldsymbol{\sigma}}_s^{(0)}\boldsymbol{\nu})_t=\boldsymbol{0} \tag{C.4.17b}$$

C.4.4 Initial conditions

$$h(0,\cdot)=h_0 \quad \text{in } \Gamma_0 \tag{C.4.18a}$$
$$\boldsymbol{u}_s^{(0)}(0,\cdot)=\boldsymbol{u}_{0,s}^{(0)} \quad \text{in } \Gamma_0 \tag{C.4.18b}$$
$$\overline{\boldsymbol{\tau}}_s^{(0)}(0,\cdot)=\overline{\boldsymbol{\tau}}_{0,s}^{(0)} \quad \text{in } \Gamma_0 \tag{C.4.18c}$$
$$\overline{\tau}_{zz}^{(0)}(0,\cdot)=\overline{\tau}_{0,zz}^{(0)} \quad \text{in } \Gamma_0 \tag{C.4.18d}$$

C.4.5 Conclusion

By combining the conservation laws (C.4.6) and (C.4.7), the constitutive equations (C.4.11), (C.4.15) and (C.4.16), the boundary conditions (C.4.17a) and (C.4.17b) and the initial conditions (C.4.18a), (C.4.18b), (C.4.18c) and (C.4.18d) and by invoking hypothesis (iv), we obtain the final system of partial differential equations valid for any $\beta \in [0,1]$:

(P_1): Find $\boldsymbol{\tau}$, τ_{zz}, $\boldsymbol{u}$ and h defined in $]0,t_f[\times\Omega$ such that

$$
\begin{cases}
-\mathbf{div}(h\,\boldsymbol{\sigma}) + \alpha \boldsymbol{u} - \boldsymbol{f}_a = \mathbf{0} & \text{in }]0,t_f[\times\Omega & \text{(C.4.19a)}\\
\dfrac{\partial h}{\partial t} + \operatorname{div}(h\boldsymbol{u}) = 0 & \text{in }]0,t_f[\times\Omega & \text{(C.4.19b)}\\
\boldsymbol{\sigma} = (\boldsymbol{\tau} - \tau_{zz}\mathbf{I}) + 2(1-\beta)(\boldsymbol{D}(\boldsymbol{u}) + \operatorname{div}(\boldsymbol{u})\mathbf{I}) & \text{in }]0,t_f[\times\Omega & \text{(C.4.19c)}\\
We\,\overset{\nabla}{\boldsymbol{\tau}} + \boldsymbol{\tau} - 2\beta\,\boldsymbol{D}(\boldsymbol{u}) = \mathbf{0} & \text{in }]0,t_f[\times\Omega & \text{(C.4.19d)}\\
We\left(\dfrac{D\tau_{zz}}{Dt} + 2\operatorname{div}(\boldsymbol{u})\tau_{zz}\right) + \tau_{zz} + 2\beta\operatorname{div}(\boldsymbol{u}) = 0 & \text{in }]0,t_f[\times\Omega & \text{(C.4.19e)}\\
\boldsymbol{u}\cdot\boldsymbol{\nu} = 0 \text{ and } (\boldsymbol{\sigma}\nu)_t = \mathbf{0} & \text{on }]0,t_f[\times\partial\Omega & \text{(C.4.19f)}\\
h(0,\cdot) = h_0 & \text{in } \Omega & \text{(C.4.19g)}\\
\boldsymbol{\tau}(0,\cdot) = \boldsymbol{\tau}_0 \text{ and } \tau_{zz}(0,\cdot) = \tau_{zz,0} & \text{in } \Omega & \text{(C.4.19h)}
\end{cases}
$$

where we dropped the orders (0) and (1), the subscripts $\boldsymbol{s}$ and the bars for notation convenience.

The problem amounts to solving a closed system: we have 4 unknowns h, $\boldsymbol{u}$, $\boldsymbol{\tau}$ and p for 4 equations, boundary conditions on the whole boundary $\partial\Omega$ of the system domain Ω and initial conditions for all the unknowns.

D Resolution of the problem in a very specific case

We place ourselves in the case under consideration at the beginning of section 2. When α is sufficiently large, the viscous term in (2.0.1a) is negligible with respect to the friction and the active force. Then $\boldsymbol{u}$ and h must satisfy the following system:

$$
\begin{aligned}
\alpha\boldsymbol{u} &= -\gamma\, h^{-1}\cdot\nabla h\, \mathbb{1}_{\Omega_c(t)} && \text{in }]0,t_f[\times\Omega && \text{(D.0.1a)}\\
\partial_t h &= -\operatorname{div}(h\boldsymbol{u}) && \text{in }]0,t_f[\times\Omega && \text{(D.0.1b)}\\
\boldsymbol{u}\cdot\boldsymbol{\nu} &= 0 && \text{on }]0,t_f[\times\partial\Omega && \text{(D.0.1c)}\\
h(0,\bullet) &= h_0 && \text{in } \Omega && \text{(D.0.1d)}
\end{aligned}
$$

i.e.

$$
\begin{aligned}
\partial_t h &= \gamma/\alpha\,\Delta h && \text{in }]0,t_f[\times\Omega_c(t)\\
h(t,\cdot) &= h_0 && \text{in } [0,t_f[\times\Omega_c(t)^c\\
\partial_{\boldsymbol{\nu}} h &= 0 && \text{on }]0,t_f[\times\partial\Omega\\
h(0,\bullet) &= h_0 && \text{in } \Omega_c(0)
\end{aligned}
$$

We recognize a heat-like equation with diffusivity parameter γ/α. By making the change of variable $s = \gamma/\alpha\, t$ (thus $s_f = \gamma/\alpha\, t_f$) and by abusing the notation, we end up with the following equation:

(P): Find h defined in $]0, s_f[\times\Omega$ such that

$$\begin{cases} \partial_s h = \Delta h \text{ in }]0, s_f[\times\Omega_c(s) & \text{(D.0.2a)} \\ h(s,\cdot) = h_0 \text{ in } [0, s_f[\times\Omega_c(s)^c & \text{(D.0.2b)} \\ \partial_{\boldsymbol{\nu}} h = 0 \text{ on }]0, s_f[\times\partial\Omega & \text{(D.0.2c)} \\ h(0,\cdot) = h_0 \text{ in } \Omega_c(0) & \text{(D.0.2d)} \end{cases}$$

It is possible to explicitly write the solution of this problem when $\Omega = \mathbb{R}$. Indeed, one can check that

$$h(s,x) = \begin{cases} c_1 - c_2 \operatorname{erf}\left(\dfrac{x}{2\sqrt{s}}\right) & \text{if } s > 0 \text{ and } c_1 - c_2 \operatorname{erf}\left(\dfrac{x}{2\sqrt{s}}\right) \geqslant h_c \\ h_0(x) & \text{otherwise} \end{cases} \tag{D.0.3}$$

where $c_1 \in \mathbb{R}$ and $c_2 \in \mathbb{R}^*$ are constant and

$$\operatorname{erf}(x) = \frac{2}{\sqrt{\pi}} \int_0^x \mathrm{e}^{-t^2} \, \mathrm{d}t \tag{D.0.4}$$

is the error function, is solution of the previous problem, as

$$\lim_{|x|\to+\infty} \partial_x h(s,x) = \lim_{|x|\to+\infty} -\frac{1}{\sqrt{\pi s}} \exp\left(-\frac{x^2}{4s}\right) = 0$$

for any $s > 0$, and if $\lim\limits_{|x|\to+\infty} h_0'(x) = 0$. The latter is a kind of compatibility condition. In practice, we need not explicitly take $\mathbb{R}$ as domain, as long as the solution h decreases fast enough not to be affected by the Neumann's condition. Eventually, to ensure the positivity of h, assuming $h_0 \geqslant 0$ in $\mathbb{R}$, a necessary and sufficient condition is

$$\left|\frac{c_1}{c_2}\right| \geqslant 1 \tag{D.0.5}$$

as for any $x \in \mathbb{R}$, $\operatorname{erf}(x) \in]-1, 1[$.

Let us try to explicit constants c_1 and c_2. For instance, for any $x \in \mathbb{R}$, $h(\cdot, x)$ will be continuous if

$$\lim_{s\to 0^+} h(s,x) = h_0(x)$$

i.e. if

$$h_0(x) = \begin{cases} c_1 - c_2 & \text{if } x > 0 \\ c_1 & \text{if } x = 0 \\ c_1 + c_2 & \text{if } x < 0 \end{cases} \tag{D.0.6}$$

Here, we clearly have $\lim\limits_{|x|\to+\infty} h_0'(x) = 0$. For example, to have $\lim\limits_{x\to+\infty} h_0(x) = 0$, we should take $c_1 = c_2$, in which case the initial condition should be equal to

$$h_0(x) = \begin{cases} 0 & \text{if } x > 0 \\ c_1 & \text{if } x = 0 \\ 2c_1 & \text{if } x < 0 \end{cases} \tag{D.0.7}$$

Case $c_1 = 1/2$ is the one we have chosen in section 3.

Coming back to the general resolution, we reverse the change of scale in time we made to get

$$h(t,x) = \begin{cases} c_1 - c_2 \operatorname{erf}\left(\sqrt{\frac{\alpha}{\gamma}} \cdot \frac{x}{2\sqrt{t}}\right) & \text{if } t > 0 \text{ and } c_1 - c_2 \operatorname{erf}\left(\sqrt{\frac{\alpha}{\gamma}} \cdot \frac{x}{2\sqrt{t}}\right) \geqslant h_c \\ h_0(x) & \text{otherwise} \end{cases} \tag{D.0.8}$$

From this relation, we deduce an explicit form for the front position at any time $t \in]0, t_f]$:

$$x_f(t) = 2 \operatorname{erf}^{-1}\left(\frac{c_1 - h_c}{c_2}\right)\sqrt{\frac{\gamma}{\alpha}t} \tag{D.0.9}$$

in which case, the tissue domain can also be defined by

$$\Omega_c(t) = \begin{cases}]-\infty, x_f(t)] & \text{if } c_2 > 0 \\ [x_f(t), +\infty[& \text{if } c_2 < 0 \end{cases} \tag{D.0.10}$$

for any $t > 0$, since erf is an increasing function. Besides, to ensure the continuity of the front in $t = 0$, we should take $h_0 \geqslant h_c$ in $\mathbb{R}_-$ if $c_2 > 0$ (R_+ if $c_2 < 0$) and 0 elsewhere. Notice the agreement between the continuity of h in time (equation (D.0.7)) and that of the front.

Finally, we can also give an explicit form to the velocity by using relation (D.0.1a):

$$u(t,x) = \begin{cases} \dfrac{\gamma^{1/2} \exp\left(-\dfrac{\alpha x^2}{4\gamma t}\right)}{\alpha^{1/2}\left(c_1 - c_2 \operatorname{erf}^{-1}\left(\dfrac{\alpha^{1/2} x}{2\gamma^{1/2}\sqrt{t}}\right)\right)\sqrt{\pi t}} & \text{if } t > 0 \text{ and } c_1 - c_2 \operatorname{erf}\left(\sqrt{\frac{\alpha}{\gamma}} \cdot \frac{x}{2\sqrt{t}}\right) \geqslant h_c \\ 0 & \text{otherwise} \end{cases} \tag{D.0.11}$$

Figure D.1 shows the curves $(x, h(t,x))$ and $(x, u(t,x))$ for $t \in \{1, 3, 5, 7\}$, $c_1 = c_2 = 1/2$, h_0 as in (D.0.7) and $\gamma/\alpha = 11.75$.

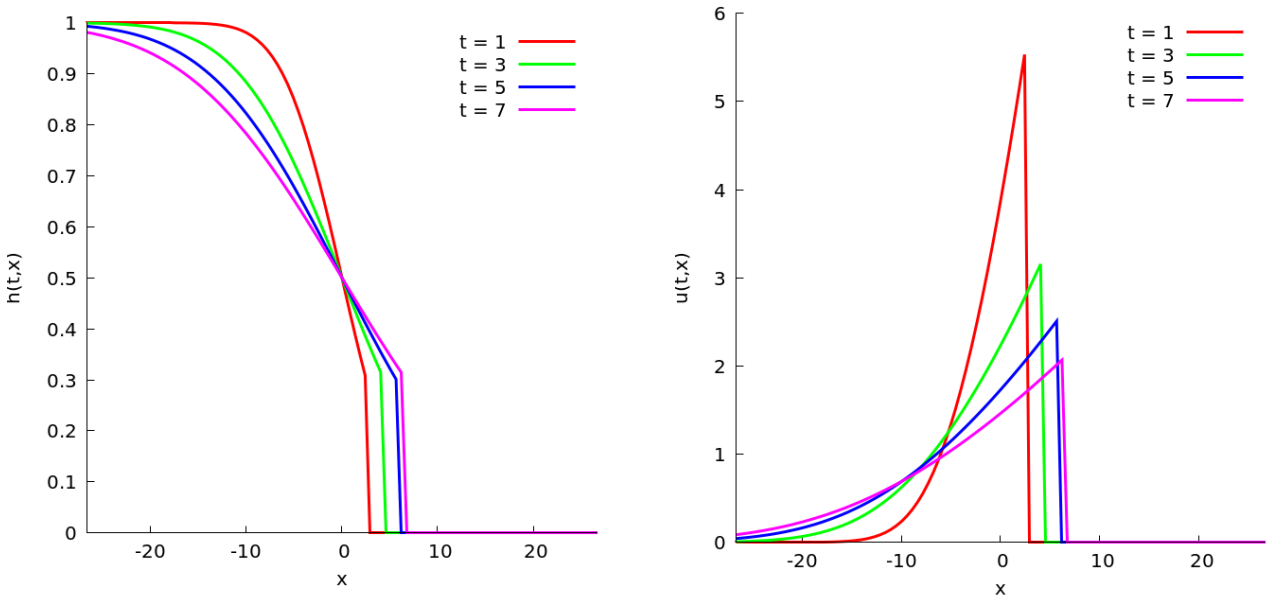

(a) (b)

Figure D.1: Exact solutions of the large α model at different times when $c_1 = c_2 = 1/2$, h_0 is like in (D.0.7) and $\gamma/\alpha = 11.75$.